Biomedical Research 2004; 15 (2): 81-84

Relationship between Renal Function and Brachial-Ankle Pulse Wave Velocity (BaPWV) in Patients with Type 2 Diabetes Mellitus

Toshiaki Kakiba, Motoi Sohmiya, Tadashi Shimizu, Masahiro Yamamoto, Yuko Yamane, Yuzuru Kato

Department of Endocrinology, Metabolism and Hematological Oncology, Shimane University School of Medicine, Izumo 693-8501, Japan.

Key words: Type 2 diabetes mellitus, Brachial-ankle pulse wave velocity, Diabetic nephropathy

Accepted March 27 2004

Abstract

We investigated the relationship between renal function and brachial-ankle pulse wave velocity (baPWV) in patients with type 2 diabetes mellitus. Fifty-six patients with type 2 diabetes mellitus were included in the present study. They were divided into three groups by urinary albumin excretion: normoalbuminuria (group N, <30 mg/g creatinine, n=32); microalbuminuria (group MI, 30 - 300 mg/g creatinine, n=16); and macroalbuminuria (group MA, >300 mg/g creatinine, n=8). The baPWV was determined by oscillometrical measurement of the pulse volume recorded at the upper arm and ankles.

The baPWV was correlated with age, systolic blood pressure, diastolic blood pressure, pulse pressure, blood urea nitrogen, serum creatinine, and urinary albumin excretion. Multiple regression analysis revealed that age and pulse pressure were independently correlated with baPWV. The baPWV was increased in patients with diabetic nephropathy, and greater in those with groups MI and MA than in group N. There was no difference in age, duration of diabetes mellitus and blood pressure between groups N and MI.

These findings suggest that baPWV is increased in patients with early stage of diabetic nephropathy in which arteriosclerosis might progress.

Introduction

Diabetes mellitus is one of the most important risk factors of cardiovascular disease [1]. The risk is 2 to 4 fold higher than the subjects without diabetes mellitus at any level of standard risk factors [1]. Renal dysfunction is well related to arterial stiffness [2,3], in which diabetic nephropathy might be more involved than other renal diseases. It has been well evaluated the relationship between arterial stiffness and plasma glucose levels and/or insulin resistance in diabetic patients [4,5].

Pulse wave velocity (PWV) is useful for evaluating arterial stiffness, which is an important risk factor for cardiovascular disease. PWV could be measured with simple and non-invasive method [6-12]. There have been a number of reports on the usefulness of PWV measurement [8,9,13,14]. PWV is consisted of brachial-ankle PWV (baPWV) and carotid femoral PWV (cfPWV). The baPWV is well correlated with cfPWV [14]

In this study, we investigated the relationship between diabetic nephropathy and baPWV in patients with type 2 diabetes mellitus.

Materials and Methods

Subjects

Fifty-six patients with type 2 diabetes mellitus (31 males and 25 females, aged from 45 to 86 yrs) were studied. The clinical characteristics of these patients are shown in Table 1. Hypertension, hyperlipidemia and smoking habits were found in 59%, 43% and 34%, respectively, in these patients. They were divided into three groups: 1) normoalbuminuria (group N, n=32, less than 30 mg/g creatinine); 2) microalbuminuria (group MI, n=16, 30 to 300 mg/g creatinine); and 3) macroalbuminuria (group MA, n=8, more than 300 mg/g creatinine). Urinary albumin was measured by radioimmunoassay in the urine samples obtained in the morning and corrected by urinary creatinine excretion for statistical analysis.

Blood samples were obtained after an overnight fasting. Blood HbA1c levels, serum C-peptide immunoreactivity (S-CPR), total cholesterol (TC), triglyceride (TG), HDL cholesterol (HDL-C), urea

nitrogen (BUN) and creatinine (Cr) levels were measured by standard laboratory methods. Serum LDL cholesterol (LDL-C) levels were calculated by the Friedewald equation. Hyperlipidemia was defined by either increased serum TC (>220 mg/dl), TG (>150 mg/dl), or LDL-C (>140 mg/dl).

Information on the smoking habits and duration of diabetes mellitus was obtained by detailed history taking.

baPWV measurement

The baPWV was measured in the supine position after bed rest for 6 min using a volume-plethysmographic apparatus (form PWV/ABI, Colin Co. Ltd, Komaki, Japan). This apparatus could record PWV, blood pressure, electrocardiogram and heart sounds at the same time. Electrodes for ECG were placed on both wrists. A microphone for detecting heart sounds was placed on the left edge of the sternum, and cuffs were mounted on both brachia and ankles. The cuffs were connected to a plethysmographic sensor for detecting volume pulse form and an oscillometric pressure sensor for measuring blood pressure. The pulse volume waveforms were recorded using a semiconductor pressure sensor. The baPWV was automatically calculated according to the following equation: baPWV = $(D1-D2)/T1$. $D1$ is the distance from the heart to the ankle, and $D2$ is the distance from the heart to the right upper arm. These distances were calculated automatically on the basis of the subject's height. $T1$ is the time from the onset of the rise in the pulse volume recorded the right upper arm to the onset of the rise in the pulse volume record of the ankle. The inter- and intra-observer variation coefficients were 8.4 and 10.0%, respectively. The mean (±SD) values of baPWV in healthy subjects were assessed based on the data reported in Japanese subjects by Yokoyama *et al.* (aged 45-75 years, 1376±373 cm/s in males and 1352±222 cm/s in females) [15].

Blood pressure and ankle/brachial blood pressure index (ABI) were measured with the use of form PWV/ABI at the same time when baPWV was measured. Hypertension was defined as systolic blood pressure (SBP) greater than 140 mmHg, or diastolic blood pressure (DBP) greater than 90 mmHg. There was no patient with ABI of less than 0.9, which suggests arteriosclerosis obliterans.

Informed consents were obtained from all the subjects examined.

Statistical analysis

Data were expressed as the means±SD. The influences of variables on baPWV were evaluated by simple linear and multiple linear stepwise regression analyses. The distribution of albuminuria was normalized by logarithmic transformation. The difference between two groups was analyzed by Student's *t*-test for parametric comparison and Mann-Whitney's *U* test for nonparametric comparison, respectively. The differences among groups N, MI, and MA were analyzed by ANOVA with Scheffe's *F* test. Data were analyzed with StatView, 5.0 software. *P* values less than 0.05 were considered significant.

Results

As shown in Table 1, the mean (±SD) baPWV was 1729.7±383.5 cm/s in all the subjects. The baPWV was increased in MI and MA groups compared with N group (1873.0±412.5 and 2004.6±276.1 vs 1589.4±333.2 cm/s, P<0.05). Duration of diabetes mellitus was longer in group MA than in groups N and MI (22.1±9.5 vs 12.7±10.0 and 14.2±5.4 years, P<0.05). SBP and PP were also increased in group MA. In contrast, there was no difference in age, diabetic duration and blood pressure between groups N and MI.

Table 2 shows the correlation coefficients between baPWV and clinical data. There were significant correlation of baPWV with age, SBP, DBP, pulse pressure (PP), BUN, Cr, and urinary albumin. As shown in Table 3, the baPWV was increased in patients with hypertension (1832.7±381.2 vs 1582.0±342.9 cm/s, P<0.05). There was no difference in baPWV among gender, smoking habits and hyperlipidemia in these patients.

Table 1. Clinical Characteristics of Patients with Type 2 Diabetes Mellitus

Group	N (n=32)	MI (n=16)	MA (n=8)	Total (n=56)
Age (years)	62.6±9.7	65.6±12.4	64.6±8.7	63.7±10.3
Gender (male/female)	17/15	9/7	5/3	31/25
BMI (kg/m^2)	23.5±4.0	23.3±3.7	24.3±4.0	23.6±3.8
Duration (years)	12.7±10.0	14.2±5.4	22.1±9.5*	14.5±9.3
HbA1c (%)	8.2±2.2	8.0±1.8	7.5±1.8	8.1±2.0
Hypertension (−/+)	15/17	6/10	2/6	23/33
Hyperlipidemia (−/+)	20/12	10/6	2/6	32/24
Smoking (−/+)	21/11	10/6	6/2	37/19
SBP (mmHg)	124.8±17.6	137.0±20.9	154.3±26.8**	132.5±22.2
DBP (mmHg)	73.2±8.7	81.6±14.3	74.8±17.7	76.5±11.7
PP (mmHg)	51.7±11.3	55.4±14.2	74.8±17.7 [a,b]	56.0±15.1
baPWV (cm/s)	1589.4±333.2	1873.0±412.5*	2004.6±276.1*	1729.7±383.5

BMI, body mass index; SBP, systolic blood pressure; DBP, diastolic blood pressure; PP, pulse pressure; baPWV, brachial-ankle pulse wave velocity. Date are means±SD. * P<0.05 vs N group. ** P<0.01 vs N group. [a] P<0.01 vs MI group. [b] P<0.001 vs N group.*

Table 2. Correlation Coefficients between baPWV and Clinical Data

Variables	r	P
Age	0.538	<0.001
BMI	-0.161	NS
Duration	0.236	NS
SBP	0.575	<0.0001
DBP	0.266	<0.05
PP	0.639	<0.0001
HbA1c	-0.056	NS
Serum CPR	-0.026	NS
Total cholesterol	-0.088	NS
HDL-cholesterol	-0.072	NS
LDL-cholesterol	-0.103	NS
Triglyceride	0.004	NS
BUN	0.421	<0.01
Creatinine	0.348	<0.01
Urinary albumin	0.394	<0.01

SBP, systolic blood pressure; DBP, diastolic blood pressure; PP, pulse pressure; CPR, c-peptide reactivity; HDL, high density lipoprotein; LDL, low density lipoprotein; BUN, blood urea nitrogen

Table 3. Group Comparison of baPWV

		baPWV (cm/s)
Gender	Males	1741.4±424.5
	Females	1715.3±333.7
Hypertension	(-)	1582.0±342.9
	(+)	1832.7±381.2 *
Hyperlipidemia	(-)	1748.1±424.3
	(+)	1705.3±328.6
Smoking	(-)	1690.3±369.1
	(+)	1806.4±409.3

baPWV, brachial-ankle pulse wave velocity.
** P<0.05 compared to (-).*

The baPWV is useful for evaluating arterial stiffness, and has been spread because it can be simply measured by oscillometry on a routine basis. The good validity and reproducibility of baPWV have been previously reported [8]. Data from necropsy studies in human shows that the atherosclerotic involvement of vessels well correlates with arterial stiffness assessed non-invasively before death [16]. The baPWV was increased in aged subjects and female in healthy subjects [9]. The PWV was increased with aging and blood pressure in patients with type 2 diabetes mellitus [13,15]. In the present study, baPWV was correlated with age, SBP, DBP and PP. These findings support the previous reports.

The PWV is increased in varicus diseases associated with atherosclerosis, including diabetes mellitus [4], hypertension [17] and renal disease [2,3]. PWV is also known to be a prognostic predictor for atherosclerotic vascular disease in patients with diabetes mellitus [4], hypertension [18] and end-stage renal failure [3]. The baPWV was increased in patients with hypertension and diabetic nephropathy in the present study. Aortic PWV correlated with the severity of independently assessed diabetic complication [6]. The baPWV was related to the risk of diabetic microvascular disease [10].

However, it is not fully elucidated whether diabetic nephropathy in the early stage influences progression of arteriosclerosis assessed by baPWV. In the present study, the baPWV was increased in diabetic patients with microalbuminuria. Although baPWV was influenced by age, duration of diabetes mellitus or blood pressure; there was no difference in these factors between groups N and MI. These findings support the hypothesis that microalbuminuria reflects general vascular damage in the body [19, 20]. The extracellular matrix composition in skeletal muscle capillary basement membranes was changed according to the level of albuminuria [21]. Therefore, the albuminuria and increased PWV might be attributed to the altered composition within vessel walls [15] and associated with increased cardiovascular morbidity and mortality independent of conventional risk factors [19].

Several studies have demonstrated the beneficial effect of angiotensin II receptor antagonist (ARB) on arterial stiffness [22,23] and urinary albumin excretion [24]. Further studies are required to evaluate whether the administration of ARB might improve arterial stiffness evaluated by baPWV in the patients with early stage diabetic nephropathy.

In the present study, such factors as hypertension, renal function and others should be evaluated by multivariate analysis. However, it is difficult to analyze in the small number of patients studied. Therefore, further studies on a large scale are required.

These findings suggest that baPWV is increased in patients with early stage of diabetic nephropathy in which arteriosclerosis might progress.

References

1. Stamler J, Vaccaro O, Neaton JD, Wentworth D. Diabetes, other risk factors, and 12-yr cardiovascular mortality for men screened in the Multiple Risk Factor Intervention Trial. Diabetes Care 1993; 16: 434-444.
2. Blacher J, Guerin AP, Pannier B, Marchais SJ, Safar ME, London GM. Impact of aortic stiffness on survival in end-stage renal failure. Circulation 1999; 99: 2434-2439.
3. Guerin AP, Blacher J, Pannier B, Marchais SJ, Safer ME, London GM. Impact of aortic stiffness attenuation on survival of patients in end-stage renal failure. Circulation 2001; 103: 987-992.
4. Cruickshank K, Riste L, Anderson SG, Wright JS, Dunn G, Gosling RG. Aortic pulse-wave velocity and its relationship to mortality in diabetes and glucose intolerance. An integrated index of vascular function? Circulation 2002; 106: 2085-2090.
5. Murakami H, Ura N, Furuhashi M, Higashiura K, Miura T, Shimamoto K. Role of adiponectin in insulin-resistant hypertension and atherosclerosis. Hypertens Res 2003; 26: 705-710
6. Lehmann ED, Riley WA, Clarkson P, Gosling RG. Non-invasive assessment of cardiovascular disease in diabetes mellitus. Lancet 1997; 350 (Supple 1): 14-19.

7. Takolander R, Rauwerda JA. The use of non-invasive vascular assessment in diabetic patients with foot lesions. Diabet Med 1996; 13: S39-42.
8. Yamashina A, Tomiyama H, Takeda K, Tsuda H, Arai T, Hirose K, Koji Y, Hori S, Yamamoto Y. Validity, reproducibility, and clinical significance of non-invasive brachial-ankle pulse wave velocity measurement. Hypertens Res 2002; 25: 359- 364.
9. Tomiyama H, Yamashina A, Arai T, Hirose K, Koji Y, Chikamori T, Hori S, Yamamoto Y, Doba N, Hinohara S. Influences of age and gender on results of noninvasive brachial-ankle pulse wave velocity measurement-a survey of 12517 subjects. Atherosclerosis 2003; 166: 303-309.
10. Aso K, Miyata M, Kubo T, Hashiguchi H, Fukudome M, Fukushige E, Koriyama N, Nakazaki M, Minagoe S, Tei C. Brachial-ankle pulse wave velocity is useful for evaluation of complications in type 2 diabetic patients. Hypertens Res 2003; 26: 807-813.
11. Wilkinson IB, Fuchs SA, Jansen IM, Spratt JC, Murray GD, Cockcroft JR, Webb DJ. Reproducibility of pulse wave velocity and augmentation index measured by pulse wave analysis. J Hypertens 1998; 16: 2079-2084.
12. Yokoyama H, Shoji T, Kimoto E, Shinohara K, Tanaka S, Koyama H, Emoto M, Nishizawa Y. Pulse wave velocity in lower-limb arteries among diabetic patients with peripheral arterial disease. J Atheroscler Thromb 2003; 10: 253-258.
13. Taniwaki H, Kawagishi T, Emoto M, Shoji T, Kanda H, Maekawa K, Nishizawa Y, Morii H. Correlation between the intima-media thickeness of the carotid artery and aortic pulse-wave velocity in patients with type 2 diabetes. Vessel wall properties in type 2 diabetes. Diabetes Care 1999; 22: 1851-1857.
14. Munakata M, Ito N, Nunokawa T, Yoshinag K. Utility of automated brachial ankle pulse wave velocity measurements in hypertensive patients. Am J Hypertens 2003; 16: 653-657.
15. Yokoyama H, Hirasawa K, Aoki T, Ishiyama M, Koyama K. Brachial-ankle pulse wave velocity measured automatically by oscillometric method is elevated in diabetic patients with incipient nephropathy. Diabet Medicine 2003; 20: 942-945.
16. Wada T, Kodaira K, Fujishiro K, Maie K, Tsukiyama E, Fukumoto T, Uchida T, Yamazaki S. Correlation of ultrasound--measured common carotid artery stiffness with pathological findings. Arterioscler Thromb 1994; 14: 479- 482.
17. Blacher I, Asmar R, Djane S, London GM, Safar ME. Aortic pulse wave velocity as a marker of cardiovascular risk in hypertensive patients. Hypertension 1999; 33: 1111-1117.
18. Laurent S, Boutouyrie P, Asmar R. Aortic stiffness is an independent predictor of all-cause and cardiovascular mortality in hypertensive patients. Hypertension 2001; 37: 1236- 1241.
19. Dinneen SF, Gerstein HC. The association of microalbuminuria and mortality in non-insulin-dependent diabetes mellitus: a systematic overview of the literature. Arch Intern Med 1997; 157: 1413-1418.
20. Deckert T, Feldt-Rasmussen B, Borch-Johnsen K, Jensen T, Kofoed-Enevoldsen A. Albuminuria reflects widespread vascular damage: the Steno hypothesis. Diabetologia 1989; 32: 219-226.
21. Yokoyama H, Hoyer PE, Hansen PM, van den Born J, Jensen T, Berden JH, Deckert T, Garbarsch C. Immunohistochemical quantification of heparan sulfate proteoglycan and collagen IV in skeletal muscle capillary basement membranes of patients with diabetic nephropathy. Diabetes 1997; 46: 1875-1880.
22. Mahmud A, Feely J. Effect of angiotensin II rece-ptor blockade on arterial stiffness: beyond blood pressure reduction. Am J Hypertens 2002; 15: 1092-1095.
23. Asmar R, Gosse P, Topouchian J, N'tela G, Dudley A, Shepherd GL. Effects of telmisartan on arterial stiffness in type2 diabetes patients with essential hypertension. J Renin Angiotensin Aldosterone Syst 2002; 3: 176-180.
24. Tan KCB, Chow WS, Ai VHG, Lam KSL. Effects of angiotensin II receptor antagonist on endothelial vasomotor function and urinary albumin excretion in type2 diabetic patients with microalbuminuria. Diabetes Metab Res Rev 2002; 18: 71-76.

Correspondence:

Dr. Toshiaki Kakiba
Department of Endocrinology,
Metabolism & Hematological Oncology
Shimane University School of Medicine
Izumo 693-8501, Japan.

Phone: +81-853-23-2111
Fax: +81-853-23-8650
e-mail: motoi@med.shimane-u.ac.jp

Biomedical Research 2004; 15 (2): 85-91

Case Report:

Effect of thyroid hormone on elliptocyte shape in a case of chronic thyroiditis associated with elliptocytosis

Motoi Sohmiya, Junko Tanaka and Yuzuru Kato

Department of Endocrinology, Metabolism and Hematological Oncology, Shimane University School of Medicine, Izumo 693-8501, Japan.

Key words: Chronic thyroiditis, Elliptocytosis, Anemia, Levothyroxine sodium

Accepted April 7 2004

Abstract

We report a rare case of primary hypothyroidism due to chronic thyroiditis associated with elliptocytosis and anemia. A 75-yr-old woman was referred to our clinic for hypothyroidism and anemia. Increased serum indirect bilirubin and LDH levels were normalized after the thyroid hormone replacement, and Hb levels were corrected promptly whereas increased mean cell volume of erythrocytes was gradually decreased to the normal range. Elliptocytosis of oval form (OH) and of rod form (RF) was persisted and the ratio of OH to RF was not changed by the treatment with levothyroxine. Although elliptocytes with the central pale indicating the central hollow were not recognized before the treatment, the percentage of the elliptocytes with the central pale was increased to 37.4±2.6% (mean±SD) after the treatment with levothyroxine sodium. The percent of elliptocytes with central pale was remarkably increased in blood samples of the patient after the incubation *in vitro* with thyroxine at the final concentration of 170 nmol/L and 1,322 nmol/L (32.6±3.8% and 60.1±6.7% vs 11.0±3.1%, P<0.0001 and P<0.0001). These findings suggest that thyroid hormone deficiency could be involved in developing anemia and elliptocytosis without central pale in the present case with chronic thyroiditis.

Introduction

Hypothyroidism is often accompanied by normochromic normocytic anemia, which is improved by replacement with thyroid hormones [1,2]. Chronic thyroiditis is also occasionally accompanied by either such macrocytic hyperchromic anemia as pernicious anemia or such microcytic hypochromic anemia as iron deficiency. There were also some case reports on chronic thyroiditis associated with either autoimmune hemolytic anemia [3-7] or spherocytosis [8,9]. Hypothyroid state itself may cause the membrane abnormality in erythrocytes, resulting in shortening the survival of erythrocytes [10].

Elliptocytosis is one of the rare erythrocyte shape abnormalities. Therefore, there has been no report for the relationship between elliptocyte shape and thyroid hormone in patients with hypothyroidism accompanied by elliptocytosis. We report the effect of thyroid hormone on ovalocyte shape in a rare case of primary hypothyroidism due to chronic thyroiditis associated with elliptocytosis and anemia, in which serum thyroid hormone levels could affect not only anemia but also the shape abnormality of elliptocytes.

Case Report

A 75-year-old woman was referred to our clinic for general fatigue and edema in 1998. She was pointed out elliptocytosis at the age of 62 year, when Hb and serum biochemistry data were normal. She was diagnosed as primary hypothyroidism at the age of 68 yr, when she was treated with levothyroxine sodium (25 μg/day, Thyradin S®, Teikoku Zouki, Tokyo). However, the treatment was discontinued after 6 weeks since serum transaminase levels were increased. Nobody in her family had jaundice or anemia.

Physical examination revealed that she was 141.4 cm tall and weighed 49.0 kg. Blood pressure was 138/70 mmHg. Her skin was dry and palpebral conjunctiva was anemic. Goiter was not palpable. There was no considerable abnormality in the chest and the abdomen.

Laboratory data are shown in Table 1. Decreased serum thyroid hormone levels associated with increased serum TSH and positive anti-microsome antibody indicated primary hypothyroidism due to chronic thyroiditis. Macrocytic hyperchromic anemia and

increased reticulocyte count were recognized. Serum indirect bilirubin and lactate dehydrogenase (LDH) levels were increased and serum haptoglobin was not detected. Although these findings suggest hemolytic anemia, both serum direct and indirect Coombs tests were negative. Ham test, sugar water test and self-hemolysis tests were negative. Glucose-6-phosphate dehydrogenase (G-6-PD) activity of erythrocytes was decreased. Serum vitamin B12 and folic acid levels were within the normal range. Anti-intrinsic factor antibody and anti-parietal cell antibody were negative. Bone marrow aspiration revealed erythroid hyperplasia but not bone marrow dysplasia in the present case. Chromosome analysis showed normal female karyotype. Occult blood in stool was negative.

Clinical course was shown in Fig. 1. In 1995, serum T3 levels were within the normal range, but serum TSH levels were increased, indicating latent primary hypothyroidism. In 1998, serum T3 and T4 levels were remarkably decreased with increased serum TSH levels, indicating apparent primary hypothyroidism. Hb concentrations were decreased when serum T3 and T4 levels were lowered. The replacement therapy with liothyronin sodium (10 - 20 μg/day, Thyronamin®, Takeda, Osaka) was started after her admission in 1998, followed by treatment with levothyroxine sodium (25 - 75 μg/day). Then, euthyroid state was maintained by levothyroxine at the dose of 75 μg/day.

Serum indirect bilirubin and LDH levels were normalized after the thyroid hormone replacement. Hb levels were corrected promptly whereas mean cell volume of erythrocytes (MCV) was gradually decreased to the normal range. Elliptocytosis of oval form (OH) and of rod form (RF) was persisted and the ratio of OH to RF was not changed by the treatment with levothyroxine. Although elliptocytes with the central pale indicating the central hollow were not recognized before the treatment, the percentage of the elliptocytes with the central pale was increased to 37.4±2.6% (mean±SD). These findings suggest that serum thyroid hormone levels may contribute to the morphological abnormality of the erythrocyte in the present case.

Materials and Methods

Blood samples were obtained into the anti-coagulant-treated tubes from the patient two weeks after stopping the treatment with levothyroxine. Control blood samples were also obtained from an age-matched normal female subject. Their serum thyroxine levels were 42 nmol/L and 132 nmol/L, respectively. Levothyroxine sodium was dissolved in 0.01M NaOH followed by neutralizing with 0.01M HCl. The levothyroxine sodium solution was diluted with the same solution to become their final volume of 10 μl. The solution of NaOH and HCl was used as control solution. Blood samples (2 ml) were added with levothyroxine sodium solution or a vehicle, and then incubated at 37°C for 3 hr. Their final concentrations of thyroxine were 42 nmol/L, 170 nmol/L and 1,322 nmol/L, respectively. Blood samples (2 ml) of a normal subject were also incubated in the presence of 132 nmol/L, 260 nmol/L and 1,412 nmol/L, respectively.

After the incubation, all the blood samples were immediately smeared on a slide glass, and stained with May-Giemsa staining. The morphological changes and the number of elliptocytes were examined at random by 5 different hematologists. The morphological changes were scored and analyzed by ANOVA. $P<0.05$ was considered significant.

Results

Blood erythrocytes consisted of elliptocytes with oval form (OF) and those with rod form (RF) in the patient as shown in Fig 2A. The ratio of OF to RF was averaged 7.22±0.28. The central pale indicating central hollow was hardly found in the erythrocytes of the patient. In contrast, all the blood erythrocytes consisted of round form with central pale in a normal subject (Fig. 2B). After the incubation with levothyroxine at the concentration of 42 nmol/L (Fig. A-1), 170 nmol/L (Fig. A-2) and 1,322 nmol/L (Fig. A-3), the ratio of OF to RF was not considerably changed. It was noted that the percent of elliptocytes with central pale was remarkably increased in blood samples of the patient after the incubation with levothyroxine at the concentration of 170 nmol/L and 1,322 nmol/L (32.6±3.8% and 60.1±6.7% vs 11.0±3.1%, $P<0.0001$ and $P<0.0001$) (Fig. 3). The percentage of the elliptocyte with central pale (Y) was close related with logarithmic values of blood thyroxine levels (X) ($Y=32.6X-41.1$, $r=0.999$, $P=0.0246$). In contrast, any morphological change was not found in the normal erythrocyte after the incubation with different doses of levothyroxine.

Discussion

We reported a rare case of primary hypothyroidism associated with elliptocytosis. In the present case, macrocytic anemia evaluated by increased MCV was recognized. In general, hypothyroidism induced normocytic normochromic [1,2]. Therefore, we could consider that microcytic hypochromic anemia associated with iron deficiency and macrocytic hyperchromic anemia associated with vitamin B12 or folate deficiency have been occasionally found in patients with hypothyroidism. Furthermore, there are some reports on autoimmune hemolytic anemia accompanied by chronic thyroiditis [3-7]. However, as iron deficiency, vitamin B12 deficiency, folate deficiency and autoimmune hemolytic anemia could be ruled out by laboratory data, we considered that elliptocytosis was hereditary and could partly affected by thyroid hormone deficient state in the present case.

We found the elliptocyte shape judging from changes of MCV and central pale was changed by L-T4 replacement therapy *in vivo* and *in vitro*. It was reported that hypothyroid state resulted in abnormal surface in red blood cells [8-10]. Glucose-6-phosphate dehydrogenase activity was decreased [11], and Na, K-pump activity was increased [12] in hypothyroidism. Glucose-6-phospate dehydrogenase activity of RBC was decreased in the present case. Therefore, elliptocyte cell surface abnormality due to hypothyroidism could partly contribute to change of elliptocyte

Table 1: Laboratory Data

CBC					
	WBC	3.2x10⁹/L		BUN	5.36 mmol/L
		Seg 49%		Crea	53.0 µmol/L
		Eos 1%		Na	143 mmol/L
		Lymph 45%		K	3.9 mmol/L
		Mono 5 %		Cl	109 mmol/L
	RBC	2.64 x 10¹²/L		Ca	2.25 mmol/L
		MCV 103.4 fL		Fe	15.0 µmol/L
		MCH 36.0pg		TIBC	46.7 µmol/L
		MCHC 348g/L		Glucose	6.11 mmol/L
		Poikilocyte (+)		HbA1c	5.0 %
		Elliptocyte (+)		Vit B12	268 pmol/L
		Reticulocyte 2.2%		Folate	22.0 nmol/L
	Hb	95 g/L		G-6-PD	179 IU/10¹²RBC
	Ht	27.3 %			
	Plt	169 x 10⁹/L	**Thyroid function**		
				T3	1.1 nmol/L
Urinalysis				Free T4	50 nmol/L
	pH	7.0		TSH	97.3 mU/L
	Pro	(-)		Anti-microsome	Ab x400
	Glu	(-)		Anti-thyroglobulin	Ab <x100
	Blood	(-)			
	Bil	(-)	**Immunology**		
	Uro	(±)		Direct Coombs	(-)
	Sediment	normal		Indirect Coombs	(-)
				Anti-nuclear antibody	Diffuse x160
Biochemistry				Anti-intrinsic factor Ab	(-)
	TP	74 g/L		Anti-parietal cell Ab	(-)
	Alb	46 g/L			
	T.Bil	25.6 µmol/L	**Hemolysis test**		
	D.Bil	3.4 µmol/L		Ham test (-)	
	I.Bil	22.2 µmol/L		Sugar water test (-)	
	GOT	0.85 µkat/L		Self hemolysis test (-)	
	GPT	0.67 µkat/L			
	CPK	2.90 µkat/L	**Bone marrow**		
	ALP	3.27 µkat/L		NCC	281 x10⁹ /L
	LAP	0.63 µkat/L		M/E ratio	0.97
	LDH	4.52 µkat/L		Erythroid hyperplasia	(+)
	r-GTP	0.52 µkat/L		Dysplasia	(-)
	ChE	4.85 µkat/L			
	T.Cho	3.72 mmol/L	**Chromosome**		
	TG	0.99 mmol/L		46XX, normal karyotype	

shape. Several observations suggested primary defect of the membrane skeleton in elliptocyte is the protein scaffolding in the cell membrane. Spectrin is the major component of the membrane skeleton in erythrocyte, and may partly contribute to formation of central pale. Spectrin extracted from elliptocyte is quantitatively normal but is structurally abnormal [13]. Major portion of the spectrin extracted from elliptocyte is presented as dimer [14]. However, it is unknown that thyroid hormone affects to spectrin structure in elliptocyte, and we could not evaluate spectrin structure in the present case.

Serum LDH and indirect bilirubin levels were increased in the Present case. These findings could be partly explained by existence of latent hemolysis. The morphological abnormality of red

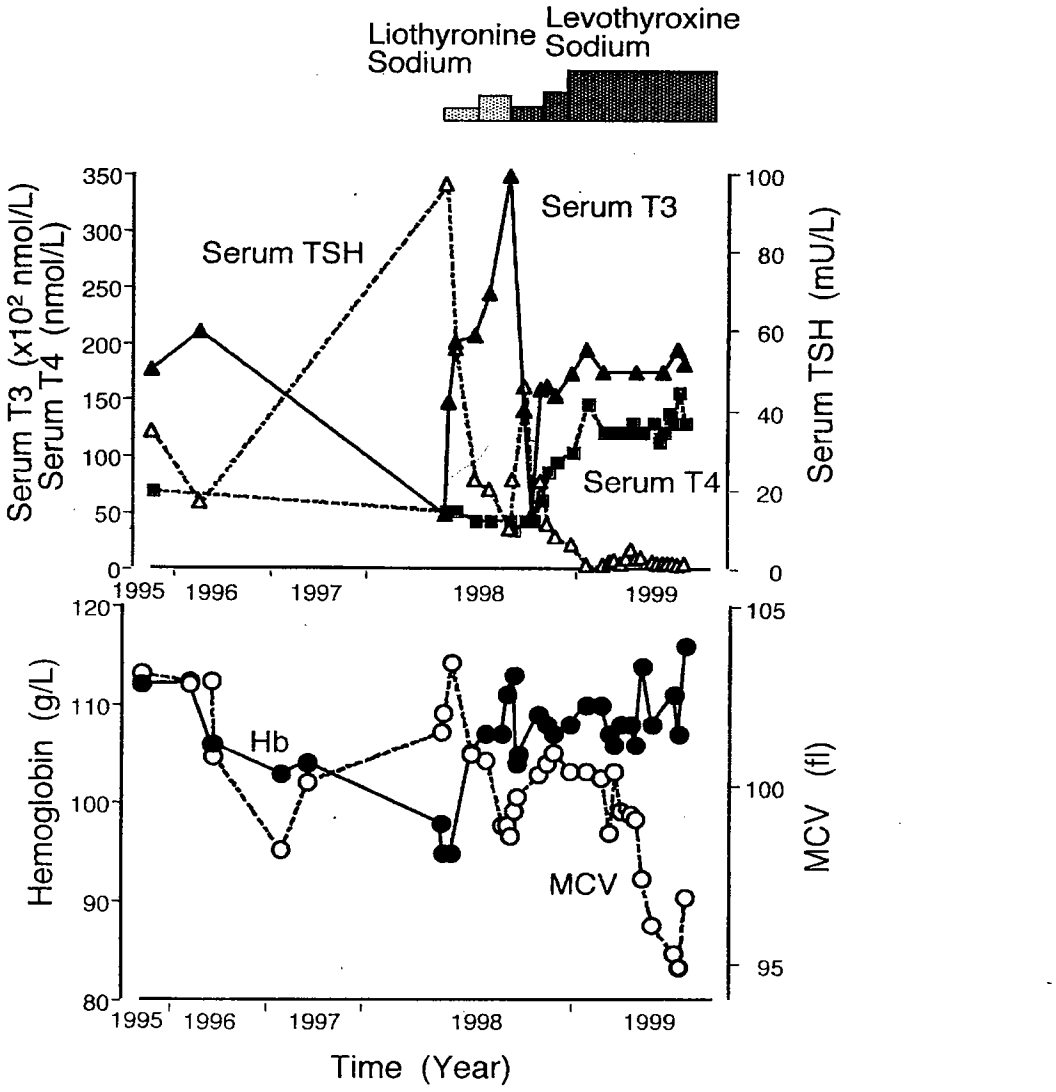

Fig. 1 *Clinical course of a patient with chronic thyroiditis associated with elliptocytosis and anemia. The upper panel shows serum T3 levels (closed triangle) and T4 (closed square) and TSH levels (open triangle). The lower panel shows Hb concentrations (closed circle) and MCV of erythrocytes (open circle) during the treatment with thyroid hormones.*

blood cells may cause hemolysis. Hereditary spherocytosis causes a common hemolytic anemia due to morphological abnormality of red blood cells. On the other hand, elliptocytosis is much more rare than spherocytosis. Elliptocytosis has various grade of ellip tocyte shape of oval form and rod form [15]. However, the relationship between elliptocyte shape and clinical severity is unclear. After the start of replacement of L-T4, serum LDH and bilirubin levels were normalized, suggesting that latenthemolysis was improved. Therefore, occasionally increased serum LDH levels and bilirubin before the replacement therapy might be derived from hemolysis based on elliptocytosis.

In conclusion, we reported a rare case of chronic thyroiditis asso ciated with and anemia. The replacement with thyroid hormones improved anemia and increased the percentage of blood elliptocytes with central pale *in vivo* and *in vitro*. These findings suggest that thyroid hormone levels could contribute to the morphological change of elliptocytes, closely related to anemia in the present case with primary hypothyroidism.

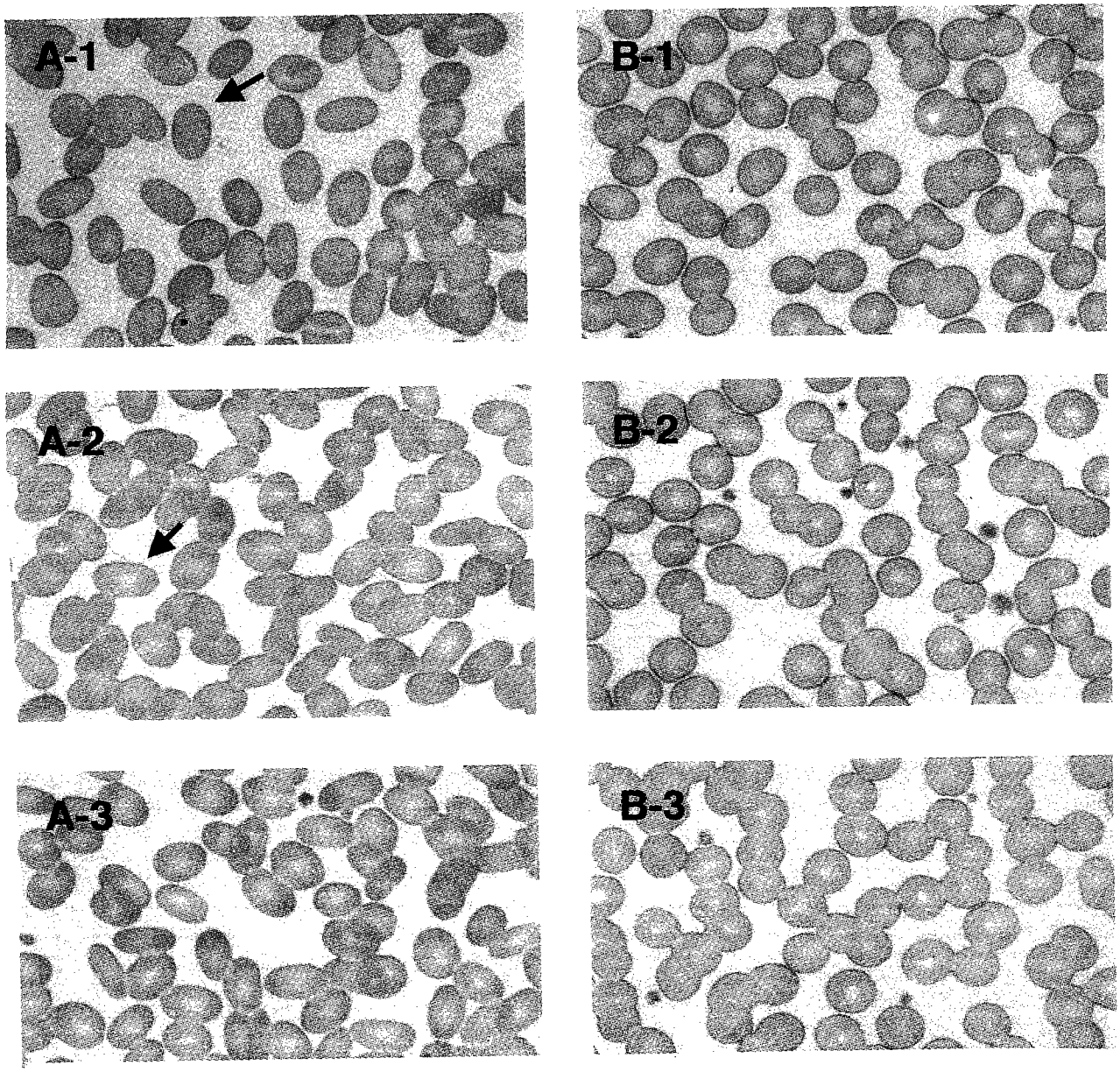

Fig. 2. *Morphological changes of blood erythrocytes incubated with different concentrations of thyroxine. May-Giemsa staining (x1,000) of blood smear is shown. Erythrocytes were obtained from the patient with primary hypothyroidism (A) and a normal control subject (B) and incubated with different concentrations of thyroxine for 3 hr. Elliptocyte without central pale of oval form and of rod form are exclusively found in the patient blood samples incubated without adding thyroxine (thyroxine levels of 46 nmol/L)(A-1). The arrows in Fig. A-1 and -2 showed representative elliptocyte of oval form without or with central pale, respectively. Percent of elliptocytes with central pale are increased in the patient blood samples after the incubation in higher thyroxine levels (A-2; 170 nmol/L, A-3; 1,322 nmol/L). Normal erythrocytes are not morphologically affected by thyroxine levels (B-1; 132 nmol/L, B-2; 270 nmol/L, and B-3; 1,412 nmol/L).*

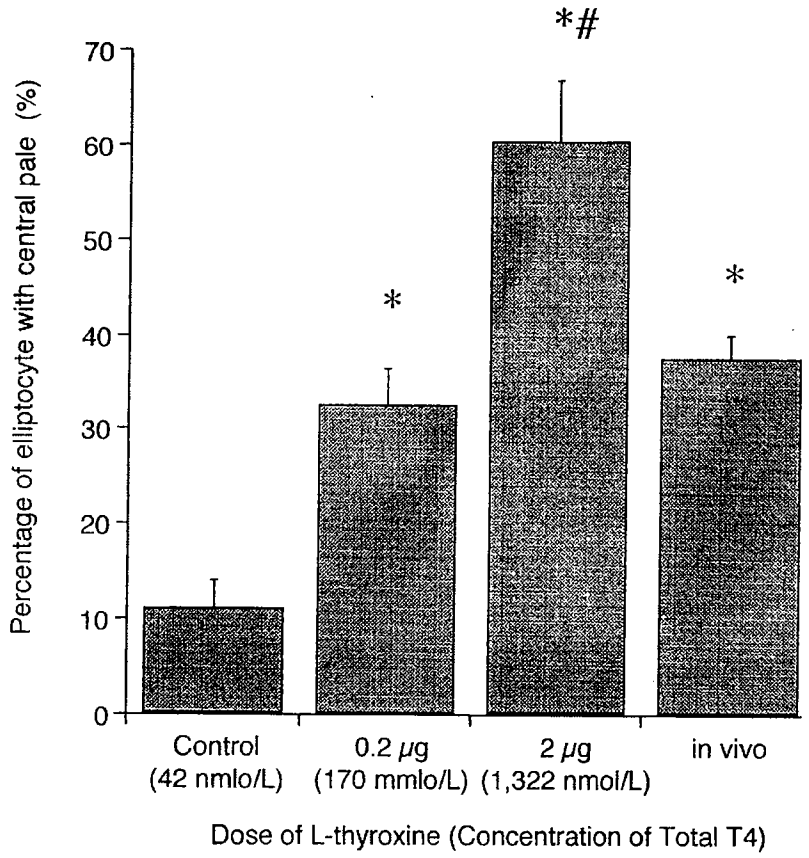

*Fig. 3. Effects of the short incubation with different thyroxine levels on the percentage of elliptocytes with central pale in a patient with primary hypothyroidism and anemia. Mean±SD values are shown. *: P<0.0001 vs control (42 nmol/L). #: P<0.001 vs control and 170 nmol/L.*

Acknowledgments

This work was supported in part by grants from the Ministry of Education, Science and Culture, Japan, and the Ministry of Health and Welfare, Japan. We are indebted to Mrs. Akiko Kawakami and Mrs. Akiko Kanayama for technical help and secretarial assistance, respectively.

References

1. Dawson MA, Yarbro JW. Anemia in hypothyroidism. South Med J 1970; 63: 966-970.
2. Fein HG, Rivlin RS. Anemia in thyroid disease. Med Clin North Am 1975; 59: 1133-1145.
3. Bouchou K, Andre M, Cathebras P, Klisnick A, Schmidt J, Aumaitre O, Rousset H. Thyroid disease and multiple autoimmune syndromes. Clinical and immunogenetic aspects apropos of 11 cases. Rev Med Interne 1995; 16: 283-287.
4. Feld S, Landau Z, Gefel D, Green L, Resnitzky P. Pernicious anemia, Hashimoto's thyroiditis and Sjogren's in a woman with SLE and autoimmune hemolytic anemia. J Rheumatol 1989; 16: 258-259.
5. Iwasaki Y, Kinoshita M. Ocular myasthenia gravis associated with autoimmune hemolytic anemia and Hashimoto's thyroiditis. Am J Ophthalmol 1989; 107: 90-91.
6. Roberts L, Seemungal T, Patrick A, Barton E. Renal acidosis, thyroiditis, hemolytic anemia: an autoimmune link? South Med J 1992; 85: 446-447.
7. Yoshida EM, Nantel SH, Owen DA, Galbraith PF, Dalal BI, Ballon HS, Kwan SY, Wade JP, Erb SR. Case Report: a patient with primary biliary cirrhosis and autoimmune hemolytic anemia. J Gastroenterol Hepatol 1996; 11: 439-442.
8. Leone NT, Narasimhan P, Watson-Williams EJ. Hypothyroidism and atypical spherocytic hemolytic anemia with high sodium, low potassium red cells. J Clin Endocrinol Metab 1971; 33: 548-550.
9. Nomura S, Eimoto T, Osawa G, Yawata Y, Horino M. Case report: Hypothyroidism as a possible cause of an acquired reversible hemolytic anemia. Am J Med Sci 1991; 302: 23-27.
10. Wardrop C, Hutchison HE. Red-cell shape in hypothyroidism. Lancet 1969; 1: 1243.
11. Viherkoski M, Lamberg BA. The glucose-6-phosphate dehydrogenase activity (G-6-PD) of the red blood cells in hyperthyroidism and hypothyroidism. Scand J Clin Lab Invest 1970; 25: 137-143.

12. DeLuise M, Filler JS. Status of the red cell Na, K-pump in hyper and hypothyroidism. Metabolism 1983; 32: 25-30.
13. Cohen, C.M. The molecular organization of the red cell membrane skeleton. Semin Hematol 1983; 20: 141-158
14. Coetzer T, Zail S. Spectrin tetramer-dimer equilibrium in hereditary elliptocytosis. Blood 1982; 59: 900-905.
15. Lee GR, Bithell TC, Foerster J, Athens JW, Lukens JN. Wintrobe's clinical hematology (ninth edition), Lea & Febiger, Philaderphia 1993; pp.972-976.

Correspondence:

Dr. Motoi Sohmiya
Department of Endocrinology, Metabolism
and Hematoloical Oncology
Shimane University School of Medicine
Izumo 693-8501
Japan.

Phone: +81-853-23-2111
Fax: +81-853-23-8650
e-mail: motoi@med.shimane-u.ac.jp

Biomedical Research 2004; 15 (2): 92-95

Comparison of two different regimens of levothyroxine/iodine combination therapy for endemic goiter

Ali Maeed Al-Shehri

Department of E.N.T,King Khalid University, College of Medicine, Abha, Saudi Arabia

Key words: iodine deficiency – endemic goiter

Acepted July 1, 2004

Abstract

The prospective study investigates the differences of two levo-thyroxine/iodide combinations (thyroxine:iodine 1:1 vs. 1:2) with regard to reduction of thyroid gland size, iodine secretion, thyroid hormone parameters and side effects. Two groups of non-treated patients with euthyroid iodine-deficiency goiter were randomized, one group received a fixed combination of 100 µg levothyroxine + 100 µg iodine, the other 75 µg levothyroxine + 150 µg iodine for a period of 6 months. Efficacy was assessed by the change in ultrasonographic size of the thyroid gland. Secondary parameters included iodine secretion, basal thyroid-stimulating hormone, bound thyroxine, free thyroxine, bound triiodothyronine and the free triiodothyronine. Under the 1:2 combination reduction in size of thyroid gland was observed as 22% while it was 17% under the 1:1 combination which was not significant. Urinary iodine excretion was found significantly raised in both the groups by 86.5% and 74.8% respectively. TSH suppression was found less under the 1:2 combination (48.9% vs. 63.3% P= 0.011) which contained 25% less hormone but the effect was comparable.

Introduction

Iodine is one f the essential elements required for normal human growth and development. Its daily per capita requirement is 150 micrograms. Deficiency of iodine in the diet may result in the development of goitre and other iodine deficiency disorder (IDD) including physical and mental retardation and endemic cretinism. More than 13% of the world's population suffer from one or the other form of iodine deficiency disorder while 1.572 billion population is estimated to be at risk of developing iodine deficiency. Approximately 655 million population living in 118 countries have endemic goitre and about 12 million suffer from endemic cretinism (WHO/UNICEF/ICCIDD 1993) [1,2].

The endemic goiter is a descriptive diagnosis, and is generally considered to be due to insufficient iodine supply in nutrition. Iodine is an essential substrate in the synthesis of the thyroid hormones T4 and L-triiodothyronine (T3). The normal human thyroid gland releases about 65 µg of hormonal iodine to the circulation per day, which is the minimum daily requirement of iodine, whereas iodine intake is considered adequate when it is between 100 and 200 µg/day. In nonendemic areas, the urinary iodine level is at least 100 µg/l. A severe iodine deficiency is considered to occur with a daily iodine excretion of less than 20 µg/l, a moderate deficiency, 20 to 49 µg/l, and a mild deficiency, 50 to 99 µg/l [3,4]. The prevalence of endemic goiter varies with the severity of the iodine deficiency.

Endemic goiter is the end-result of physiological and morphological changes in the thyroid gland as adaptation to an insufficient supply of dietary iodine. When the iodine intake is low, thyroid hormone synthesis is impaired. Mobilization of local regulatory mechanisms, e.g. the release of growth factors like tissue growth factor-ß (TGF-ß) or endothelial growth factor (EGF), lead to hyperplasia of the thyreocytes, and the increased release of the thyroid stimulating hormone (TSH) leads to a hypertrophy of the thyreocytes, too. In a chronic iodine deficiency, the follicles become inactive and distended with colloid accumulation. These changes persist into adult life, and focal nodular hyperplasia may develop to nodule formation.

The final objective of correction of iodine deficiency is not only to increase the access of the population to iodized salt and to normalize the urinary iodine concentration, but mostly to normalize thyroid size and function tests. Only the application of iodine can supply the intrathyroidal iodine deficiency so as to affect hypertrophy and hyperplasia of the thyreocytes. On the other hand the application of iodine alone in adults (others than in children) is critical, as there is need for a higher dosage with the risk of hyperthyroidism and appearance of TPO antibodies [5]. Therefore

combinations of levothyroxine and iodide are favorized, as numerous studies proved a higher efficacy for combination preparations as for levothyroxine resp. iodide alone [5,6,7].

The present prospective study shall determine the efficacy and compatibility of two commonly applied combinations of levothyroxine and iodine to normalize thyroid function, both preparations characterized by different combination ratios (thyroxine : iodine 1:1 vs. 1:2). Differences were analyzed with regard to the development of the thyroid gland size, iodine secretion, and thyroid hormones.

Patients and Methods

The study was conducted as a prospective, randomised, verum-controlled multi-center study in the Region of Bonn (Germany). People measuring the goitre volume were blinded to the experimental treatment. All patients as well as the local ethic commission submitted their agreement to the study.

Between 1998 and 2000, the data of all patients, who underwent general endocrinological diagnostic measures, were checked for the criteria of endemic goiter. Patients with nodule formations, autonomous areas, as well as those with medical pre-treatment were excluded. Patients, who's data matched the criteria, were assigned to a random list for the two treatment groups.

Each group was treated over a period of six months. The patients were instructed to take their medicament every morning half an hour before breakfast. One group (group A) received a fixed combination of 100 µg levothyroxine + 100 µg iodine (Jodthyrox®), the other (group B) a fixed combination of 75 µg levothyroxine + 150 µg iodine (Thyronajod®).

All patients underwent clinical examination and evaluation of medical history before and after six months of therapy. For the assessment of tolerability, TPO antibodies, undesired adverse reactions, reasons for abandonment of treatment, clinical findings and patient's assessment were specified.

The primary parameter for efficacy was the variation of ultrasonographic volume of the thyroid gland. The ultrasonographic volume of the thyroid gland was determined in real-time sonography with a Siemens, Sonoline Elegra, 7.5 MHz ultrasound assembly according to the method of Brunn [8].

Secondary parameters were variations in concentrations of urinary iodine, basal thyroid stimulating hormone (TSH), TSH after thyroid releasing hormone (TRH), bound thyroxine (TT4), free thyroxine (FT4), bound triiodothyronine (TT3), and free triiodothyronine (FT3). Basal TSH (standard: 0.3 - 4 mU/l), FT4 (standard: 11-23 pmol/l) and FT3 (standard: 3.4-7.6 pmol/l) were quantified with commercially available validated enzymatic or radioimmunoassay. The iodine concentrations in casual urine were determined with high-pressure liquid chromatography (HPLC).

Statistical analysis was based on all randomized patients. Differences to initial values were tested as conjoint samples with the Wilcoxon-Test, in the comparative check the Mann-Whitney-Test was used. The level of significance was assessed at $\alpha = 0.05$ bidirectional. As there was no adjustment of the probability value for the multiplied secondary parameters, only the statistical analysis of the variation of the thyroid gland volume as primary parameter was evidentiary. Concerning TSH only the difference of the logarithms were used as test values, as only in these cases there is a linear dose-effect relationship to thyroxine as approximatively equivalent to percentual reduction.

Results

Table 1 shows the demographic data of the patients involved in the study. 104 patients took part in the study, and none of them abandoned treatment. 65 % of the patients were female with a median age of 36 years (18 to 78 years) in both groups. There was no statistical difference in height in both groups (men: 182.9 $\pm$ 7.4 in group A, 181 $\pm$ 7.4 in group B; women: 169.4 $\pm$ 7.1 in group A, 167.7 $\pm$ 6.7 in group B), but there was a statistical significant difference between both groups concerning the weight of the men (90.3 $\pm$ 14.2 in group A, 79.6 $\pm$ 12.4 in group B), whereas there was no statistical difference concerning the weight of the female patients (72.2 $\pm$ 14.9 in group A, 73.4 $\pm$ 11.4 in group B). Seven patients of group B mentioned additional medication: one patient took insulin and furosemid, one metoprolol and cumarin, one more patient took magnesium, one amlodipin, two ibuprofen, and one propranolol. In both groups one third of the women used estrogene preparations.

70 % of the patients complained of neck disturbances. In only 2 % of the patients goiter was primarily diagnosed, whereas in 98 % of these untreated patients there was a history of goiter with no statistical difference between the two groups.

Before therapy the ultrasonographic volume of the goiter was between 18 and 78 ml with a median of 30 ml, and there was no statistical difference between both groups. Thyroid hormones (basal TSH, FT4, TT3, urine iodine) in the beginning of the study showed no statistical differences between both groups either (Table 2). The data for TSH after TRH, TT4 and FT3 were incomplete and could not be analyzed.

After six months of treatment the thyroid volume had decreased in both groups with a high statistical significance (Fig. 1). Within group A there was a reduction of 5 ml (median) or 16.5 % respective, with an arithmetic mean of 17.7 %. Within group B there was a reduction of 6 ml (median) or 20.3 %, with an arithmetic mean of 22 %. There was no significant difference between the results of both groups.

In both groups urine iodine as an indirect parameter of the thyreoidal iodine supply had increased significantly. Within group A there was an increase of iodine secretion of 36 ng/g creatinine (median) or 46 % (arithmetic mean: 74.8 %). As expected, within group B the increase of iodine secretion was much higher with 61 ng/g creatinine (median) or 65 % (arithmetic mean: 86.5 %), and there was a significant difference between both groups (group A: $p = 0.013$, group B: $p = 0.001$).

Table 1: Demographic Data of all patients before therapy (mean ± standard deviation; m = male, f = female)

	Group A	Group B
gender (p=0.83)	19 (m) / 32 (f)	17 (m) / 36 (f)
age (years) (p=0.98)	36.8 ± 9.2	36.2 ± 7.1
Height(cm)(p=0.45)	182.9 ± 7.4 (m)	181.0 ± 7.4 (m)
(p=0.37)	169.4 ± 7.1 (f)	167.7 ± 6.7 (f)
Weight(kg)(p=0.05)	90.3 ± 14.2 (m)	79.6 ± 12.4 (m)
(p=0.23)	72.2 ± 14.9 (f)	73.4 ± 11.4 (f)
Broca-Index(p=0.04)	1.09 ± 0.17 (m)	0.98 ± 0.13 (m)
(p=0.23)	1.05 ± 0.20 (f)	0.98 ± 0.13 (f)
sonographic volume of the thyroid gland (ml) (p=0.31)	35.3 ± 15.2	32.3 ± 12.3
history of goiter (months) (p=0.70)	7.5 ± 20.4	4.2 ± 11.0

Table 2: Thyroid hormones before therapy

	Group A	Group B
basal TSH	1.19 ± 0.35	1.34 ± 0.41
FT4	1.30 ± 0.24	1.26 ± 0.23
TT3	1.42 ± 0.25	1.35 ± 0.24
urine iodine	91.8 ± 29.9	102.1 ± 52.4

Basal TSH was reduced below the initial value. Within group A the reduction was 0.70 mU/l (median) or 70.0 % (arithmetic mean: 63.3 %), within group B the reduction was 0.68 mU/l (median) or 56.3 % (arithmetic mean: 48.9 %). The difference of the logarithms in relation to the initial values was significant in both groups as well as the difference between the two groups (p = 0.011).

The increase of FT4 within group A was 0.20 ng/dl (median) or 15.4 % (arithmetic mean: 16.4 %), within group B 0.20 ng/dl (median) or 11.5 % (arithmetic mean: 15.1 %). The difference in relation to initial values was significant in both groups, whereas there was no difference between the groups.

Concerning TT3, only data of 36 patients in each group (72 %) were available, statistical analysis is restricted to these data. Within group A the reduction of TT3 was 0.1 µg/l (median) or 6.0 % (arithmetic mean: 1.3 %), within group B 0.1 µg/l (median) or 8.0 % (arithmetic mean: 5.9 %). The difference in relation to initial values was significant in both groups, whereas there was no difference between the groups.

Both prescriptions were tolerated very well. The patient's assessment of therapy was estimated good or very good in 74 % of group A and 82 % of group B (not significant). There was one case in each group which developed TPO antibodies > 35 IU/ml,

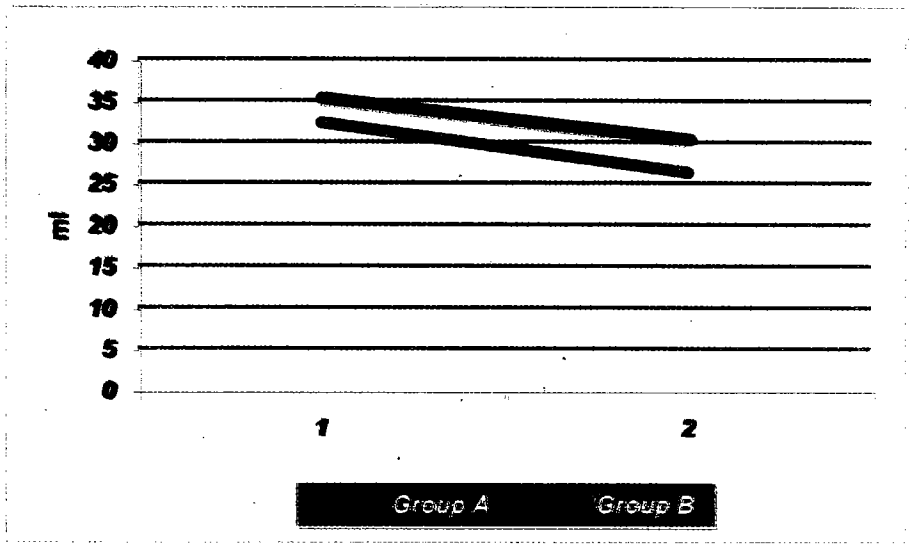

Fig. 1: Sonographic volume (mean volume) of the thyroid gland before (1) and after (2) 6 months of therapy

but below 100 IU/ml during treatment. There were no severe adverse reactions and no abandonment of treatment. After six months of treatment there was one case of occasional tachycardia in group B, whereas there were 10 cases with these complaints in group A. There was no case of increased defecation in group B, but 6 cases in group A. The differences in clinical effects were statistical significant.

Discussion

Prescriptions of hormone-iodide-combinations for the treatment of euthyroid goiter have increased in recent years. The present prospective study compared two commonly applied combinations of levothyroxine and iodine, characterized by different combination ratios (thyroxine : iodine 1:1 vs. 1:2). The intention of the development of the 1:2-combination was to avoid a too intense suppression of TSH and to keep or increase the level of iodine concentration in the thyroid gland. The application of thyroxine in TSH suppression dosages is supposed to decrease osseous density in post-menopausal women [9,10], and to increase the incidence of tachycardia or atrial fibrillation. Although these side effects until now are not proved as facts [11], a total TSH suppression should be avoided, as a too intense suppression of TSH anticipates thyroidal iodine uptake [12].

In everyday practice reduction of the thyroid volume is the main criterion to estimate the success of therapy. The thyroid volume decreased in both groups significantly with the efficacy of the 1:2 combination similar to that of the 1:1 combination. The result of this study is in accordance with previous studies, especially with a study on more than 200 patients treated with the same 1:2 combination [13], whereas in other studies with different thyroxine/iodine ratios efficacy was lower [14]. However, because of the varieties in study design restrictions to compare the data must be followed. Treatment with the combination of 75 µg levothyroxine and 150 µg iodine was associated with a lower reduction in TSH and higher iodine excretion, which is in accordance with the intention of the preparation. Although this combination preparation contains 25 % less hormone, its efficacy is comparable. But for this preparation, too, it must be taken into account that in case of undesirable TSH suppression the thyroxine dosage still must be consecutively reduced.

Conclusion

It can be concluded that combination therapy had a lower excretion of TSH and higher iodine excretion. To avoid undesirable TSH suppression, the dosage of thyroxine may be reduced.

Recommendation

Such type of prospective comparative studies are recommended to be conducted elsewhere also.

Acknowledgment

I would like to express my gratefull thank Dr. Mohd. Yunus Khan of Family & Community Medicine Department, College of Medicine, King Khalid University for revising this manuscript.

References

1. Dunn JT, Van der Haar F. A practical guide to the correction of iodine deficiency. WHO/ICCIDD/UNICEF, Wageningen, 1990, p 14.
2. WHO/UNICEF/ICCIDD. Indicators for assessing iodine deficiency disorders and their control through salt iodization (document WHO/NUT/94.6). Geneva: World Health Organization, 1994.
3. Stanbury JB, Hetzel B. Endemic goiter and endemic cretinism. New York, Wiley, 1980.
4. Pan American Health Organisation. Scientific publication No 292 and 267, 1974.
5. Koutras DA, Karaiskos KS, Piperingos GD et al. Treatment of endemic goitre with iodine and thyroid hormones, alone or in combination. Endocrinol Exp, 1986, 20: 57-65.
6. Hintze G, Emrich D, Köbberling J. Treatment of endemic goitre due to iodine deficiency with iodine levothyroxine or both: results of a multicenter trial. Eur J Clin Invest, 1989, 19: 527-534.
7. Benson K, Hartz AJ. A comparison of observational studies and randomized, controlled trials. N Engl J Med, 2000, 342: 1878-1886.
8. Delange F, Bastani S. Benmiloud M.: Definitions of endemic goiter and cretinism, classification of goiter size and severity of endemias, and survey techniques. In: Dunn JT, Pretell EA, Daza CH, et al. (Eds.): Towards the eradication of endemic goiter, cretinism and iodine deficiency (no.502). Washington, DC: Pan American Health Organization, 1986, 373-375.
9. Novack DV. TSH, the bone suppressing hormone. Cell, 2003, Oct 17; 115(2): 129-130.
10. Knudsen N, Faber J, Sierbaek-Nielsen A, Vadstrup S, Sorensen HA, Hegedus L. Thyroid hormone treatment aiming at reduced, but not suppressed, serum thyroid-stimulating hormone levels in nontoxic goitre: effects on bone metabolism amongst premenopausal women. J Intern Med, 1998; 243: 149-154.
11. Hegedus L, Nygaard B, Hansen JM: Is routine thyroxine treatment to hinder postoperative recurrence of nontoxic goiter justified? J Clin Endocrinol Metab, 1999; 84: 756-760.
12. Koc M, Ersoz HO, Akpinar I, Gogas Yavuz D, Deyneli O, Akalin S. Effect of low- and high-dose levothyroxine on thyroid nodule volume: a crossover placebo-controlled tria. Clin Endocrin (Oxf) 2002; 57: 621-628.
13. Meng W, Schindler A, Spieker K, Krabbe S, Behnke N, Schulze W, Blumel C. Iodine therapy for iodine deficiency goiter and autoimmune thyroiditis. A prospective study. Med Klin (Munich) 1999; 94: 597-602.
14. Kreissl M, Tiemann M, Hanscheid H, et al. Comparison of the effectiveness of two different dosages of levothyroxine-iodide combinations for the therapy of euthyroid diffuse goiter. Dtsch Med Wochenschr (Germany) 2001; 126 p227-231

Correspondence:

Dr. Ali Maeed Al-Shehri
Department of E.N.T.
College of Medicine and Health Sciences
King Khalid University
P.O Box 641, Abha
Saudi Arabia

e-mail: namas1@hotmail.com

Biomedical Research 2004; 15 (2): 96-99

Evaluation of cytotoxic activity of new GABA mimetic drugs

Capasso A.°, Saturnino C.°, Buonerba M.*, Rocco F.°, Diversi E.° and De Martino G.°

* Department of Pharmaceutics Sciences, via Ponte Don Melillo, I-84084 Fisciano (Sa), ITALY.
° Department of Sciences and Tecnology of Drugs, via Pietro Giuria 9, I-10125 Torino, ITALY.

Key words: GABA, citotoxicity, anticonvulsive

Accepted February 29 2004

Abstract

GABA (γ-aminobutyric acid) is the main inhibitory neurotransmitter in the central nervous system. The inhibitory action of GABA is mediated by the receptors present on the cell membrane, and results in a reduction of neuronal excitability. It may be useful in the treatment of Huntington's disease, epilepsy and Parkinson's disease [1,3]. The aim of this investigation was to develop a new pro-drug molecules able to increase the uptake of the GABA molecule in the brain, Here we report preliminary pharmacological results of 11 new pirrolidin-2-one derivatives, as potential anti-convulsive drugs.

Introduction

GABA (gamma-aminobutyric) is the most important and abundant inhibitory neurotransmitter in the brain (it's actually an amino acid classified as a neurotransmitter). It helps in due relaxation and sleep. It acts as a "balancer" for the brain where excitation of the brain is balanced with inhibition. In addition to it's positive effect on the nervous system, medical studies have also proven GABA to have many other important positive effects on the body following supplementation [1-4]. First, GABA naturally stimulates the anterior pituitary gland to secrete higher levels of *Human Growth Hormone (HGH)*. Second, studies have shown GABA to improve sleep cycles leading to more restful sleeping and more interesting, vivid dreaming. Third, GABA has shown powerful stabilizing effects on blood pressure.

Finally, research has demonstrated GABA to be a very effective analgesic, eliminating pain from chronic conditions such as arthritis and lower back pain. HGH is a hormone that is widely known for its powerful anabolic (muscle building) effects as well as its lipotropic (breakdown and utilization of body fat) effects [1-4]. The overall result of these effects is an increase in lean tissue mass and a decrease in body fat. The development of new pro-drug molecules able to increase the uptake of the GABA molecule in the brain, is a very important target in this field. Different GABA pro-drugs are reported in literature [4,7]. The aim of this work was to present a new pharmacological study of new pirrolidin-2-one derivatives, as potential anti-convulsive drugs. These compounds, called **N1-N11** (Figure 1), are structural GABA cyclic analogous [8-15] and here we report their preliminary results on the synthesis and on the anticonvulsive activity [16-23].

Materials and Methods

Experimental Session

Pharmacology

Cytotoxic assay: Citoxicity test is based on inhibition of proteic synthesis, that is caused by tested drugs. The drugs are incubated at scalar concentrations in different experimental conditions. Results are reported as percent of proteic synthesis, compared to controls cultures, background values being substrated. It is performed on human cancer cells growing in adherence: HT-29 and Igrov 1.

Mean ^{3}H-leucine incorporation in untreated control cultures is 12.000 cpm for HT-29 and 25.000 for Igrov 1 cells. Evalueting the results, it is evident that IC_{50} values of the different drugs tested are not influenced by time of drug exposure.

The HT-29 are colon-rectal adenocarcinoma cells obtreined from ATCC (ref. N° HTB-38), whereas the Igrov 1 are human ovarian carcinoma cells culture medium containing 10% of fetal cow serum (FCS), glutamine (2mM) and antibiotics (penicillin 100 UI/ml, kanamicyn 100 mg/ml, streptomycin 100 μg/ml).

They are cultivated in thermostat in wet atmosphere at 5% of CO_2 at 37 C°.

In 96 flat bottom wells plates, $3x10^4$ cells/wells are put in a culture volume of 100 μl and they are left to ad there for 3-8 hours in incubator. Meanwhile, diluitions of the substances having final mo-

larity from $1x10^{-3}$ to $1x10^{-9}$ one prepared; the substances are tested in drug scalar concentrations and each point is tripled.

100 µl of each diluition is put in each well. These tests are performed incubating for 24 and 72 hours. Wells are then emptied and 150 µl of RPMI containing a 1 µCi of triziatic leucine (L-[4,5]-leucine, 58Ci/mmols) are added and all is incubated for 16-17 hours. Wells are then emptied, quickly washed using 100 µl of trypsin and incubated for 15 min. at 37°C using 100 µl more of the enzymatic solution.

We perform then the lysis of the ticking up the colture of the cells in order to determine the quantity of marked aminoacid incorporated in the protein. The content of the wells is aspirated, transferred to filter-paper and, once dried it is put in polyten vial adding 3ml of Ready Gel scintillation liquid so as to measure the radioactivity at the β-counter. Results are expressed ad ^{3}H-leucine incorporation referred to the white, in function of the different cytotoxic substances dilutions. Usually, controls present a radioactivity of about 12.000 cpm for the HT-29 and 25.000 cpm for the Igrov1.

Results and Conclusions

Glutamate and gamma-amino butyric acid (GABA) systems are emerging as targets for development of medications for mood disorders [1-4]. The preponderance of available evidence suggests that glutamatergic and GABAergic modulation may be an important property of available antidepressant and mood-stabilizing agents [24]. It is involved in a wide spectrum of physiological functions and behaviours, from sleep and sedation to convulsions. Here we report cytotoxic activity of 3 compounds of a new series of GABA cyclic analogues. Evaluating the results, we can demonstrate that IC_{50} values of the different drugs tested are not influenced by time of drug exposure (Table 1). GABA analogous showed a very low toxicity and further studies are performed towards this direction to identify GABA analogues miming better the functions of this endogenous neurotrasmettiter.

Table 1: IC_{50} values of the N5, N10 and N11 drugs tested

		IC_{50}			
Cell line	Drug Incubation	N5	N10	N11	GABA
HT-29	24 & 72 h	$3.2x10^{-4}$	$3.2x10^{-4}$	$2.5x10^{-4}$	___

		IC_{50}			
Cell line	Drug Incubation	N5	N10	N11	GABA
Igrov 1	24 & 72 h	$3.0 x10^{-4}$	$3.0 x10^{-4}$	$2.5x10^{-4}$	___

In fact future research will be needed to develop and evaluate new agents with specific glutamate and GABA receptor targets in the treatment of mood disorders [1-4].

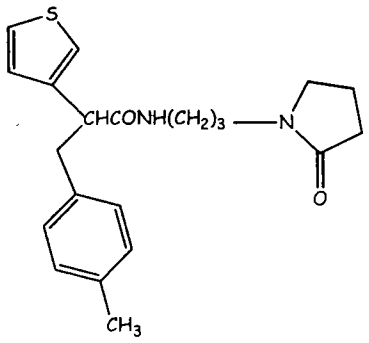

N 1

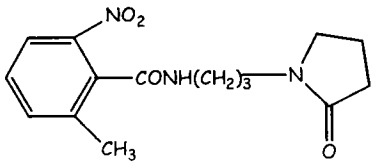

N 2

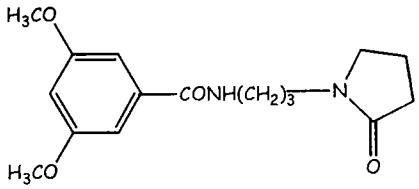

N 3

Fig. 1: Chemical Structure for Compounds **1-3**

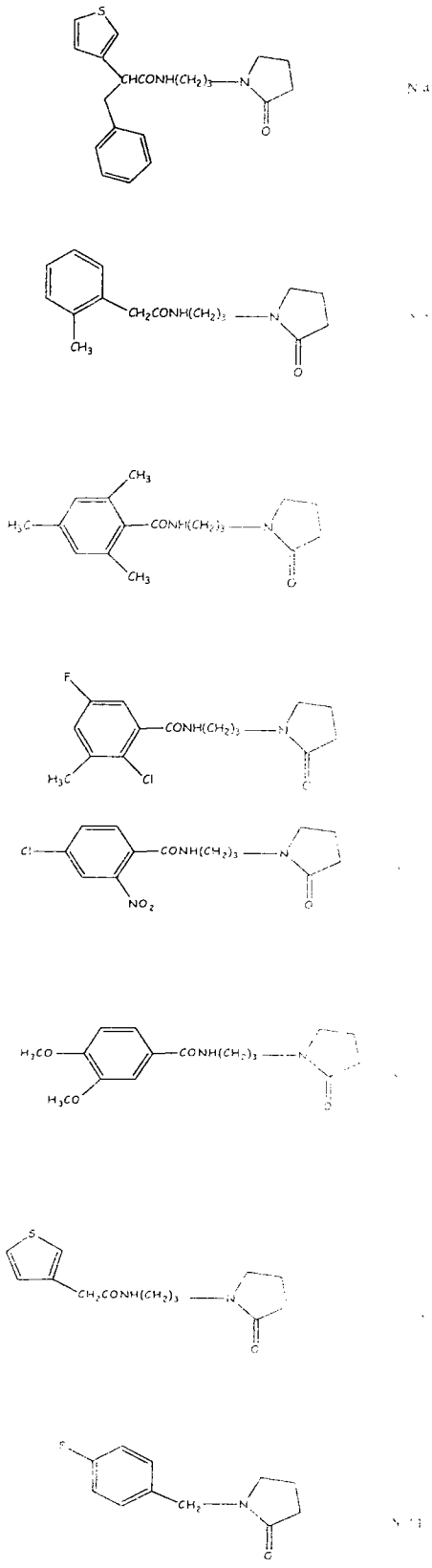

Fig. 2: Chemical Structure for Compounds 4-11

References

1. Amabeoku G.J. and Chikuni O. Effects of some GABAergic agents on quinine-induced seizures in mice. Experientia 1992; 48: 659-662.
2. Bormann J., and Kettenmann H. Patch-clamp study of gamma- aminobutyric acidreceptor Cl channels in cultured astrocytes. Proc Natl Acad Sci U.S.A. 1988; 85: 9336-9340.
3. Bakay R.A.E., Harris A.B. Neurotransmitter, receptor and biochemical changes in monkey cortical epileptic foci. Brain Res 1981; 206: 387-404.
4. Bianchi M, Deana R, Quadro G, Mourier G, Galzigna L. 4-Aminobutyric acid methyl ester hydrochloride, a precursor of 4-aminobutyric acid. Biochemical Pharmacology 1983; 32: 1093-1096.
5. Bodor NS. U.S. Patent 4 824 850. Chem. abstr 1989; 112: 7383 (1990).
6. Bowery NG. $GABA_B$ receptor pharmacology. Annu Rev Pharmacol Toxicol 1993; 33: 109-147.
7. Severre JR, Loiseau P, Couvreur P, Letourneux Y, Gayral P, Renoir JP. J Pharm Pharmacol 1991, 41, 191 Jacob JN 1990, Lambert DM 1993.
8. Enna SJ, Stern LZ, Wasiek GJ, Yamamura HI. Neurobiology and pharmacology of Huntington's disease. Life Sciences 1977, 20: 205-211.
9. Galzigna L, Garbin L, Bianchi M, Marzotto A. Properties of two derivatives of γ\-aminobutyric acid (GABA) capable of abolishing cardiazol- and bicuculline-induced convulsions in the rat. Arch Int Pharmacodyn 1978; 235: 73-85.
10. Jonnston GAR, Mitchell JF. Effect of bicuculline, metrazole, picrotoxin and strychnine on the release of [3H]-GABA [γ-aminobutyric acid] from rat brain slices. J Neurochem 1971; 18: 2441-2446.
11. Kaplan JP, Raizon BM, Desarmenien M, Feltz P, Headley PM, Worms P, Lloyd KG, Bartholini G. New anticonvulsants: Schiff bases of gamma-aminobutyric acid and gamma-aminobutyramide. Journal of Medicinal Chemistry 1980, 23: 702-4.
12. Kelly JS and Beart PM Amino acid in CNS II GABA in supraspinalregions. In, Handbookof Psycopharmacology, Sect. I, Vol.4 Plenum Press, New York, 1975. 129-209. meldrum B.S. Int Rev Neurobiol 1975; 17 : 1.
13. Lloyd KG, Arbilla S, Beaumont K, Briley M, De Montis G, Scatton B, Langer SZ, Bartholini G. Gamma-Aminobutyric acid (GABA) receptor stimulation. II. Specificity of progabide (SL 76002) and SL 75102 for the GABA receptor. Journal Of Pharmacology And Experimental Therapeutics 1982, 220: 672-677.
14. Madrid Y, Langer LF, Brem H, Langer R. New directions in the delivery of drugs and other substances to the central nervous system. Advances In Pharmacology 1991, 22: 299-324.
15. Murray R.J., Schmiesing R.J.: PCT Int. Appl. WO 95 2 23, 135 (1995); Chem. Abstr. (1996), Vol. 124, N° 3, 29607.
16. Nishino N, Hanada S, Mita T, Fujiwara H, Tanaka C, Noguchi-Kuno SA, Ionikawa K. Neurochemical pathology of GABAergic and cholinergic systems in Parkinson disease: an autopsy study. Rinsho shinkeigaku. Clinical neurology 1984, 24: 1029-1035.
17. [illegible] R.W. GABA-benzodiazepine-barbiturate receptor interactions. J Neurochem 1981; 37: 1-13.
18. Quian [illegible] and Dani JE. Novel GABA responses from rod-[illegible] of [illegible] cells. Nature (Lond.) 1993; 361: 162-164.

19. Rubin RP. The role of calcium in the release of neurotransmitter substances and hormones. Pharmacol Rev 1970; 22: 389-428.
20. Reddy P, Armuta H, Bonnie CH, Latifi T, Ferrendelli JA, Covey DF. J Med Chem 1996; Chem Abstr 1996; 124: 21, 277982v.
21. Shashoua VE, Jacob JN, Ridge R, Campbell A, Baldessarini RJ. Gamma-aminobutyric acid esters. 1. Synthesis, brain uptake, and pharmacological studies of aliphatic and steroid esters of gamma-aminobutyric acid. Journal of Medicinal Chemistry 1984; 27. 659-664.
22. Toffano GG., Guidotti A and Costa E. Proc. Natl. Acad. Sci. U.S.A. 1978; 75: 4024-4028.
23. Toffano G, Leon A, Masotti M, Guidotti A. and Costa E. Receptors for Neurotransmitters and Peptide Hormones Pepeu G, Kuhar MJ and Enna SJ (Eds), 1980; 133-142. Raven Press, New York.
24. 24. Krystal J H; Sanacora G; Blumberg H; Anand A. Charney D S; Marek G; Epperson C N; Goddard A; Mason G F Glutamate and GABA systems as targets for novel antidepressant and mood-stabilizing treatments. Molecular Psychiatry 2002; 7: 71-80.

Correspondence:

Professor Anna Capasso
Dipartimento di Scienze Farmaceutiche
Università di Salerno
Via Ponte don Melillo
84084 Fisciano, Salerno
Italy

Phone/Fax 0039-089-964357
e-mail: annacap@unisa.it

Biomedical Research 2004; 15 (2): 100-102

Azetidinone structures: Antibacterial activity

C. Saturnino*, M. Buonerba*, S. Martini°, E.R. Rinaldi°, F. Gorga°, G. De Martino*, A. Capasso*

*Department of Pharmaceutical Science, University of Salerno - Ponte don Melillo, 84084 Fisciano (Salerno) ITALY.
°Institute of Microbiology, II University of Naples, S. Aniello a Caponapoli 2, Naples ITALY.

Key words: Azetidinones, antibacterial, β-lattamic

Accepted March 15 2004

Abstract

Aztreonam, the first monobactam antibiotic to be released, has excellent activity against aerobic and gram-negative bacteria, including *P. aeruginosa*. It is not ototoxic or nephrotoxic and therefore its use is a good alternative in a lot of clinical situations to amino glycosides.. The aim of this preliminary study was to show an antibacterial effect of a new series of azetidinone derivatives, which we synthesized in our laboratory. The antibacterial effect of these compounds exhibited a greater activity than penicillin G, taken as references substance.

Introduction

The monolattamics are a class of β-lattamic antibiotics introduced in therapy in 1980 [1]. The lead compound, the aztreonam (Figure 1), is a simple β –lattamic compound, used in the treatment of the Gram (-) bacteria's infections and often involved in nosocomial infections, particularly in some infections by P. aeruginosa. Its use is useful when there are bacterial resistences to the classical β –lattamic compounds; infact aztreonam is a resistant drug to β-lattamase [2].

Its clinical use includes the treatment of the urinary tract's infections, bronchial airways, septicaemia and cutaneous infections due to Gram (-). It can be used in association with other antibiotic, such as clindamicin, for the treatment of the post-surgery pelvic infections and other pelvic infections [3].

The advantages of the use of aztreonam, in comparison to aminoglucosides, include a reduced ability to penetrate the cerebrospinal liquid, reduced ototoxicity and nefrotoxicity. There is not interference with the coagulation processes and small immunogenicity. A further advantage is its possible use in patients allergic to penicillins and cefalosporines, which show a different mechanism of action [4]. Disadvantages of aztreonam compared to amnoglycosides include the cost of the drug (50 times more expensive than gentamicin), the lack of post antibiotic effect, resistance to P. aeruginosa, and lack of significant activity against Enterobacter cloacae and E. aerogenes. The restricted anti- microbial spectrum of aztrenoam has been proposed as an advantage. Theoretically, this would permit targeting of a gram-negative pathogen with minimal disruption of the (largely anaerobic) intestinal flora. In fact, use of this drug has been associated with colonization of gram positive organism, especially enterococci. Although aztreonam appears to be an excellent antibiotic, its use has been limited by its relatively high cost, narrow spectrum of activity and the availability of numerous alternative agents. On the basis of these considerations, we have prepared some monolattamic [5] antibiotics [6,7] and we have studied their antibacterial activity (Figure 2).

Materials and Methods

Used substances: *Azetidinones –1 2 3 4 5 6.*

Escherichia strains; Citrobacter spp.; Staphylococcus epidermidis; Pseudomonas aeruginosa; Pastaurella multocida (clinical isolation fetters) Pastaurella multocida ***(log ATCC)***

Kirby-Bauer's Method

The substances tested were dissolved in DMSO (dimethylsulfoxid) and were loaded by imbibitions on sterile disks of 6mm of diameter.

The solid medium used for the assay of the sensibilities is the Muller-Hinton with a agar concentration of about 1.5-2%, pH between 7.2 and 7.4, Mg^{++} concentration about to 20-35 mg/litr and 50-100 mg/litr Ca^{++}. The thickness was 4 mms, uniform in the whole plate with the purpose to avoid different diffusion times.

The bacterial inocule had fixed to the 0.5 Mac Farland and protect to a concentration of ~10-8 mycro organisms/mls. In this way it was take with an ansa 4-5 colonies of the examined strain and inoculated in 4-5 mls of broth (Trypticase soy-broth). The suspension was incubated at 35°C until its turbidity reached the fixed standard previously.

Therefore the surface of a Muller-Hinton agar plate was inoculated by a cotton sterile imbibed of culture broth and rotated 60° degree before every series of you crawl in order to assure an uniform distribution for the inoculon on the whole plate.

The sensibility's halos were measured in mm by a caliber in order to outline also including in the survey the diskette.
The results of this studies, reported in Table I, show the sensibility's halos (expressed in mm), related to the tests done at different concentration and in particular at 1200 μg, 1000 μg, 500 μg for each tested substance.

Results and Conclusion

Aztreonam is a synthetic monobactam antibiotic that has excellent activity against aerobic gram-negative bacilli. It can be used as a single agent for the treatment of upper urinary tract infections caused by organisms resistant to the cephalosporins and ampicillin, others byciclic beta lactamic drugs.

Compounds with antibacterial activity are a class of pharmaceuticals that clearly do not share a common mode of action. Further more, there is no "typical" antibacterial pharmaceutical compound, and they are structurally diverse. In fact the pharmacological profile can be attributed to their different chemical proprieties. Anyway, in this preliminary studies it is evident that the compound **1** show a good antibacteric activity especially on Pastaurella at the dose of at 1200 μg, 1000 μg, while it is reduced at 500 μg.

The compound **2** , **3** ,**4** e **6** always show a dose-dependent activity but less than compound **1**.

Compound **2** and **6**, are the only two possessing an inhibing activity on St. aureus.

Structurally the compounds 1-6 show the same azetininone ring on which an nitrogen's atom brings an aromatic ring variously replaced; evaluating the results it seems that compound **1** is the best in this series, in fact may be that the presence of an alchylic chain on the aromatic ring which divided the amidic function from the other one acid, play a key role for its activity.

Further studies are performed towards this directions in order to identify other analogues having a better activity and a wide range of use.

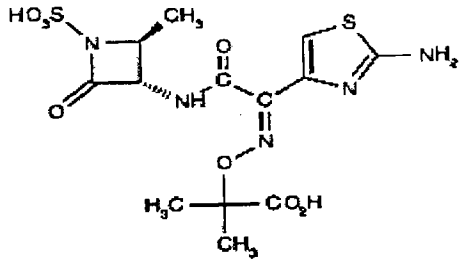

Fig. 1: Chemical Structure for AZTREONAM

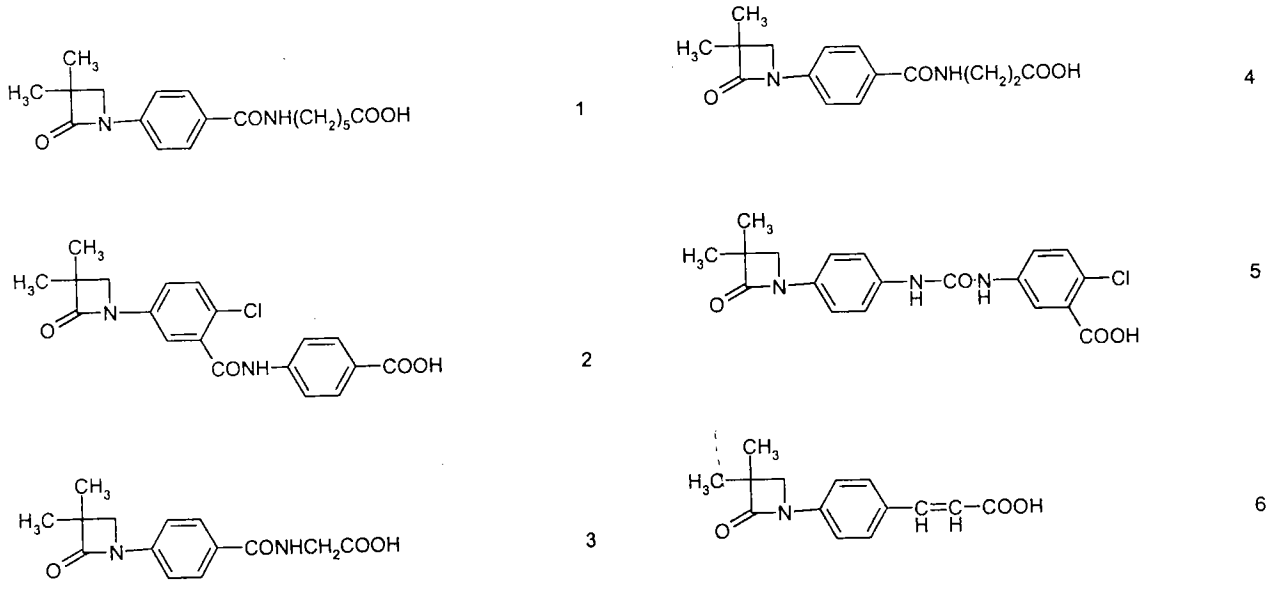

*Fig. 2: Chemical Structure for monolattamic antibiotics **1-6***

Table i: The table indicate the haloes (expressed in mm) of sensibility related to the tests done at concentrations of 1200 µg, 1000 µg, 500 µg, for each tested substance

1200µg	*E. colii*	*Citrobacter*	*St. epid.*	*Pasteurella*	*St. aureus*	*P. auruginosa*
1	3	1.6	0	3.5	0	0
2	0	1	0.9	2.7	1.2	0
3	2	1.1	1.15	1.8	0	0
4	1.8	1.25	1.22	1.19	0	0
5	0	0.8	0	0	0	0
6	1.2	1	0.9	0	0	0

1000µg	*E. coli*	*Citrobacter*	*St. epid.*	*Pasteurella*	*St. aureus*	*P. auruginosa*
1	2.5	1.2	0	2.8	0	0
2	0	0.9	0.7	2	0.8	0
3	1.7	0.7	0.9	1.3	0	0
4	1.4	0.65	0.63	0.61	0	0
5	0	0	0	0	0	0
6	0.75	0.64	0.8	0	0	0

500µg	*E. coli*	*Citrobacter*	*St. epid.*	*Pasteurella*	*St. aureus*	*P. auruginosa*
1	0.75	0	0	0.9	0	0
2	0	0	0	0	0	0
3	0	0	0	0	0	0
4	0	0	0	0	0	0
5	0	0	0	0	0	0
6	0	0	0	0	0	0

References

1. Ennis MD Cobbs CD. Infect Dis Clin North Am 1995; 9: 687-713.
2. Neu HC Aztreonam activity, pharmacology, and clinical uses. Am J Sci. 1990; 88: 38-42
3. Clark P. Aztreonam Obstet Gynacol. Clin North Am 1992; 19: 519-528.
4. Westley-Horton E, Koestner J A. Aztreonam: a review of the first monobactam. American Journal of the Medical Sciences 1991; 302: 46-49.
5. Sykes RB, Bonner DP, Cimarusli CM Monobactams and the development of aztreonam. Proc Int Congr Chemother 1983, 1: 3021-3027.
6. Lancelot JC., Latois B., Saturnino C., Perrine D., Robba M. Efficient synthesis of new beta-lactams, Synthetic Comm 1993; 23: 1535-1542.
7. Lancelot JC., Saturnino C., El-Kashef H., Perrine D., Mahatsekake C., Prunier H., Robba M. A facile synthesis of new beta-lactams. J Heterocyclic Chem 1996, 33: 427-430.

Correspondence:

Professor Anna Capasso
Dipartimento di Scienze Farmaceutiche
Università di Salerno
Via Ponte don Melillo
84084 Fisciano
Salerno, ITALY

phone/ Fax 0039-089-964357
e-mail: annacap@unisa.it

Biomedical Research 2004; 15 (2): 103-106

Significant factors in conversion of laparoscopic cholecystectomy: A retrospective study

Hasan Qayyum, MBBS and Syed Amjad Ali Rizvi, MS, FRCS (Edin.)

Department of Surgery, Jawaharlal Nehru Medical College, A. M. U., Aligarh, India

Key words: Laparoscopic cholecystectomy, symptomatic gall stone disease, logistic regression

Accepted June 07 2004

Abstract

Laparoscopic cholecystectomy has become the gold standard for the treatment of symptomatic gall stone disease. However, there are still patients requiring conversion to open cholecystectomy. Our aim in this study is to identify significant factors that predict conversion.

A single institutional study of 110 patients, in whom laparoscopic cholecystectomy was attempted from April 2003 till April 2004, was conducted. A retrospective analysis of 32 parameters including patient's demographics, clinical history, laboratory data, ultrasonic evidence, and intra-operative details was performed. Logistic regression was used to determine statistical significance of the studied factors for conversion to open cholecystectomy .

Twenty three cases (20.9%) of attempted laparoscopic cholecystectomy required conversion. A binary logistic regression model employing the forward L-R method showed that dense adhesions, elevated SGPT levels, and common bile duct stones diagnosed intra-operatively were consecutively significant.

The results show that laboratory tests and routine ultrasonography can be recommended for predicting conversion of laparoscopic cholecystectomy. Knowledge of predictive factors along with their explanation to patients and their attendants will serve to strengthen the surgeon-patient therapeutic alliance.

Introduction

Cholelithiasis is a benign condition commonly seen in outpatient clinics. Surgery is the preferred modality of treatment due to the relative inefficacy of medical therapy. Laparoscopic cholecystectomy is generally chosen over conventional open cholecystectomy, since it results in shorter hospital stay, reduced postoperative pain, and has obvious cosmetic advantages.

Over a history spanning close to 20 years, the threshold for selecting patients for laparoscopic cholecystectomy has been lowered. Previous contraindications like obesity, past laparotomy, and acute cholecystitis are no longer regarded as absolute [1].

Today, laparoscopy is attempted in all patients except those with portal hypertension and serious bleeding disorders, although conversion is still required in 1.5 % to 19 % of patients [1].

The specific aim of our study is to highlight significant conversion factors of laparoscopic cholecystectomy using a retrospective view.

Patient and Methods

110 cases of laparoscopic cholecystectomy were randomly selected between April 2003 and April 2004 at the Jawaharlal Nehru Medical College, India. A retrospective analysis of 32 parameters including patient's demographics, clinical history, laboratory data, ultrasonic evidence, and intra-operative details was performed.

Demographic data included the age, sex, duration of illness, weight, and associated co-morbid factors of tuberculosis, diabetes mellitus, hypertension, and chronic obstructive pulmonary disease. Clinical data included fever, tenderness in the right upper quadrant, icterus, and past surgical scar.

Preoperative laboratory analysis included complete hemogram including neutrophil counts and levels of SGPT, SGOT, alkaline phosphatase and bilirubin. Ultrasonic evidence included the size of the gall bladder, thickness of the gall bladder wall, number of gall stones, pericholecystic fluid, and common bile duct status.

Intraoperative details included the number of gall stones, evidence of pericholecystic fluid, common bile duct stones, anatomy of the Calot's triangle, adhesions, peroperative complications, and whether conversion done or not.

The operations were performed by consultants only using a standard 4-point technique. They were assisted by senior residents.

More than 20 episodes of biliary colic were regarded as continuous pain in right hypochondrium. Fever was present when body temperature measured in axilla was more than 100°F. Tenderness was defined as tenderness in right hypochondrium on deep palpation.

The reference range of SGPT and SGOT was found to be 0-30 U/ml. Reference range of alkaline phosphatase was found to be 30-300 U/ml from the Biochemistry Laboratory of Jawaharlal Nehru Medical College, Aligarh.

Size of gall bladder was studied as normal or distended. Ultrasonic gall bladder wall thickness of 3 mm or less was considered as normal. Thickness more than 3 mm was regarded as thick walled gall bladder. Number of gallstones more than 1 was classified as multiple. Common bile duct status was studied as either dilated or with stones. Dilatation was defined as a common bile duct diameter of 6 mm or more.

Intra-operative complications studied included dense adhesions around the biliary tree, inability to dissect the gall bladder, iatrogenic bile duct injury, iatrogenic bleeder, ruptured gall bladder with iatrogenic bile duct injury, ruptured gall bladder with iatrogenic bleeder.

Statistical Analysis

A step-wise binary logistic regression model which used 'forward L-R method' was designed to determine the statistically significant factors amid the 32 independent variables studied.

Our model showed that the significant independent predictors were the presence of adhesions, elevated SGPT levels, and presence of common bile duct stones missed on routine ultrasonography.

The upper and lower values of significance of odds ratio (see Table 1) for all the significant predictors are unidirectional. For adhesions and common bile duct stones, both are below 1, while for SGPT, both values are above 1. This statistical fact ensures that we can generalize the performance of our significant predictors for the entire population of patients in whom laparoscopic cholecystectomy is attempted and hence the result is not limited to our sample only.

Furthermore, apart from the above-mentioned significant predictors, we found that the intra-operative complication of inability to dissect the gall bladder (Roa's score = 6.067, $df = 1$, $p = .01$) can also contribute to conversion of laparoscopic cholecystectomy

Table 1 Step-wise binary logistic regression of significant conversion predictors for overall series

PREDICTORS	Wald	df	p	ODDS RATIO	% CONFIDENCE INTERVAL	
					Lower	Upper
Adhesions	21.140	1	.000	.084	.029	241
SGPT	14.596	1	.000	1.083	1.040	1.128
CBD stone	4.2340	1	.000	.045	.002	864

Results

Out of the 110 patients in whom laparoscopic cholecystectomy was attempted, 23 (20.9%) required conversion. The reasons for conversion in our study are summarized in Table 2.

The most common factor for conversion in our study was dense adhesions around the gall bladder, which prevented accurate identification of the biliary anatomy in 16 patients. Adhesions were associated with 2 cases of inability to dissect the gall bladder requiring conversion, 2 cases of iatrogenic bile duct injury requiring conversion, 3 cases of iatrogenic bleeders requiring conversion, and 2 cases of ruptured gall bladder with iatrogenic bleeder requiring conversion

Common bile duct dilation was found in 8 cases by routine ultasonography. The cause of dilatation was identified as biliary sludge in 4 cases (all ultrasonologically) and stones in the remaining 4 cases. Common bile duct stones were identified ultrasonologically in only 1 out of 4 cases where duct stones were eventually found at the time of laparoscopy. In this single preoperatively diagnosed bile duct stones case, laparoscopy was attempted but conversion was required due to inability to extract the stones by laparoscopic choledocholithotomy. Common bile duct stones were identified in the remaining 3 cases intraoperatively out of which 2 were converted and 1 was successfully completed as a laparoscopic procedure.

SGPT was found to be elevated in 40 cases, and was raised in 13 out of the 23 converted cases. No significant relation was found between the likelihood of conversion and any of the following variables: age, sex, duration of illness, number of biliary colic attacks, fever, jaundice, associated co-morbid conditions, weight, tenderness in right hypochondrium, past surgical scar, hemogram, SGOT levels, alkaline phosphatase levels, bilirubin levels, size of gall bladder, thickness of gall bladder wall, number of gall stones, and pericholecystic fluid.

Table 2: Reasons for conversion to open cholecystectomy in 110 patients

Intra-operative complication	Total	CONVERTED	% out of 110 cases CONVERTED
Adhesions	30	16	14.5%
Iatrogenic bile duct Injury	7	3	2.7%
Iatrogenic Bleeder	6	4	3.6%
Ruptured Gall Bladder with Iatrogenic Bile Duct Injury	2	1	0.9%
Ruptured gall bladder with Iatrogenic bladder	1	1	0.9%
Inability to dissect gall bladder	2	2	1.8%

Discussion

Laparoscopic cholecystectomy has become the surgical procedure of choice in the treatment of symptomatic cholelithiasis. With experience, it is a safe and cost efficient procedure. However, surprises like dense adhesions and ultrasonologically missed bile duct stones call for conversion to a conventional technique. Identifying significant predictors for conversion help in patient counseling and better pre-operative preparation

In our study, conversion was required in 20.9% of the studied laparoscopies. The actual rates of conversion reported in the literature are variable [1-3]. However, our reported rate is relatively high.

In concordance with other studies [1], we believe that conversion to open cholecystectomy should not be considered a failure but a step towards safety in dealing with challenging cases. A decision to convert should be treated as a measure of safety and not as a sign of surgical incompetence.

In conformity with the findings of Fried et al [3] and Chi-Leung et al [4], the commonest cause of conversion in our study is the inability to define biliary anatomy. We found dense adhesions of the gall bladder to the common bile duct and adjacent structures caused this. Although these dense adhesions may be a pathological consequence of prolonged duration of symptoms due to delay in operation, the latter was not found to be a statistically significant independent predictor in our study. This is contrary to the report of Rattner et al [5].

The second commonest significant factor was found to be elevated SGPT levels. This was present in 36.4% of our patients and 56.5% of converted patients.

The other commonest significant factor was the surprise of bile duct stones missed ultrasonologically . In our study, only 25 % common bile duct stones were diagnosed pre-operatively despite dilatation present in all cases where bile duct stones were eventually found. Hence, we agree with Fahlke et al [6] that the presence of CBD dilatation alone does not reliably predict presence of common bile duct stones.

Although gall bladder wall thickness was present in 46.3% laparoscopies and 56.5% converted laparoscopies, our statistical analysis showed that it was of little use in predicting per-operative difficulty. This is in corroboration with the findings of Mcloughlin et al [7]. Hence, we do not regard it as a significant factor for conversion.

In contrast to the findings of Fried et al [2], we could not establish the male sex or increasing age as significant pre-operative predictors in conversion. However, we agree with his study that patients with multiple previous laparotomies have not proved to have a problem with laparoscopic cholecystectomy.

In summary, to determine the risk factors for conversion of laparoscopic cholecystectomy to open cholecystectomy, preoperative and intra-operative data were collected and analyzed retrospectively from 110 randomly selected patients. The analysis showed that both patient factors and surgeon factors predicted conversion of laparoscopy.

Factors found statistically significant were dense adhesions, elevated SGPT levels, and common bile duct stones missed in routine ultrasonography consecutively. Knowledge of these factors may therefore, facilitate surgeons to choose the appropriate modality of surgery and convey the chances of conversion to the patient.

Acknowledgement

The authors are thankful to Dr. Lalit Singh, Surgery Resident, Jawaharlal Nehru Medical College for his cooperation in the preparation of this manuscript.

References

1. Alponat A, Kum CK, Koh BC, et al. Predictive factors for conversion of laparoscopic cholecystectomy. World J Surg 1997; 21: 629-633

2. Fried GM, Barkin JS, Sigman HH, et al. Factors determining conversion to laparotomy in patients undergoing laparoscopic cholecystectomy. Am J Surg 1994; 167: 35-41
3. Sanabria JR, Gallinger S, Croxford R, Strasberg SM. Risk factors in elective laparoscopic cholecystectomy for conversion to open cholecystectomy. J Am Coll Surg 1994; 179: 696-704.
4. Chi-leung liu, Sheung-tat Fan, Edward C.S. Lai et al. Factors affecting conversion of laparoscopic cholecystectomy to open surgery. Arch Surg 1996; 131:98-101
5. Rattner DW, Ferguson C, Warshaw AL. Factors associated with successful laparoscopic cholecytectomy for acute cholecystitis. Ann Surg 1993; 217: 233-236
6. Fahlke J, Ridwelshi, Manger Th, Grote R, Lippert H. Diagnostic workup before laparoscopic cholecystectomy- Which diagnostic tools should be used? Hepato-Gastroenterology 201; 48: 59-65
7. McLoughlin RF, Gibney RG, Mealy K et al. Radiological investigations in laparoscopic compared with conventional cholecystectomy- an early assessment. Clinical Radiology 1992; 45: 267-270

Address:

Dr. Hasan Qayyum
6-B Manzar
Sir Syed Nagar
Aligarh 202 002
India

e-mail: hasanq_2000@hotmail.com

Biomedical Research 2004; 15 (2): 107-109

Short communication

A case of malignant catarrhal fever by OHV-2 in Italy

C. Benazzi*, A. Gentile°, B. Brunetti*, S. Sconza°, G. Sarli*

*Department of Veterinary Public Health and Animal Pathology, oVeterinary Clinical Department, School of Veterinary Medicine of Bologna, Via Tolara di Sopra, 50 – 40064 Ozzano Emilia (BO), Italy

Key words: Sheep-associated malignant catarrhal fever (SA-MCF), OHV-2, gammaherpesvirus, PCR

Accepted March 9 2004

Abstract

The first case of malignant catarrhal fever by OHV-2 in bovine in Northern Italy is presented in a 9-month-old Holstein heifer. The diagnosis was suspected on the basis of clinical signs and histopathological lesions of microangiopathy. It was confirmed by PCR performed on the blood of the subject, and immunohistochemical features showed a prevalence of CD3, suggesting that T-lymphocytes are the major cell type in this case.

Introduction

A typical case of Malignant Catarrhal Fever (MCF) is the object of this case report that concerns the [1,2] characterized by high mortality rate (3, 4, 5), but morbidity is irregular and usually low (6, 7). The disease is caused naturally by at least two distinct but related gammaherpesviruses, namely alcelaphine herpesvirus 1 (AHV1) and ovine herpesvirus 2 (OHV-2). This paper refers the first case in Northern Italy and the third in Italy of sheep-associated malignant catarrhal fever (SA-MCF) in bovine in which it has been possible to isolate the OHV-2 genomic DNA via the PCR technique [8,9,10].

Case report

The history of the animal, a 9-month-old Holstein heifer, reported clinical evidence of chronic diarrhea associated with appetite disturbances and progressive weight loss. On the basis of these symptoms the referring veterinarian had sent blood samples to Istituto Zooprofilattico Sperimentale of Bologna that excluded the presence of bovine viral diarrhea-mucosal disease (BVD-MD) by serological (ELISA and Kit-IZS-BS) and virological (ELISA) exams. As the clinical symptoms progressed, bilateral corneal opacification appeared and the heifer was referred to the Veterinary Clinical Department of the Veterinary School of Bologna for more accurate exams. The first clinical approach evidenced a retarded development of the body compared to the head, anxiety, cachexya (the weight was 150 kg), dry skin, with crusts in some areas, bilateral corneal opacity, diarrhea, and ruminal hypotonia. An evaluation of the spinal fluid (obtained by post-occipital rachicentesis) gave the following results: protein 32.9mg/dl (normal <30mg/dl), creatinchinase 56 IU/l (normal <15 IU/l) and leucocytes 38/µl (normal <5leucocytes/µl) all mononuclear cells. These values let the authors suspect a non-suppurative encephalitis, probably due to MCF virus. The heifer was put down.

Clinical and postmortem examinations revealed, bilaterally, scarring of the cornea and congestion of scleral vessels, extensive necrotic ulcerative lesions (Fig. 1) located on the epithelium of the tongue and palate; the mucosa of the stomach presented spread reddened patches and, in the pyloric area, ulcerative lesions with slightly raised margins. An ulcer was visible on the vulva. Grey foci of interstitial nephritis could be seen in the cortex of both kidneys. These lesions were 3-5 mm in diameter and slightly indented. Similar foci were visible in the myocardium as well. The brain presented meningeal melanosis.

The histopathological changes were those of a multifocal mononuclear inflammation: lymphoblasts, lymphocytes, macrophages, and plasma cells were observed in the kidney, spleen, lymph nodes, myocardium, skin, eyes, and mucosa of the tongue and abomasum. The most typical lesions were vascular alterations, in particular arteritis, characterized by mononuclear infiltrations in the adventitia and fibrinoid necrosis. The myocardium showed obliteration of a branch of a coronary artery, caused by hyperplasia of the *tunica muscolaris* of the wall. The brain presented severe non-suppurative inflammation: mononuclear cuffing, passive hyperemia and perivascular edema. Satellitosis and neuronal necrosis were especially severe in the Satellitosis and neuronal necrosis were especially severe in the cerebellum, in addition to lymphoid inflammation of the meninges. Follicular hyperplasia and neuronal necrosis were especially severe in the cerebellum,

Fig. 1. *Gross aspect of the right eye of the heifer affected by MCF showing opaque cornea thickened by scarring. An ulceration is visible in the internal edge of the eye.*

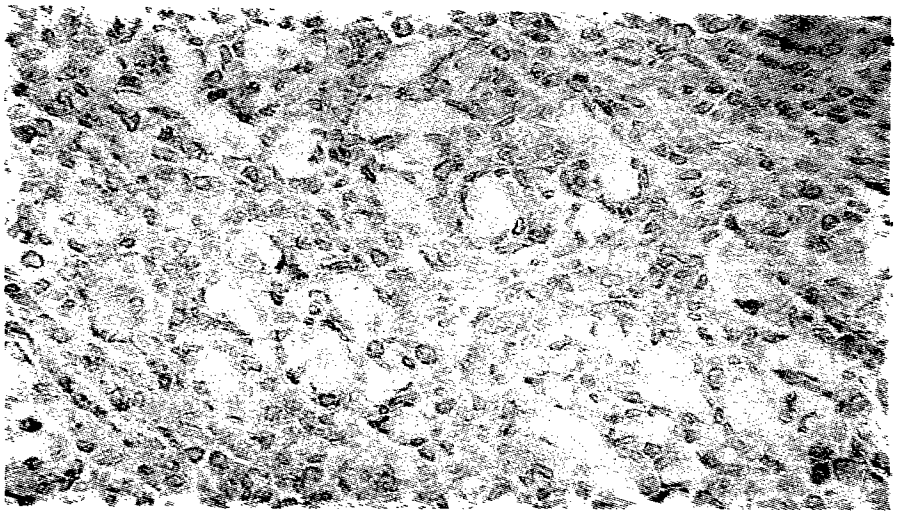

Fig. 2. *Immunohistochemically the heart presents abundant CD3 infiltration among cardiac muscle cells. 63x.*

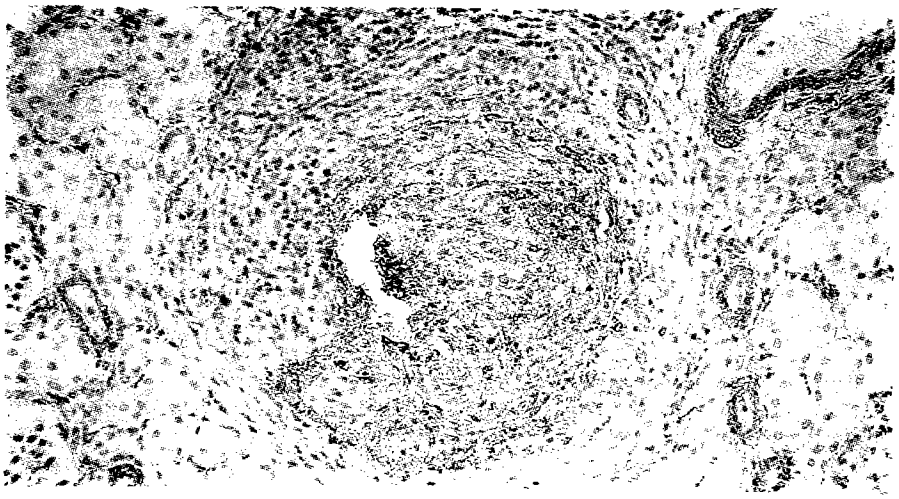

Fig. 3. *Immunohistochemical stain for actin reveals hyperplasia of muscle cells in renal artery. 20x.*

In addition to lymphoid inflammation of the meninges. Follicular hyperplasia was observed in the paracortex and medulla of lymph nodes and in the spleen, with congestion and haemosiderosis. Besides infiltration of mononuclear cells, the skin showed diffuse hyperkeratosis, foci of necrosis and ulcerations.

Immunostaining was carried out by means of monoclonal antibody anti-CD3, clone F7.2.38 (Dako), diluted 1: 75 for the identification of a T lymphocyte population, and anti-CD79, clone HM57 (Dako), diluted 1:50, for the detection of B lymphocytes, in the inflammatory infiltrates of the heart (Fig. 2), skin, abomasal mucosa, and kidney, and in the periarteriolar spaces of the brain, kidney and heart. Lymphocytes presented stronger positivity for CD3 than for CD79, indicating that T-lymphocytes are the major infiltrating cells in this case of MCF. Moreover, a monoclonal antibody anti-smooth muscle actin, clone 1A4 (Dako), diluted 1:100, was employed to evidence marked hyperplasia of blood vessel walls in the heart and kidney (Fig. 3).

The diagnosis of MCF was strongly suggested by the clinical signs, postmortem and histopathological findings. However, to identify which virus was responsible for this form of MCF, PCR was performed on the blood of the subject, at the Bayerisches Landesamt für Gesundheit und Lebensmittelsicherheit of Munich (Germany), and ovine herpesvirus 2 (OHV-2) DNA was amplified. This is the first account of a virologically confirmed OHV-2 case in Northern Italy.

References

1. Cortez PP, Dias Pereira P, Cortes A. et al. First confirmed case of malignant catarrhal fever in a cow in Portugal. Vet Rec 2001; 149: 558-559.
2. Muller-Doblies UU, Egli J, Hauser B, et al. Malignant catarrhal fever in Switzerland: 2. Evaluation of the diagnosis. Schweizer Archiv Tierheilkunde 2001; 143: 581-591.
3. Campbell RSF. Malignant catarrhal fever in Asian livestock. Eds P. W. Daniels, Sudarisman, P. Rohohardjo. Canberra, Australian Centre for International Agricultural Research. 1988 p 64.
4. Plowright W. Virus infections of vertebrates 3. Virus infections of ruminants. Eds Z. Dintner, B. Morein. Amsterdam, Elsevier Science Publishers. 1990; p 123.
5. Smith BP. Large Animal Internal Medicine. 2nd edn. St. Louis, Mosby-Year Book. 1996; p 814.
6. O'Toole D, Li H, Miller D, et al. Chronic and recovered cases of sheep-associated malignant catarrhal fever in cattle. Vet Rec 1997; 140: 519-524.
7. Yus E, Guitian J, Diaz, A et al. Outbreak of malignant catarrhal fever in cattle in Spain. Vet Rec 1999; 145: 466-467.
8. Baxer SI, Pow I, Bridgen A, et al. PCR detection of the sheep-associated agent of malignant catarrhal fever. Arch Virol 1993; 132: 145-159.
9. Crawford TB, Li H., O'Toole D. Diagnosis of malignant catarrhal fever by PCR using formalin-fixed, paraffin-embedded tissues. J Vet Diagn Invest 1999; 11: 111-116.
10. Decaro N, Tinelli A, Pratelli A, et al. First two confirmed cases of malignant catarrhal fever in Italy. New Microbiol 2003; 26; 339-344.

Correspondence:

Dr. C. Benazzi
Department of Veterinary Public Health and Animal Pathology
School of Veterinary Medicine of Bologna
Via Tolara di Sopra,
50- 40064 Ozzano Emilia (BO)
Italy

Phone: ++39 051 2097955
Fax: ++39 051 2097967
e-mail: Benazzi@vet.unibo.it

Biomedical Research 2004; 15 (2): 110-116

Quantitative motor unit potentials analysis in healthy horses

B. Ciminaghi, S. Mazzola, M. Albertini, V. Scaioli*, M. Costanzi, F. Patrese, F. Pirrone, M.G. Clement

Department of animal pathology, section of Biochemistry and Physiology, University of Milan, Via Celoria 10, 20133 Milano, Italy
*Istituto Neurologico C. Besta, Section of Neurophysiology, Milan, Italy; Corresponding author: E-mail: ciminagh@utenti.unimi.it

Key words: |Electromyography (EMG), motor unit potential (MUPs), horse

|Accepted May 7 2004

Abstract

Electromyographic examination (EMG) is a diagnostic technique, useful to discriminate between myogenic and neurogenic problems. In our study we used a multi-MUP EMG analysis, an online method that, permitting to know the results in real time, may be advantageous especially in uncooperative and not sedated animals. The EMG examination was performed in ten healthy horses on splenius, trapezius and triceps muscles, using concentric needle electrodes. The signals were acquired and analyzed online with a dedicated software that proposed some grouping of the motor unit potentials (MUPs). For each subset of MUPs the program analysed duration, amplitude, area/amplitude ratio and firing rate.

The results indicate that no significant differences have been evidenced among the three muscles studied. The MUPs had a duration of 8.04 ms ± 2.32 (S.D.) in splenius, 7.85 ms ± 2.61 (S.D.) in trapezius and 7.35 ms ± 2.32 (S.D.) in triceps, while amplitude values were 2.52 μV ± 0.22 (S.D.) in splenius, 2.56 μV ± 0.21 (S.D.) in trapezius and 2.59 μV ± 0.29 (S.D.) in triceps. The plotting of amplitude versus duration, for all three muscles studied, showed a homogeneous range of normality. We believe that the present method may be adopted to create a normative data base for evaluation of muscular function in clinical studies.

Introduction

Electromyography is a well-established technique for evaluating the electrical activity of the motor unit (MU) [1]. The recording electrode is placed directly into the muscle belly and the muscle action potentials, discrete discharges of the motor neurons, are recorded from the interstitial fluid. Consequently, the distance of the recording electrode from the active muscular fibre is responsible for the waveform and amplitude of the recorded signal, and it is of great importance in the assessment of motor unit potential.

The first electromyographic qualitative studies have been made by Adrian and Bronk in 1929 by Adrian and Bronk in 1929 [2], by means of some specially manufactured concentric needle electrodes. In this method the electromyographers assess the traces subjectively, by viewing them on an oscilloscope screen and by listening to their sound on an audio monitor, providing a semi-quantitative evaluation of the muscle activity.

In the middle of the 1950s, Buchthal et al. introduced quantitative motor unit potential analysis, but this method had some inconveniences, because it could request a lot of time for analysis of filmed traces [3-5]/ Both the semi-quantitative and quantitative methods, evidencing changes in physical properties of MUPs, provides clues for clinical diagnosis of neuromuscular diseases, but, in order to record activity from the entire motor unit, Stålberg et al. [6] developed in 1980 a non selective technique (Macro EMG) correlated with the number and size of muscle fibres. Recently, Wijnberg et al. [7] have performed, in horses, the offline analysis of the MUP in a semiautomatic way, where the MUPs were selected and analyzed manually. This method is user friendly, with good accuracy, reliability and reproducibility and it is sufficiently fast to be used in routine EMG analysis, also in uncooperative animals.

To know the results in real time without manual trigger or delay line, in our study we use a method in which the sweep is free running; in this program the algorithms are based on a "turns" analysis described by Willison [8].

The aim of our study is to establish normal values of the physical properties of the MUPs in terms of amplitude, duration, area/amplitude ratio and firing rate in healthy horses, in order to create a data base usable in clinical studies for electromyographic evaluation of muscular function.

Materials and Methods

Animals

Ten healthy horses, 4 geldings and 6 mares, aged 15.4 ± 2.65 trained to riding lessons, were used. The animals were not anesthetized or sedated and were maintained in a stable, without any form of restraint.

EMG equipment

The EMG examination was performed by inserting a disposable concentric needle electrode (75 mm x 0.64 mm – 23G, Medtronic, Denmark) in the muscle and gently searching for a site where the EMG signal was crisp. The EMG signal has been acquired and analyzed online with a portable commercial EMG equipment (Keypoint, Dantec, Denmark) with dedicated software (Quantitative EMG including Multi-MUP). This equipment used a pass-filter, usually setting at 20 HZ to 10 KHZ.

Signal procedure

Before inserting the concentric electrodes to record EMG signals, the animals were connected to ground with a subcutaneous needle electrode, positioned near a bony prominence, such as spina scapulae or ischial tuber. Since the concentric electrode recorded the muscle action potentials from fibres close to the tip of the electrode, it was necessary to move the needle, advancing or withdrawing it in small steps and maintaining it in each new position with a firm grip, to sample some different areas (at least three for each insertion).

In our study we have evaluated each muscle at rest and during different degrees of contraction, obtained during horse's own movements or inducing the shift from one limb to the other.

The EMG examination was performed in two steps: 1) insertional activity and spontaneous activity, evaluated at rest; 2) motor unit potentials, evaluated during "voluntary" activity.

1. Insertional activity lasted little longer than the movements of the needle and it represented the muscular fibre membrane irritability due to the insertion of the electrode. Spontaneous activity was detected at the end of insertional activity and, in healthy subjects, it was characterized by an electrical silence.

2. Motor unit potentials were recorded during mild contraction of the muscle. In the horses, this step was very difficult to perform, because the animals were often uncooperative and consequently it was necessary to force them to slowly move. We have chosen to analyze three muscles: splenius, trapezius and triceps.

Quantitative EMG evaluation

The software that we used proposed a grouping of the MUPs, sampled from each different insertional areas. All the MUPs belonging to a group were shown superimposed in a window of the monitor and a weighted average of these MUPs was shown highlighted over them. Tags, that defined some of the MUP's characteristics, were set on suggested positions by the program. Before accepting the results, the operator deleted inconsistent groups and adjusted tags position for definitive measurements.
Many different MUPs were usually obtained from each recording site and there were different parameters that could be used for their classification. According to the number of phases, evaluated as the section of the MUP that fell between two baseline crossing, the MUPs were divided in monophasic and polyphasic. Until 4 phases, the MUPs were classified as monophasic. For each subset of MUP (simple or polyphasic), the software analysed the following MUPs properties: duration, amplitude, area/amplitude ratio and firing rate. The duration, a function of synchrony in the firing of many muscle fibres belonging to a common motor unit, was measured from the initial take-off to the return to baseline, and the amplitude of the MUP was measured peak-to-peak within the duration. The thickness was represented by area/amplitude ratio, and the area was calculated within the duration of the MUP. The firing rate was the reciprocal of the time between the interdischarge interval.

Although our equipment permitted to evaluate many other MUP parameters, we deemed not to report them in the paper, owing to little clinical usefulness.

Statistical analysis

All the values were expressed as mean ± S.D. To describe the characteristics of duration and amplitude of the MUP, a descriptive statistic has been used. The values that were not normally distributed, have been transformed in natural logarithm. The statistical significance of differences between two sets of data was assessed by two tiled t-test for unpaired data. A p value < 0.05 was regarded as statistically significant.

Results

We have identified and classified a total number of 608 MUPs; the mean number of MUPs that we have recorded was 27.2 ± 4.87 in splenius, 26.2 ± 6.41 in trapezius and 18.5 ± 9.71 in triceps. In six horses we could not detect any MUPs from triceps because, in the standing position, this muscle did not evidence a significant and recordable electrical activity.

In Table 1 are reported the data regarding the main characteristics of motor unit action potentials of the three muscles under study. Most of the MUPs were simple, in fact the polyphasic MUPs were 9% ± 6.2 for splenius, 4.8% ± 5.6 for trapezius and 4% ± 0 for triceps. In the splenius and trapezius the amplitude as well as the duration of the MUPs were very homogeneous among the animals, while the examination of area/amplitude ratio evidenced that about 50% of the horses draw from the mean. For all the parameters that we had considered, the percentage of MUPs out of the range was very low. The firing rate of active motor units was 4.75 Hz ± 0.51 in splenius and 4.02 Hz ± 0.43 in trapezius, that are normal values for muscles at rest, when the degree of MU activation is low. On the contrary, in the triceps we have found a much higher firing rate, probably because the difficulty of recording MUPs from this muscle at rest leads us to force the horses to a much stronger muscular contraction.

The characteristics of duration and amplitude of the 608 MUPs, evaluated from the splenius, trapezius and triceps muscles, are reported in figg. 1-5. The duration values were normally distrib

Table 1: Main characteristics of motor unit action potentials of the three muscle under study.

	SPLENIUS			*OUT range %MUP*			*OUT range %MUP*			*OUT range %MUP*		
horse	**n.MUP**	**%Poli**	**Ln Amp**	**± 2**	**± 2.5**	**Dur**	**± 2**	**± 2.5**	**Ar/Amp**	**± 2**	**± 2.5**	**Fr**
1	24	8.0	2.41*	0.00	0.00	8.70	0.37	0.37	1.65*	1.10	0.37	5.40
2	37	5.0	2.55	1.10	0.37	7.86	0.37	0.00	1.51	0.74	0.74	4.56
3	26	15.0	2.60*	0.37	0.00	8.79	0.74	0.74	1.75*	1.84	0.37	4.30
4	19	0.0	2.43	0.00	0.00	7.79	0.00	0.00	1.45	0.74	0.00	4.36
5	23	9.0	2.58	1.10	0.00	7.50	0.00	0.00	1.11*	0.00	0.00	4.49
6	30	0.0	2.55	0.74	0.00	6.57*	0.00	0.00	1.14*	0.37	0.00	5.24
7	28	14.0	2.50	0.00	0.00	8.13	1.10	0.00	1.38	0.37	0.37	5.06
8	26	15.0	2.59	0.74	0.37	8.65	0.37	0.37	1.41	0.74	0.37	3.87
9	29	17.0	2.57	0.37	0.37	8.55	0.74	0.00	1.20*	0.00	0.00	5.33
10	30	7.0	2.36*	0.37	0.00	8.03	0.00	0.00	1.35	0.00	0.00	4.91

	TRAPEZIUS			*OUT range %MUP*			*OUT range %MUP*			*OUT range %MUP*		
horse	**n.MUP**	**%Poli**	**Ln Amp**	**± 2**	**± 2.5**	**Dur**	**± 2**	**± 2.5**	**Ar/Amp**	**± 2**	**± 2.5**	**Fr**
1	25	4.0	2.63	0.00	0.00	11.14*	1.91	0.76	1.91*	0.76	0.76	4.28
2	43	0.0	2.52	0.38	0.00	7.34	0.38	0.38	1.13*	0.38	0.38	3.96
3	19	5.0	2.53	0.00	0.00	7.73	0.00	0.00	1.34	0.00	0.00	3.72
4	26	4.0	2.61	0.00	0.00	8.13	0.00	0.00	1.66*	0.38	0.38	3.67
5	24	4.0	2.52	1.15	0.76	6.76*	0.00	0.00	1.16*	0.00	0.00	3.13
6	26	8.0	2.53	0.00	0.00	8.45	0.00	0.00	1.44	0.38	0.38	4.43
7	25	0.0	2.54	0.00	0.00	8.19	0.38	0.00	1.8*	0.76	0.38	4.44
8	21	19.0	2.76*	1.91	1.15	8.42	0.76	0.76	1.15*	0.38	0.00	4.42
9	26	0.0	2.45*	0.38	0.00	6.38*	0.38	0.00	1.24	0.00	0.00	3.87
10	27	4.0	2.62	0.00	0.00	6.47*	0.00	0.00	1.19	0.38	0.38	4.31

	TRICEPS			*OUT range %MUP*			*OUT range %MUP*			*OUT range %MUP*		
horse	**n.MUP**	**%Poli**	**Ln Amp**	**± 2**	**± 2.5**	**Dur**	**± 2**	**± 2.5**	**Ar/Amp**	**± 2**	**± 2.5**	**Fr**
1	24	8.0	2.68	1.35	0.00	8.83*	1.35	1.35	1.46*	1.35	0.00	5.67*
5	24	8.0	2.65	1.35	1.35	7.43	1.35	0.00	0.84*	0.00	0.00	31.36*
7	4	0.0	2.13*	1.35	0.00	2.85*	1.35	0.00	0.59*	0.00	0.00	15.03
8	22	0.0	2.52	0.00	0.00	6.45*	0.00	0.00	1.10	0.00	0.00	15.60

In fig. 4 A, B, C are reported the amplitude data, transformed into natural logarithm, because the distribution of amplitude values was not normal. We observed that these normalized data were equally distributed around mean values, such as 2.52 ± 0.22 in splenius (Fig. 4 A), 2.56 ± 0.21 in trapezius (Fig.. 4 B) and 2.59 ± 0.29 in triceps (Fig. 4 C).

For each muscle under study, we have plotted the values of logarithm of MUP amplitude versus those of MUP duration, to construct a two-dimensional graph, in which the two rectangular areas represent the normal range of values (Fig. 5 A,B, C). For the computation of these areas, we have chosen a confidence interval representing the mean ± 2 S.D. or ± 2.5 S.D. In these graphs, the cross inside the cloud represents the barycentre of the two variables. In our case, almost all the points, representing the MUPs of the three muscle considered, fell inside the cloud, making immediately clear that the muscles under study belonged to healthy subjects.

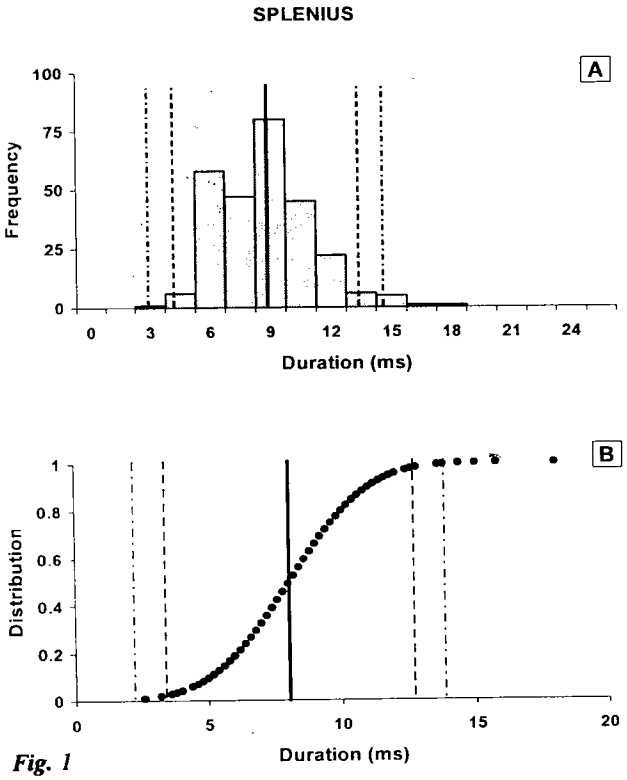

Fig. 1

Fig. 1: in A: histogram of the duration of the MUPs and in B: distribution of the duration values of the MUPs of the splenius muscle. The dashed lines indicate the confidence intervals representing the mean ± 2 S.D. or ± 2.5 S.D.

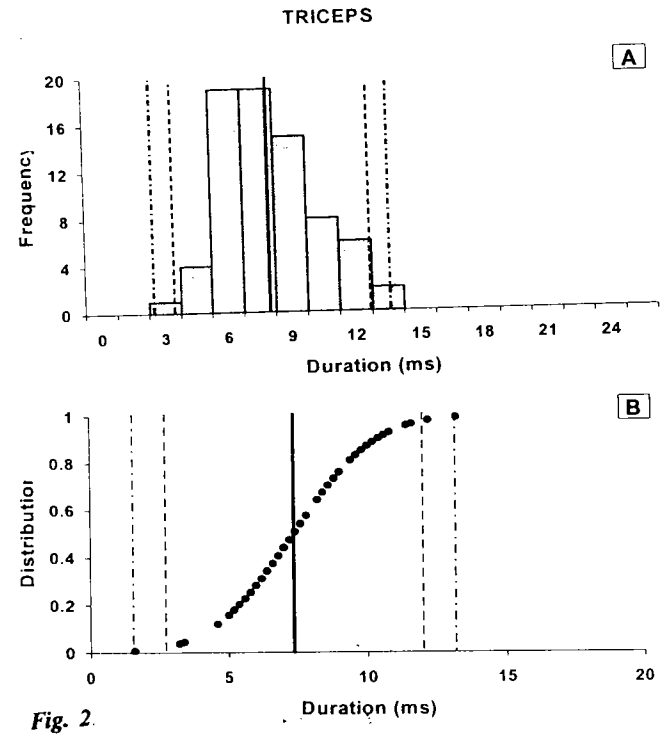

Fig. 2

Fig. 2: in A: histogram of the duration of the MUPs and in B: distribution of the duration values of the MUPs of the trapezius muscle. The dashed lines indicate the confidence intervals representing the mean ± 2 S.D. or ± 2.5 S.D.

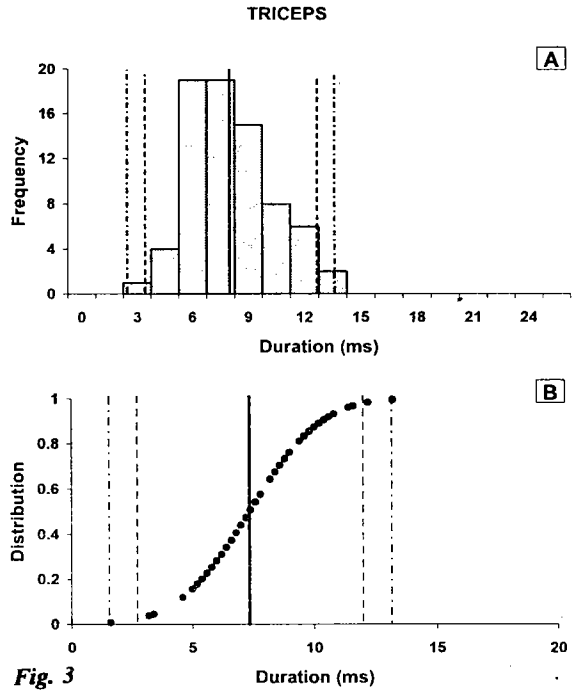

Fig. 3

***Fig. 3**: in A: histogram of the duration of the MUPs and in B: distribution of the duration values of the MUPs of the triceps muscle. The dashed lines indicate the confidence intervals representing the mean ± 2 S.D. or ± 2.5 S.D.*

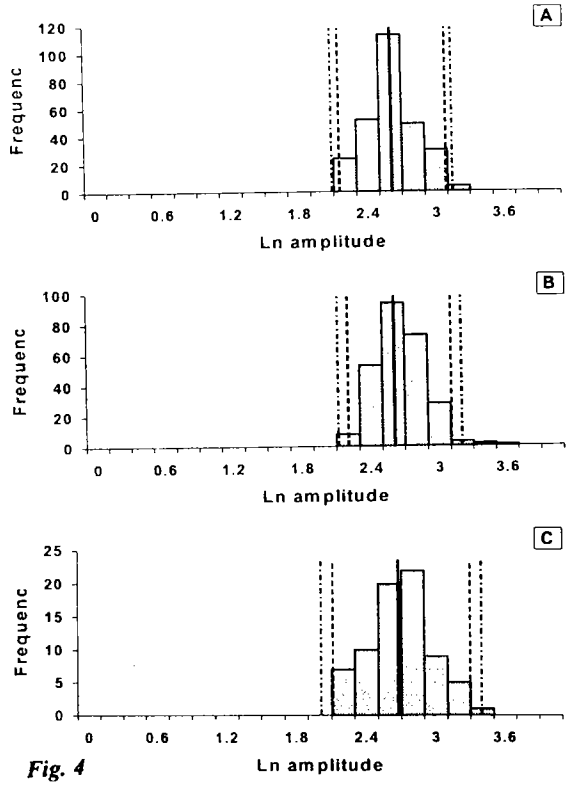

Fig. 4

***Fig. 4:** Histogram of the amplitude of the MUPs in the three muFscles under study. The dashed lines indicate the confidence intervals representing the mean ± 2 S.D. or ± 2.5 S.D. Ln: natural logarithm.*

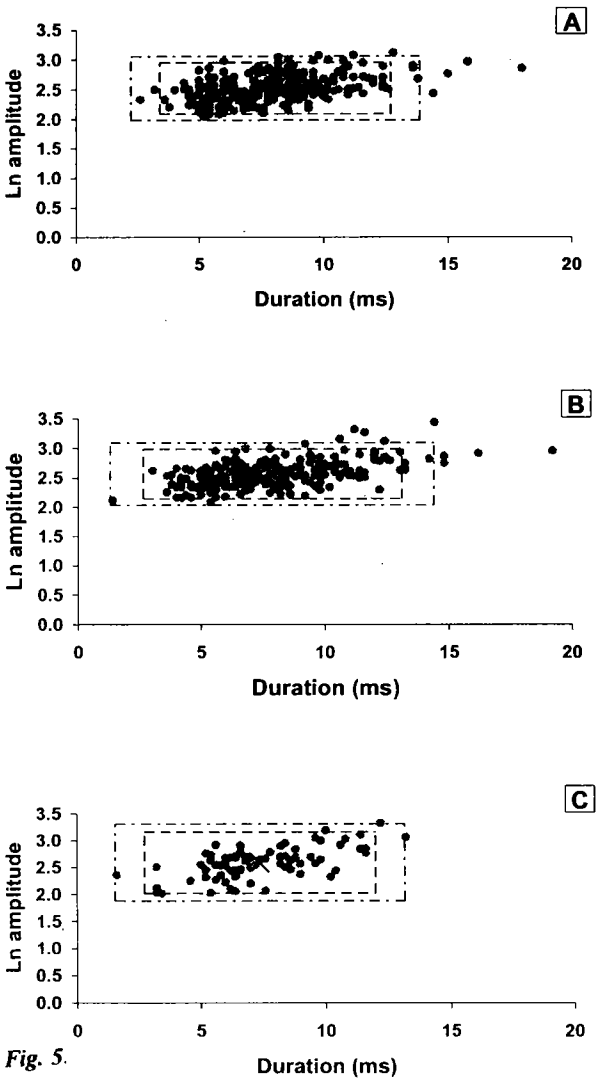

Fig. 5.

Fig. 5: Two-dimensional graph representing the normal range of duration and amplitude values for splenius (A), trapezius (B) and triceps (C). The cross inside the cloud represents the barycentre of the two variables. The dashed lines indicate the confidence intervals representing the mean ± 2 S.D. or ± 2.5 S.D. Ln: natural logarithm.

Discussion

The electrophysiology of the motor units may be studied with various qualitative and quantitative EMG methods, using needle electrodes. Although many electromyography laboratories are still evaluating assess the traces subjectively, by viewing them on an oscillocope screen and by listening to their sound on an audio monitor [9].

Since 1950s, some authors have introduced a quantitative motor unit potential analysis manually performed, that permits a detailed measurement of the duration, amplitude and number of phases of the MUPs; but this method is time consuming. Currently, in human medicine, single fibre EMG (SFEMG), that

allows precise study of the microphysiology of the motor units, is widely used [10]. SFEMG assesses the muscle fibre membrane characteristics, propagation velocity, function, of individual motor end-plates and organization of muscle fibre in the MU territory. Unfortunately, this SFEMG technique is not suitable for animal studies, because requires substantial subject cooperation.

In order to record activity from the entire motor unit, a non selective technique (Macro EMG) has been developed by Stålberg et al. in 1980 [5,6]. Macro EMG, often used to assess the MU size, provides information from the entire cross-sectional area of the motor unit, representing the temporal and spatial summation of each singular muscle fibre action potentials (Cengiz et al,[9]. Recently Wijnberg et al. have performed an offline and semiautomatic analysis of the MUP in horses, using a variable trigger line that selects signals above a certain chosen amplitude [7]. The MUPs having a rise time of less than 0.8 ms and occurring repeatedly at least 4 times are selected and analyzed manually. This method is quite reliable and easy to use also in non-cooperating animals.

In our study we have used a multi-MUP EMG analysis, a method of decomposition analysis based on template matching. The main advantages of multi-MUP EMG analysis are: A) it is an online method that permits the automatic extraction of more than one MUP obtained from each recording site, and this assures sampling from many different MUs; B) it is faster to be used routinely; C) it does not require special electrodes; D) it is reproducible.

Nevertheless, this technique has also some disadvantages. The software may accept only the MUPs with the highest firing rate, and, due to the weighted averaging of the MUPs, it is possible to detect a certain degree of signal distortion, a reduction of MUPs amplitude and a change of the number of phases.

All the results measured in this study correspond to the normal values observed in humans and, still to date, in horses [11;12]. The duration of the MUPs, evaluated from the initial take-off until the return to baseline, ranges from 3 to 11 ms, with a mean value of 7.45 ms, that corresponds to normal values reported in literature. From the results we can also deduce that the duration is positively correlated with the percentage of polyphasic PUMs and hence with the synchronicity of the discharge of the fibres. In healthy muscles the proportion of polyphasic MUP varies from one muscle to another; in our study, the mean of polyphasic PUMs in splenius is 9 %, in trapezius is 4.8% and in triceps is 4

%, all percentages that are included in the range of normal values.

The amplitude is primarily determined by few fibres located near the tip of the recording needle and it is affected by the number and diameter of these fibres. The amplitude values, normally reported in literature, range from several hundred microvolts to a few millivolts; in our study, we have reported the normalized values of amplitude and we can observe that these data are equally distributed around mean values, that is 2.52 in splenius, 2.56 in trapezius and 2.59 in triceps.

In our study, the firing rate of active motor units is 4.75 Hz ± 0.51 (S.D.) in splenius and 4.02 Hz ± 0.43 (S.D.) in trapezius; these are normal values for muscles at rest, when the degree of muscular fibres activation is low. On the contrary, in the triceps the frequency is much higher (16.92 Hz ± 10.65), probably because, at rest, this muscle does not always discharge and an increasing force of contraction is necessary.

All these parameters characterize the physical properties of the MUPs, and they reflect morphological or physiological features that change with neurogenic or myogenic pathology. Neurogenic diseases are characterized by MUP which display high amplitude and long duration, while myogenic diseases are characterized by MUP with low amplitude and short duration. The Fig. 5 is particularly useful to easily evidence some kind of pathology that can occur in the MU of the muscle under study. In fact, when the plotted points fall outside the normal cloud, it can be possible to discriminate if the pathology is neurogenic or myogenic.

To conclude, our study provides normative MUP data, which can be used for clinical diagnosis in patients with suspected myogenic disorders, lower motor neuron disease or locomotion disturbances of unknown origin.

Acknowledgements

This work was supported by two grants FIRST 2002, COFIN 2002.

References

1. Platt SR. Advancing the role of electrodiagnostic techniques in equine neuromuscular disease. Equine Vet J 2000; 34: 538-539.
2. Adrian ED, Bronk DV. Discharge of impulses in motor nerve fibres. The frequency of discharge in reflex and voluntary contraction. J Physiol 1929; 67: 119-151.
3. Buchthal F, Guld C, Rosenfalck P. Action potential parameters in normal human muscle and their dependence on physical variables. Acta Physiol. Scand. 1954a: 32, 200-215.
4. Buchthal F, Pinelli P, Rosenfalck P. Action potential parameters in normal human muscle and their physiological determinants. Acta Physiol Scand 1954b: 22: 219-229.
5. Nandedkar SD, Stalberg E. Simulation of macro EMG motor unit potentials. Electroenceph Clin Neurophysiol 1983: 56: 52-62.
6. Stålberg E, Macro EMG. A new recording technique. J Neurosurg Psychiatr 1980; 43: 45-482.
7. Wijnberg JD, Franssen H, Van Der Kolk JH, Breukink HJ. Quantitative motor unit action potential analysis of skeletal muscles in the Warmblood horse. Equine Vet J 2002: 34, 556-561.
8. Willison RG. Analysis of electrical activity in healthy and dystrophic muscle in man. J Neurol Neurosurg Psychiat. 1964; 27: 386-394.
9. Cengiz B, Ozdag F, Ulas UH, Odabasi Z, Vural O. Discriminant analysis of various concentric needle EMG and macro-EMG parameters in detecting myopathic abnormality. Clin Neurophysiol 2002; 113: 1423-1428.
10. Gooch CL, Moisier DR. Stimulated single fiber electromyography in the mouse: techniques and normative data. Muscle Nerve 2001; 24:, 941-945.
11. Stålberg E, Falck B, Sonoo M, Stalberg S, Astrom M. Multi-MUP EMG analysis - a two year experience in daily clinical work. Electroencephalogr. Clin Neurophysiol 1995; 97: 145-154.
12. Bischoff C, Stalberg E, Falck B. Reference values of motor unit potentials recorded with decomposition EMG. Muscle Nerve 1994; 13: 247-253.

Correspondence:

Professor M.G. Clement
Department of animal pathology, section of Biochemistry and Physiology
University of Milan
Via Celoria 10, 20133 Milano
Italy

e-mail: mariagiovanna.clement@unimi.it

Biomedical Research 2004; 15 (1): 117-120

Bioactivity of isosaline stem-bark extract of *Lantana camara*

J. A. Olagunju[1], O. T. Aregbe, A. B. Sokunle and A. O. Ogunnupe

Department of Biochemistry, Obafemi Awolowo College of Health Sciences, Olabisi Onabanjo University (Formerly Ogun State University), PMB 2002, Ago-Iwoye, Nigeria

Key Words: *Lantana camara* (Labiatae), hypoglycaemia, hyperinsulinaemia, gluconeogenesis

Accepted February 9 2004

Abstract

The isosaline stem-bark extract of *Lantana camara* was investigated for its biological activity in albino rats of the Sprague-Dawley strain. Treatment of albino rats resulted in a significant reduction ($p<0.05$; $p<0.0l$) in blood glucose, liver and kidney alanine aminotransferase and aspartate aminotransferase activities, kidney alanine glucose 6-phosphatase and fructose 1,6-diphosphatase activities. While the liver glycogen was comparable rats and the kidney glycogen was significantly reduced ($p<0.05$) in the experimental rats. Also unaffected ($p>0.05$) by the treatment are the liver glucose 6-phosphatase and fructose l,6-diphosphatase activities, serum urea, total proteins, total triglycerides, pyruvate, lactate and cholesterol. The results suggest that the induced hypoglycaemia in the experimental rats probably resulted from the depressed activities of the enzymes regulating gluconeogenesis known to prevent hypoglycaemia. Since high insulin levels reduce the activities of these enzymes, it is being speculated that hyperinsulinaemia or an inappropriate plasma insulin levels and reduced gluconeogenesis induced by this extract may be responsible for the observed hypoglycaemia.

Introduction

Lantana camara (Labiatae), a cosmopolitan ornamental plant, grows throughout Tropical Africa. The plant bears orange or bright red flowers with dark blue fruits. The leaves emit a characteristic aroma and contain *lantanine*, a quinine-like alkaloid [l,2] known to be toxic and exert antispamodic property [2]. Aside from *lantanine* contained in the leaves, its seeds and leaves also contain essential oils known to exert antiseptic effects [3]. The fresh leaves also tested positive for the presence of *saponins*, *tannins* and *flavonoids* [4].

In folklore medicine, the leaves of this plant are mixed with *Ocimum*, banana leaf, *Morinda lucida* and other herbs are used as a remedy for yellow fever. This mixture is also used as febrifuge and known to exert diaphoretic action [2,5,6].

Biochemical investigations into the anti-inflammatory property of the whole plant and ethanolic extracts of its fresh leaves using a cotton-pellet anti-inflammatory bioassay technique revealed an inactivation of phosphatases and aminotransferases and stimulation of adenosine triphosphatase activities in the plasma and exudates of the experimental rats [4]. A survey of the literature however, revealed a dearth of reports on the pharmacological and biochemical effects elicited by this plant. We therefore decided to probe into the other possible biochemical effects of the isosaline stem-bark extract which could elicit an *in vivo* effects other than the ones reported earlier. This paper, therefore, reports the bioactivity of isosaline extract of the stem-bark of the plant in albino rats.

Materials and Methods

Plant Material

The stem-bark of *Lantana camara* was collected during the month of August at a location along Ile-Ife-Ibadan road, Osun State, Nigeria. The plant was botanically identified and authenticated by Dr. J. O. Faluyi of the Department of Botany, Obafemi Awolowo University, Ile-Ife, Nigeria. Specimens were air-dried at 25-27°C in the laboratory for two weeks and voucher specimens were deposited at the Herbarium (IFE).

Preparation of Plant Material

The air-dried and powdered stem-bark (558g) was homogenized and extracted by maceration in 250 ml 0.9% (w/v) NaCl solution at 4°C for 24 hours. The suspension was centrifuged at 5,000rpm for 20 minutes at room temperature after which the filtrate obtained was lyophilized to obtain a greenish-brown solid residue, which was reconstituted in 0.9% (w/v) NaCl solution to a final concentration of 400mg/ml.

Animals

Ten healthy albino rats of the Sprague-Dawley strain of either sex weighing between l20 and 200g were used. They were obtained from the Animal House Colony of the Department of Physiology, Olabisi Onabanjo University (formerly Ogun State University), Ago-Iwoye, Nigeria. The animals were housed individually and provided with a balanced diet and water *ad libitum*.

Experimental Design

The animals were divided into two groups of five rats in each each. The first group of animals was served as controls and treated with the vehicle [0.9% (w/v) NaCl solution] at a dose of lml/kg body weight, while the animals of the experimental group were treated with the extract at a sub-lethal dose of 400mg/kg body weight. The vehicle and the extracts were administered intraperitoneally once daily for 2l days. At the end of experimentation, rats were bled from the heart under anesthesia to remove blood for sera preparation after which they were sacrificed and their livers and kidneys removed and stored wet-frozen until they were ready for use.

Preparation of Liver and Kidney Homogenates

Liver and kidney homogenates (5%) were prepared as described by Olagunju *et al.* [7] except that post-mitochondrial supernatants were recovered by centrifugation at l0,000rpm for 25 minutes at 4°C in a Sorvall RC-2B Automated Refrigerated Centrifuge fitted with SS-34 rotor. The supernatants were kept wet-frozen until ready for use.

Phytochemical Screening

Tests for phytochemicals present in the extract were done according to the standard procedures described by Sofowora [8].

Biochemical Assays

Biochemical assays were carried out on the serum, liver and kidney of both the control and experimental rats. Serum urea, total proteins, total triglycerides, lactate and cholesterol were determined with the aid of Autoanalyzer (Hitachi Model), while glucose of the whole blood was measured with One-Touch® Glucometer. Serum pyruvate was determined by the method previously described by Friederman and Haugen [9].

The activities of liver and kidney alanine aminotransferase (ALT) and aspartate aminotransferase (AST) were determined by the method of Reitman and Frankel [10], while liver and kidney glycogen were isolated by the method descrived by Seifter *et al.* [11] and assayed using the procedure described by Jermyn [12]. Liver and kidney glucose 6-phosphatase activities were assayed as described by Swanson [13], while fructose l,6-diphosphatase assays were carried out according to the method of Pogell and McGilvery [14]. Inorganic phosphate was determined by the method of Fiske and SubbaRow [15], while supernatant protein assay was done according to the method of Lowry *et al.* [16].

Statistical Analysis

All data generated were expressed as Mean ± SEM and analyzed statistically using the Student's t-test [17]. All p values less than 0.05 were considered statistically significant.

Results and Discussion

The extraction of a 558g sample of the ground stem-bark of *Lantana camara* gave a yield of 22.7%. The product obtained was reconstituted in normal saline and used for the study. Our choice of the intraperitoneal route was aimed io obtain a quick biochemical response as delay may be experienced if the extract was administered orally. Besides, digestion may have modified the active principle extracted and the biochemical responses obtained may not necessarily have been due to the extracted principle but metabolite arising from its digestion.

The biological effects elicited by the isosaline stem-bark extract of *Lantana camara* in experimental albino rats are presented in Tables I and 2. No significant differences ($p<0.05$) were observed in the mean serum urea, total protein, total triglycerides, pyruvate, lactate and cholesterol in each of the two groups (i.e. the experimental and the control). However, blood glucose in the extract-treated rats decreased significantly ($p<0.05$) by 28.2% when compared to the controls (Table I). The decrease in blood glucose levels suggests that the induction of hypoglycaemia is possibly mediated by the active principles present in the extract. Phytochemical screening of the extract revealed the presence of alkaloids, saponins, tannins and flavonoids.

Table I: Effects of Isosaline Stem-Bark Extract of Lantana camara on Some Blood Parameters

Biochemical Variable	Experimental Rats	Control Rats
Serum Urea (mg/dl)	33.00±1.25	35.28 ± 0.48
Blood Glucose (mg/dl)	55.60±7.47*	77.40± 6.73
Serum Total Proteins (g/dl)	6.10 ± 0.07	6.29 ± 0.l6
Serum Total Triglycerides mg/dl)	53.42 ± l.57	54.57±1.17
Serum Pyruvate (μmol/ml)	75.45 ± l.61	77.l0±4.34
Serum Lactate (mg/dl)	0.99 ± 0.01	0.99±0.02
Serum Cholesterol(mg/dl)	77.59 ± 0.71	76.82±0.53

Each value represents Mean ± SEM
**Significantly different from control at p<0.05*

Liver alanine aminotransferase and aspartate aminotransferase activities were significantly reduced ($p<0.05$) by 14.5% and 18.5%, respectively (Table 2). Liver glucose 6-phosphatase and fructose 1,6-diphosphatase activities were, however, comparable in the extract-treated rats and controls. In the kidney, both alanine aminotransferase and aspartate aminotransferase activities were significantly reduced ($p<0.05$; $p<0.01$) by 15.6% and 33.5%, respectively. Kidney glucose 6-phosphatase and fructose 1,6-diphosphatase activities were also significantly reduced ($p<0.05$) by 19.7% and 21%, respectively. While the liver glycogen remained unaffected in both the extract-treated rats and the controls. The kidney glycogen was significantly increased ($p<0.05$) by 27.1% in the extract-treated rats suggesting increased glycogenesis in the kidney (Table 2). All these biochemical changes in the experimental rats were suspected to have been induced by the extract.

Table 2: Effects of Isosaline Stem-Bark Extract of Lantana camara on Some Liver and Kidney Enzymes and Glycogen

Biochemical Variable	Experimental Rats	Control Rats
Liver Alanine Aminotransferase (U/mg Protein/min)	3.12± 0.29*	3.65± 0.39
Liver Aspartate Aminotransferase (U/mg Protein/min)	1.85± 0.20*	2.27± 0.19
Liver Glucose 6-Phosphatase (U/mg Protein/min)	0.123±0.01	0.120± 0.01
Liver Fructose l,6-Diphosphatase (U/mg Protein/min)	0.180±0.01	0.184± 0.01
Liver Glycogen (mg/l00g Wet Wt.)	2.82± 0.61	2.79± 0.58
Kidney Alanine Aminotransferase (U/mg Protein/min)	3.36+ 0.44*	3.98± 0.20
Kidney Aspartate Aminotransferase (U/mg Protein/min)	1.23±0.18**	1.85± 0.12
Kidney Glucose 6-Phosphatase (U/mg Protein/min)	0.49± 0.02*	0.61± 0.02
Kidney Fructose l,6-Diphosphatase (U/mg Protein/min)	0.124±0.01*	0.157±0.01
Kidney Glycogen (mg/l00g Wet Wt.)	2.11± 0.08*	1.66± 0.11

Each value represents Mean ± SEM of five rats
**Significantly different from control at p<0.05*

It is a well-established fact that blood glucose concentration is maintained within relatively narrow limits through a tightly controlled balance between glucose production in the fed state and utilization in fasting and post-absorptive states with the liver playing a central role in normal glucose homeostasis [18]. In addition to the role of the liver in maintaining glucose homeostasis, the interaction between insulin and glucagon also regulates blood glucose concentrations in the fed and post-absorptive states with insulin enhancing glucose storage by promoting gycogenesis, lipogenesis and protein synthesis, and thus capable of inducing hypoglycaemia, while glucagon functions primarily to prevent hypoglycaemia by stimulating glycogenolysis and gluconeogenesis [19].

Drug-induced hypoglycaemia has been widely reported. Sulphonylurea drugs either singularly or in combination with other drugs account for the majority of drug-induced hypoglycaemia in diabetic patient [20]. Salicylate overdose has been associated with hypoglycaemia in children while quinine has also been shown to stimulate insulin secretion and its intravenous use in the treatment of *falciparum* malaria has been associated with profound hypoglycaemia [19]. The fact that a quinine-like alkaloid, *lantanine*, had earlier been identified in *Lantana camara* [l,2]. It is not unlikely that this substance or related ones may be present in the extract which may be responsible for the hypoglycaemia induced in the rat.

Various mechanisms have been proposed for drug-induced hypoglycaemia. Most commonly implicated is hyperinsulinaemia or inappropriate plasma insulin levels due to non-clearance of insulin from circulation [19,21,22]. Insulin is known to inhibit gluconeogenesis, a condition that is known to prevent hypoglycaemia. It is also well known that the aminotransferases, glucose 6-phosphatase and fructose 1,6-diphosphatase are stimulated during gluconeogenesis [18]. In the present study, key enzymes of gluconeogenesis (i.e., alanine aminotransferase, aspartate aminotransferase, glucose 6-phosphatase and fructose 1,6-diphosphatase) were significantly reduced in the kidney. It is not unlikely that some active principles in this extract may cause hyperinsulinaemia leading to the depressed activity of the enzymes regulating gluconeogenesis and hence, leading to hypoglycaemia.

Kidney glycogen in this study was also significantly increased in the experimental rats. Insulin is also known to promote glycogenesis, while in the process can induce hypoglycaemia [19]. The increased insulin levels induced by the extract may probably stimulate the significant increase in kidney glycogen. All these observations indirectly tend to support the fact that hyperinsulinaemia or inappropriate plasma insulin levels may be responsible for the observed hypoglycaemia in the experimental rats.

The situation appears to be a little bit different in the liver. While the activities of the key enzymes of gluconeogenesis were depressed in the kidney, only the activities of the aminotransferases were depressed by the extract in the liver. The activities of glucose 6-phosphatase and fructose 1,6-diphosphatase as well as glycogen were not affected in the experimental rats (Table 2). Since the liver is the major organ that regulates the level of blood glucose through gluconeogenesis and glycogenolysis, it is therefore expected that the high insulin levels possibly induced by the extract could possibly affect the liver more than any other organ of the body. In the present study, while the activities of insulin-regulated enzymes were reduced in the kidney, the enzymes showed some resistance in the liver possibly in a way of resisting hypoglycaemia induced by the extract. The implication of these observations is that the liver and the kidney enzymes may exhibit differential sensitivities to insulin regulatory effect. The sparing effect on the activities of the liver enzymes in preference to those of the kidney may be a compensatory mechanism to oppose what could lead to a more severe hypoglyceamia than presently observed in the extract-treated rats. However, the reduction in the activities of alanine aminotransferase and aspartate aminotransferase in the liver of the experimental rats possibly suggests the impaired delivery of precursors of gluconeogenesis to the gluconeogenic pathway, a pathway whose operation is important in preventing hypoglycaemia.

The data obtained in the present study are therefore, consistent with the fact that hyperinsulinaemia or inappropriate plasma insulin levels may be responsible for the observed hypoglycaemia in the experimental rats. It is possible that certain active principles are present in the extract that induce an excess of insulin production or prevent insulin clearance from the blood. Further studies by way of measuring hormonal changes induced by the extract in the treated rats will certainly elucidate the mechanism of induction of hypoglycaemia evident by the treatment with the extract of *Lantana camara*.

References

1. Tyler VE, Brad LR, Roberts JE. Poisonous plants. In: *Pharmacognosy, 8th Edition*, Lea and Febiger, Philadelphia 1981; 449-467.

2. Oliver-Bever B. Medicinal plants in tropical West Africa. 2. Plant acting on nervous system. Journal of Ethnopharmacology 1983; 7: I-93.
3. Loun PGJ. Lantaden A: The active principle of *Lantana camara*. Ondestepoort Journal of Veterinary Sciences 1949; 24: 321-329.
4. Oyedapo OO, Sab FC, Olagunju JA. Bioactivity of fresh leaves of *Lantana camara*. Biomedical Letters 1999; *59*: I75-I83.
5. Thomas OO. Perspectives of ethno-phytotherapy of Yoruba medicinal herbs and preparations. Fitoterapia 1989; LX: 49-60.
6. Dalziel JM. *The useful plants of West Tropical Africa*. Crown Agents for Overseas Government and Administration, Milbank, London 1959; 223-224.
7. Olagunju JA, Jobi AA, Oyedapo OO. An investigation into the biochemical basis of the observed hyperglycaemia in rats treated with ethanol root extract of *Plumbago zeylanica*. Phytotherapy Research 1999; 13: 346-348.
8. Sofowora A. In: Medicinal plants and traditional medicine in Africa, 2nd Edition, Spectrum Books Limited, Ibadan 1993; 150-152.
9. Friederman TE, Haugen GE. The determination of keto acids in blood and urine. J Biol Chem 1943; 147: 415-442.
10. Reitman S, Frankel S. A colorimetric method for the determination of glutamic oxaloacetic and glutamic pyruvic transaminases. Am J Clin Path 1957; 28: 56-66.
11. Seifter S, Dayton S, Novic B, Muntwryler E. The estimation of glycogen with anthrone reagent. Arch Biochem 1950; 25: 191-199.
12. Jermyn MA. Increasing the sensitivity of the anthrone method for carbohydrate. Analyt Biochem 1975; 68: 322-335.
13. Swanson MA. Glucose-6-phosphatase from liver. In: *Methods* in Enzymology, *Vol. 2*. Academic Press, Inc., New York, 1955; 541-543.
14. Pogell BM, McGilvery RW. Fructose-l,6-diphosphatase from liver. J Biol Chem 1954; 208: I49-I52.
15. Fiske CH, SubbaRow Y. The colorimetric determination of phosphorus. J Biol Chem 1925; 66: 375-385.
16. Lowry ON, Rosebrough NJ, Farr L, Randell RJ. Protein measurement with folin-phenol reagent. J Bioll Chem 1951; 193: 265-275.
17. Snedecor GW. *Statistical Methods, 5th Edition*, The Iowa State College Press, Amees, Iowa, 1956; 52-62.
18. Newsholme EA, Start C. Regulation of carbohydrate metabolism in the liver. In: *Regulation in Metabolism*, John Wiley & Sons, New York, 1976; 247-292.
19. Labib M. Hypoglycaemia. In: Clinical Biochemistry-Metabolic and Clinical Aspects. (Marshall, W. J. and Bangert, S. K., Eds.), Churchill Livingstone, New York, 1995; 281-294.
20. Marks V, Rose FC. *Hypoglycaemia, 2nd Edition*. Blackwell Scientific Publications. 1981; 225-247.
21. Service FJ. *Hypoglycemic Disorders*. G. K. Hall Medical Publishers, 1983; 127-141.
22. Cryer PE, Gerich, JE. Glucose counter regulation, hypoglycemia and Intensive insulin therapy in diabetes mellitus. New England J Med 1985; 313: 232-241.

Correspondence:

Dr. J. A. Olagunju
Department of Medical Biochemistry
Lagos State University College of Medicine
PMB 21266, Ikeja-Lagos
Nigeria

e-mail: joelagus@yahoo.com
Phone: +234-1-4735199

Biomedical Research 2004; 15 (2): 121-127

Structural and biochemical changes induced by chronic chloroquine administration in the liver of rabbits

A.A Ngokere[1]* and T.C. Ngokere[2]

Departments of Morbid Anatomy[1], Medicine[2], College of Medicine, University of Nigeria Teaching Hospital, Enugu, Nigeria.

Key words: Histology, liver, cholesterol, enzyme, Ngokere bodies .

Accepted 27 October 2003

Abstract

The histopathologic and biochemical changes produced by chloroquine phosphate in the liver in doses 3, 10 and 15mg/kg over 30, 60 and 90 days in the albino (n = 10) and pigmented (22) rabbits with mean weight value of 1.46± 0.44kg and mean age value of 9.0± 0.25 months were investigated in the college of medicine, University of Nigeria, Enugu Campus, Enugu. Histology results showed chloroquine – induced lesions in the liver. Mixed cells infiltration of the liver parenchyma, proliferation of the bile ducts, presence of 'Ngokere' inclusion bodies which were argyrophilic, sinusoidal dilatation, haemorrhage and parenchymal cell degeneration were evident. On the otherhand, total serum cholesterol levels showed statistically significant (P< 0.05) decreases at different periods of the study. Acid phosphatase in the serum of both the kidney and liver tissues was also significantly elevated (P< 0.05) at different periods of the study. The histologic findings in the present study were in agreement with the biochemical observations. Chloroquine should be administered with circumspection in view of its toxic potential.

Introduction

Chloroquine (CHQ) has been widely used in man for the treatment and suppression of malaria and for prolonged treatment of chronic diseases such as rheumatoid arthritis, discoid lupus and systemic lupus erythematosus [,2]. Malaria continues to represent a major public problem in tropical countries in terms of geographical spread, high mortality and severe morbidity, especially among children. Two billion people, or about 40 percent of the worlds population, live in the 90 countries at risk [3]. Global estimates of the malaria disease burden for 1992 indicated at least 300-500 million clinical cases were recorded annually, 90% of them in sub-Saharan Africa.

The retinal changes described consist of impaired central vision, peripheral constriction of the visual field, marked attenuation of the retinal vasculature, pigmentary changes of the macula, peripheral pigmentary and retinal edema [4]. Wetherholm and Winter (5) described the retinal changes as a destructive loss of the rod and cone elements with accumulation of pigment-laden cells in the outer nuclear and plexiform layers, whereas Bernstein and Ginsberg [6] have described it as a destruction of the rods and cones and a migration of pigment clumps from the pigmented epithelium to the inner nuclear layer. The first case of chronic cardiac toxicity due to an antimalarial agent, chloroquine phosphate, was reported in 1971 and since then several cases of heart failure, restrictive cardiomyopathy or atrioventricular block have been ascribed to this family of drugs [7]. Although Histologic studies were not performed in their patient, the clinical evidence of toxicity, absence of underlying heart disease and fairly young age of the patient pointed to chloroquine toxicity. Recently numerous cytoplasmic inclusions or "myeloid" bodies were observed in all neurons and in the retinal ganglion cells of rats given chloroquine 3 to 6 months. These bodies were identified as lysosomal in origin by localization of acid phosphatase activity [8]. Such bodies have also been demonstrated in the liver cells following acute and chronic chloroquine administration [8,9]. In both reports these bodies were attributed to lysosomal autophagy. Chloroquine has been known to cause an increase in phospholipid and a significant decrease in the activities of mitochondrial inner membrane enzymes in the liver such as NADH dehydrogenase, succinate dehydrogenase and cytochrome C Oxidase [10]. Their results confirm drug-induced inhibition of mitochondrial respiration, thereby impairing availability and utilization of energy. Amodiaquine, an analogue of chloroquine has been found to cause adverse side effects such as agranulocytosis and liver damage and the observed drug toxicity is believed to be related to the formation of an electrophilic metabolite, which can bind to cellular macromolecules and initiate hypersensitivity reactions [11].

Plethora of literature on chloroquine –induced histologic lesions of organs and tissues exists, little information on its histologic and biochemical effects on the liver warrants the present study. In the current study, ascertaining the clinical observation, gross, biochemical and light microscopic changes induced by chloroquine

phosphate in rabbits was intended. The onset of toxicity and its relationship with dose as well as the pattern of progression of chloroquine- induced lesions with time was determined.

Materials and Methods

Animals

Thirty-two specific – pathogen free (SPF) rabbits each approximately 9 months of age, 22 pigmented and 10 albino were bought from the veterinary house, Ogbete, Enugu, Nigeria and kept in the animal house of the college of Medicine, University of Nigeria, Enugu Campus for 4 weeks for acclimatization. They were housed in bottom – wired stainless metal cages and were allowed food and tap water ad libitum. Individual identification of the animals was by metal ear tags. Rooms were well ventilated and constantly maintained at room temperature. The Pfizer Pharmaceutical company Ltd., Nigeria supplied drugs used in this study.

Experimental Design

The experimental animals were divided into 4 groups comprising 8 sex-matched rabbits in each of the 4 groups. Those in groups 1, 2, and 3 constituted the test groups, whereas the 4th group acted as the control. The animals in group 1 were given doses of chloroquine 5mg/kg daily. The animals in group 2 received 10mg/kg (twice the dose). While the 3rd group received 15mg/kg (thrice the dose), all given intraperitoneally dose daily for a period of 90 days. The 4th group received equal volume of normal saline daily.

Experimental Procedure

The rabbits were weighed fortnightly and the weights recorded. Blood samples were taken from the marginal ear vein for enzyme and cholesterol parameters prior to drug administration. Thereafter, similar samples were collected at days 30, 60, and 90. Blood samples collected prior to drug administration produced enzyme and cholesterol values which represented the baseline value. Two animals from each of the test groups and two from the control group were painlessly sacrificed after 30, 60 and 90 days. All the rabbits were still living when the study terminated and were anaesthetized by intraperitoneal injection of sodium thiopentane and were exsanguinated. Necropsies were performed immediately. Representative samples of the liver were fixed promptly in 10% neutral formal saline, histologically processed, embedded in paraffin wax, sectioned at 5μ thick using Rotary microtome and stained by both Haematoxylin and Eosin (H&E) (12) and Gordon and Sweet (13) techniques respectively.

Statistical Analysis

The results were expressed as mean ± SEM and significance of differences between control and treated as well as before and following treatment for enzyme and serum cholesterol parameters were determined using paired student
t-test and one-way analysis of variance (ANOVA). Statistical significance was set at $P< 0.05$.

Sample Collection

Whole blood samples were collected for serum cholesterol and kidney and liver acid phosphatase estimation in plain test tubes. The animals were fasted overnight before collecting blood samples for serum cholesterol estimation.

Biochemical Analysis

The method used for the estimation of serum cholesterol was according to Zak and his colleagues [14]. The method of Gutman and Gutman [15] was used in the estimation of non-prostatic acid phosphatase in the serum.

Results

Clinical Observation

Clinical changes were observed in all the animals receiving chloroquine phosphate. The most consistent clinical findings were sluggishness, depressed appetite, especially in group 3, and poor general appearance. Group 1 received chloroquine phosphate in the amount of 5mg/kg with no apparent ill effect. Two animals in this group lost weight after the first 2weeks of the drug administration. The rest of the animals also maintained consistent slight weight loss till sacrifice. Overall, all the animals except those mentioned above, had slight weight losses during the treatment period. On the first day of chloroquine administration, one gravid rabbit in group 2 spontaneously aborted one fetus 3 hours later, whereas on the 9th day of treatment, 2 of 8 animals aborted in group 3.

The obvious clinical changes in the rabbits in the groups were mild dermatitis which affected more of the albino rabbits than the pigmented and hyperpigmentation of the faces. Onset of dermatitis was at day 65 and involved entire body which was found dry and scurfy with prominent loss of hair in most albinos and in some of the pigmented on which bleaching of hair was also observed. All the rabbits in all the groups survived the treatment regimen and generally experienced slight weight losses and some losses throughout the test period. The rabbits in the control group appeared in excellent health condition throughout the period of study.

Gross Pathology

Multiple haemorhages were seen in the heart, lungs and in the stomach. These observations were especially noted in the animals in groups 2 and 3 particularly. Alopecia, dermatitis and hyperpigementation occurred in the rabbits in all the groups. Bullae were observed on the abdominal regions of the animals in all the study groups particularly 2 and 3. After some days the bullae were observed to have ruptured and the site ulcerated. Shortly after, the ulcers healed with scar tissue formation. At necropsy, all the animals in groups 2 and 3 showed ulcerated mucosa of the stomach with no overt macroscopic haemorhage. Liver of the animals in group 3 showed yellowish discoloration. Kidney showed cortical depressions and slight shrunkenness in some instances.

Histopathology and Histochemistry

Light microscopy of the liver section showed periportal fibrosis with mononuclear infiltration and architectural disorganization in all the treated groups. There was obvious and frank centrolobular necrosis in liver of all the animals in the test groups. All liver necropsy sections of the animals showed sinusoidal dilatation with parenchymal infiltration of mononuclear cells suggestive of reactive hepatitis.

Histochemical demonstration of the tissue by Gordon and Sweets revealed total architectural loss of the liver reticular framework. This finding was indicative of severe liver damage as shown in Fig. I. Interestingly but surprisingly 2 of 18 sacrificed rabbits revealed well circumscribed solitary structure. This structure, stained by Haematoxylin and Eosin (H&E) and Gordon and Sweets respectively showed thick fibrous band heavily permeated with chronic inflammatory infiltrates as shown in Figures 2a and 2b. In the center of the ovoid structure were found numerous eosinophilic membranous oval-shaped or round laminated or whorled bodies. Similar bodies were also found at various locations within the fibrous band and were also argyrophilic. The bodies were not found within the cytoplasm of hepatic cells but rather, perhaps, fused and found in the parenchyma of the rabbits liver administrated 10mg/kg chloroquine in the first 30 days of the study. Identical bodies called membranous cytoplasmic bodies or "myeloid" bodies were usually found in the cytoplasm of hepatic cells and other tissues in chloroquine- administrated animals. Since this finding was made outside the cytoplasm of hepatocytes, it should be distinguished from the well-documented bodies by being called "Ngokere" bodies, since, in this study, the bodies were found at 5μ thick, unlike the 'myelin" figures found at ultrathin sections of 1μ or at electron microscopic level. The liver necropsies of both the 10mg and 15mg/kg treated groups showed proliferation of the bile ducts, intraportal fibrosclerosis, haemorrhage and parenchymal cell degeneration.

Biochemical Findings

Table 1 shows the serum cholesterol profile of baseline and test mean values at 5, 10, and 15mg/kg doses. Accordingly, the baseline and test mean values at 5mg/kg dose were 2.46± 0.09, and 1.44 ± 0.07, 10.3 ± 0.08 and 1.03± 0.05 at days 30, 60 and 90 respectively. Although the analysis of variance (ANOVA) was not statistically significant at P = 0.0909, there were statistically significant decreases of test over the baseline mean value at P< 0.0001, P < 0.001 and P< 0.0001 at days 30, 60 and 90 respectively. This result showed that 5mg/kg chloroquine administration produced statistically significant decrease in serum cholesterol level over the period of study and this fall in level was dose and not time dependent.

Table 1: Mean (Mean ± SEM) Values of serum cholesterol (MMOL/L).

group	Baseline	day 30	P value	Day 60	P value	Day 90	P value	ANOVA
1.	2.46 ± 0.09	1.44 ±0.07	P < 0.0001	1.03 ±0.08	P < 0.0001	1.03 ±0.05	P< 0.0001	P = 0.09
2.	3.26 ±0.43	1.96 ±0.19	P = 0.0141	1.42 ±0.20	P = 0.0057	0.75 ±0.06	P = 0.0023	P = 0.03
3.	2.5 ±0.12	1.38 ±0.10	P = 0.0001	0.95 ±0.11	P = 0.0001	0.73 ±0.11	P = 0.0001	P=0.005
4.	2.7 ±0.12	2.7 ±0.11	2.62 ±0.05	2.73 ±0.09	-	-		

**P<0.05 Considered Significant*

Table 2: Mean (Mean ± SEM) Values of Non Prostatic Phosphatase (IU/L)

Group	Baseline	day 30	P value	Day 60	P value	Day 90	P value	ANOVA
1.	5.25± 0.14	7.6 ±0.77	P = 0.0088	8.85 ±0.94	P = 0.009	8.05±0.14	P = 0.0006	P= 0.38
2	4.49 ±0.24	7.61±0.67	P = 0.0007	9.63±114.14	P= 0.0003	12.23±0.93	P = 0.0001	P= 0.15
3.	4.49±0.19	5.98±0.14	P < 0.0001	9.52±0.70	P < 0.0001	10.98±0.76	P< 0.0001	P< 0.0001
4.	4.74±0.11	4.71±0.11	-	4.83±0.12	-	4.85±0.10		

**P<0.05 Considered Significant*

The baseline and test mean values were 3.26± 0.43 and 1.96 ± 0.19, 1.42 ± 0.20 and 0.75 ± 0.06 at days 30, 60 and 90 respectively which showed statistically significant decreases over the baseline at P = 0.0141, P = 0.0057 and P = 0.0023 respectively in the 10mg/kg dose category. The ANOVA was statistically significant at P = 0.0253. These results showed that the 10mg/kg dose induced a significant fall in serum cholesterol level which was both dose and time dependent over the period of study.

The table also represents the baseline and test mean values which were 2.5± 0.12, and 1.38± 0.10, 0.95± 0.11, and 0.73 ± 0.11 at dose 15mg/kg. This result showed that there were statistically significant decreases in serum cholesterol levels at P =

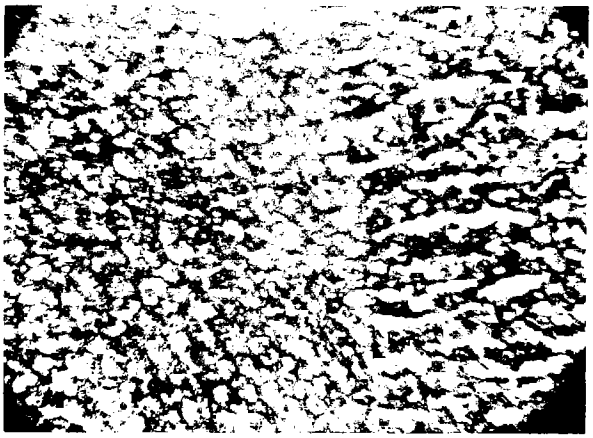

Fig. I: represents liver necropsy sections from all the dose regimen which revealed total architectural derangement of reticular framework of the parenchyma. This lesion is suggestive of liver damage. Stained by Gordon & Sweets method. X 100.

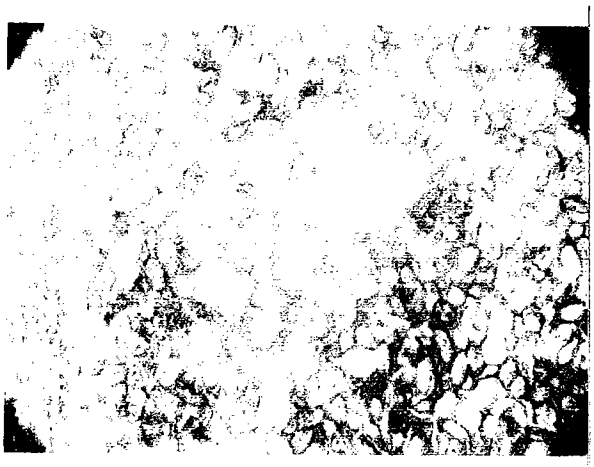

Fig. 2a: shows liver necropsy section displaying the "Ngokere" inclusion bodies circumscribed by thick fibrous band heavily infiltrated by mononuclear cells. Similar bodies are also discernible at different sites within the fibrous band. Stained by H & E technique. X 100.

0.0001, P = 0.0001 and P= 0.0001 at days 30, 60 and 90 respectively. The ANOVA was significant at P= 0.0052. In all, the result has shown that 15mg/kg dose of CHQ produced a very significant decrease in serum cholesterol level over the period of study and were both dose and time dependent.

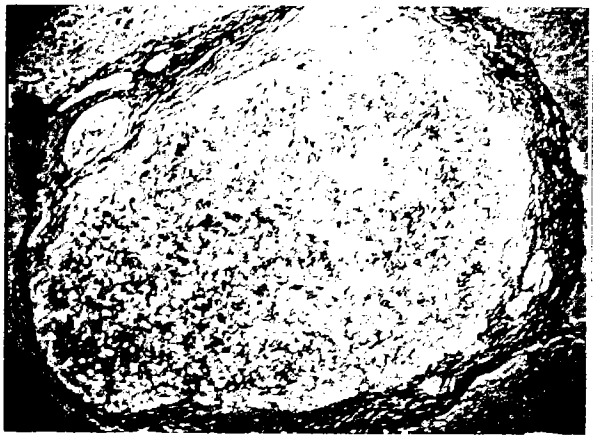

Fig. 2b: Shows liver necropsy section from the 10mg/kg dosed rabbit at day 30 displaying similar features as in Fig. 2a but are argyrophilic. Stained by Gordon & Sweets' silver impregnation technique. X. 100

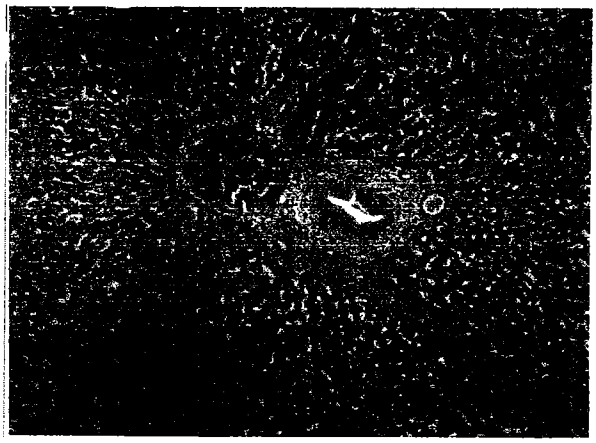

Fig. 3a: Figure represents liver necropsy section of the untreated rabbits showing normal architecture. Stained by H & E technique. X 100

Fig. 3b: Figure represents liver section from the control rabbit showing normal architecture of simusoidal reticulin meshwork. Stained by Gordon & Sweets technique. X 100.

Fig. 1: Mean values of Serum Cholesterol

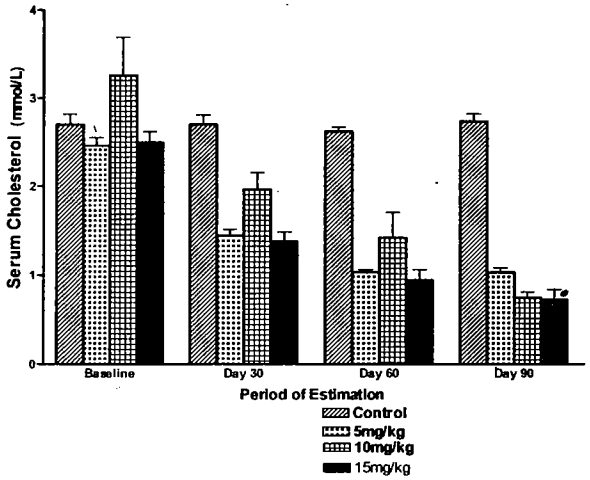

Fig. 2: Mean values of Acid Phosphatase

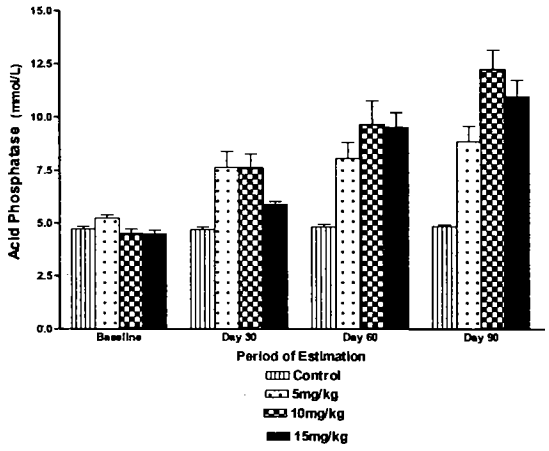

Table 2 reflects the non prostatic acid phosphatase profile of 5mg, 10mg and 15mg/kg doses of CHQ administration. The baseline value was 5.25± 0.14, and at dose 5mg/kg the test mean values were 7.6± 0.77, 8.85± 0.94 and 8.05 ± 0.14 I.U/L at days 30, 60 and 90 respectively. This showed statistically signify-cant increases over the baseline at P = 0.0088, P = 0.009 and P = 0.0006 respectively. However, the ANOVA was statistically not significant at P = 0.3768 which showed that 5mg/kg dose produced a statistically significant elevation in acid phosphatase level in circulation which was dose but not duration dependent The table also shows the baseline and test mean values at 10mg/kg dose of CHQ were 4.49± 0.24 and 7.61 ± 0.67, 9.63 ± 1.14 and 12.23 ± 0.93 I.U/L at days 30, 60 and 90 respectively. These results showed that there were statistically significant increases in serum acid phosphatase levels at P = 0.0007, p = 0.0003 and P <0.0001 at the different periods of the study.

The ANOVA was at P = 0.1459. This showed that the rise in non-prostatic acid phosphatase level was only dose and not time dependent.

The table also displays the acid phosphatase profile at 15mg/kg dose over the period of study. The baseline and test mean values were 4.49 ± 0.19, and 5.89 ± 0.14, 9.52 ± 0.70 and 10.98 ± 0.76 at days 30, 60 and 90 respectively. It was observed that this dose produced statistically significant increases in mean values of test over the baseline at P < 0.0001, P < 0.0001 and P < 0.0001 at the different periods of study.

The ANOVA stood at P < 0.0001. These results indicate that the rise in acid phosphatase level at 15mg/kg dose was both dose and time dependent.

Discussion

In view of the prevalence of the diseases such as rheumatoid arthritis, systemic lupus erythematosus and liver amoebiasis in this part of Nigeria, we decided to administer the dose regimen to the experimental animals as shown in the current study. Since the treatment of these diseases, aside from malaria, lasts for a long period of time we also decided to undertake a chronic study to determine the cumulative toxic effect of chloroquine in the liver of rabbits. However, our treatment regimen is in conformity with that of Wilkinson and his colleague [15].

It has been the general impression that chloroquine (CHQ) toxicity was limited to retinopathy and cardiomyopathy following our observation and little experience of chloroquine effects over the years. The current study has shown that chloroquine administered in doses of 5, 10 15mg/kg daily over 90 days caused hepatic damage, nerosis, mononuclear cell infiltration of the liver parenchyma, haemorrhage as well as periportal fibrosis and disorganization of the architecture at this area. Ovoid bodies limited by fibrous band heavily infiltrated by chronic inflammatory cells and containing varied membranous structures without obvious nuclear or any other substance and which proved to be argyrophilic were discerned. Previously "myeloid" or "membranous cytoplasmic bodies" had been identified in the liver of rats fed chloroquine [9]. In their case, these inclusion bodies were identified at 1μ ultrathin or electron microscopic levels in the cytoplasm of the hepatocytes but in our series, the "Ngokere" bodies so named because not only were they identified by silver impregnation method at $5\mu_m$ section thick level but they were also seen outside the cell cytoplasm and were diffusely distributed in hepatic parenchyma. These findings suggest an increase in the synthesis of lysosomes and increase in their autophagic activity, but the persistence and continual accumulation of these membranous structures indicates that digestion was partial and incomplete at best. Formation of new lysosomes does appear to be a primary feature of chloroquine toxic effect. Whether alteration of organelle membranes was due to the attered lysosomal activity or whether the increase in lysosomal autophagy was a response to changes in organelle membranes is still open to speculation. That membranous organelles were damaged and contributed to the formation of the membranous inclusions was supported by the observation that the location of the inclusions was most consistently related to areas within the cell. Present knowledge indicates that CHQ toxic effect produces a widespread membrane alteration, which is probably associated with

abnormal or increased lysosomal activity. The basic cytoplasmic lesion probably results from widely distributed cellular injury in chloroquine toxicity. The origin of these "Ngokere" inclusion bodies, their significance in relation to cell function, and the basic biochemical pathogenesis of this lesion are presently the subject of further investigation.

The current investigation has also demonstrated that CHQ administration at both 5,10, and 15mg/kg doses induced statistically significant decrease in serum cholesterol levels of the liver and kidney respectively. The fall in serum cholesterol levels, in this case, was dose dependent and time dependent from 10mg/kg up to 15mg/kg dose. Numerous population studies have linked elevated concentration of total cholesterol or Low-density lipoprotein (LDL)- cholesterol in serum with inceased incidence of atherosclerotic events [16,17].

It has been further shown that the clinical complications of atherosclerosis could be diminished and life prolonged when plasma lipids are lowered by hypocholesterolemic agents [18,19, 20]. Many drugs with proven hypocholesterolemic activity are available clinically to ameliorate cases of individuals with premature arterosclerosis and those with other risk factors such as hypertension or diabetes mellitus [21]. The present work has shown that CHQ administration caused marked elevation of acid phosphatase level at different periods of the study. This biochemical finding is strongly reinforced by the histologic finding of the presence of "Ngokere" bodies which are also inclusion bodies due to hepatic lysosomal damage associated with increased acid phosphatase production. It was also observed that acid phosphatase increases were only dose dependent for the first 60 days, whereas it became both dose and duration dependent at 15mg/kg dose of administration of chloroquine.

The plausible explanation for the significant decrease in serum cholesterol and increase in acid phosphatase levels can be derived from the works of Filkins [22] and Stein et al [23]. Filkins observed that CHQ administered intraperitoneally (IP) to 300± 20g rats was at doses of 1, 5, 10, 15 and 25mg/kg elicited moderate to marked lysosomal activities of acid β- glycerophosphatase in either liver homogenates or large granule fraction (autophogy). In another study, Stein et al noted rapid disappearance of cholesterol ester- labeled human very low density liprprotein (VLDL), enriched with cholesterol ester by preincubation with unlabeled erythrocytes was also cleared from circulation at rapid rate. In their view, cholesterol ester labeled VLDL seemed more appropriate to evaluate the effect of CHQ on the hydrolysis of the lipid portion of VLDL remnants. Their findings indicate that acid phosphatase participates in the degradation of VLDL cholesterol ester. It was further explained that the different degree of inhibition of degradation of various lipoproteins obtained in the presence of high concentrations of CHQ suggests that other capthepsins, which are not inhibited by CHQ, participate also in the catabolism of these lipoproteins. Accordingly, cathepsin has been shown to degrade dog high-density lipoprotein (HDL), and since this enzyme is not inhibited by CHQ, it seems it might have participated also in the degradation of lipoproteins containing apolipoprotein AI. Histologically, it was observed, in this series, that silver impregnation of the liver necropsy sections showed reticulin fibres with architectural derangement. This finding is indicative of liver damage and a significant increase in serum cholesterol levels would have been expected, but for the lysosomal membrane destruction induced by CHQ administration, which produced elevated levels of acid phosphatase which, on the otherhand, caused the degradation of cholesterol ester and VLDL to produce a significant fall in cholesterol in systemic circulation in the rabbits.

Our finding suggests that CHQ therapy could be useful in artherosclerosis treatment but its overall toxicity constitutes a source of worry.

Acknowledgement

We thankfully acknowledge the wonderful advice of Dr. Anselem A. Ofodile in the preparation of this manuscript. We are also indebted to Benjamin Nworji and his team of workers for procuring and caring specially for the animals in the animal house. We gratefully appreciate the effort of Victor Orieji in bleeding the animals and the assistance of Gideon Ekeoma in the secretarial work.

References

1. Goldman L, Preston RH. Reactions to chloroquine observed during the treatment of various dermatologic disorders. Amer J Trop Med 1957; 6: 654-657
2. Seideman P, Albertoni F, Beck O, Eksborg S, Peterson C. Chloroquine reduces the biovailability of methotrexate in patients with rheumatoid arthritis: A possible mechanism of reduced hepatotoxicity. Arthritis –Rheum. 1994; 37: 830- 833.
3. World Health Organisation: World Malaria Situation in 1992. Weekly epidemiological record 1994, 309-314
4. Kellner U, Kraus H, Foerster MH. Multifocal ERG in chloroquine retinopathy: regional variance of retinal dysfunction. Graefes-Arch-Clin-Exp-Ophthalmol 2000; 238: 94-97.
5. Wetherholm DH, Winter FC. Histopathology of chloroquine retinopathy. Arch Ophthal 1964; 71: 238-245.
6. Bernstein WN, Ginsberg J. The pathology of chloroquine retinopathy Arch Ophthal 1964; N.Y. 71: 238-240
7. Guedira N, Hajjaj Hassouni N, Srairi JE, El-Hassani S, Fellat R, Benomar. Third degree atrioventricular block in a patient under chloroquine therapy. Rev-Rhum-Engl- Ed 1998; 65: 58-62.
8. Abraham R. Hendy RJ. Effects of chloroquine treatment on lysosomes of rat liver cells. Exp Molec Path 1979; 12: 148-149
9. Abraham R, Hendy RJ Grasso P. Formation of myeloid bodies in rat liver lysosomes after chloroquine administration. Exp Molec Path 1968; 9: 121-128.
10. Deepalakshmi PD, Parasakthy K, Shanthi S, Pvaraj NS. Effect of chloroquine on rat liver mitochondria. Indian J Exp Biol 1994; 32: 797-799.
11. O'Neill PM,; Harrison AC, Storr RC, Hawley SR, Ward SA, Park BK. The effect of fluorine substitution on the metabolism and anti malarial activity of amodiaquine. J Med Chem. 1994; 37: 1362-1370.
12. Ehrlich P. Staining of tissue general structures. Z WissMikr 1886; 3: 150.

13. Gordon H, Sweets HH. Demonstration of reticulin fibres. Amer J Path 1936; 12: 545.
14. Zak B, Slatkis A, Boyle AJ. Serum cholesterol estimation. J Lab Clin Med 1957; 4: 486.
15. Wilkinson RJ, Davidson RN. Drug therapy of falciparum malaria- present practice and future prospects. JAMA 1996; 380: 1-3.
16. Goldstein JL, Schrott HG, Hazzard WR, Bierman EL, Motulsky AG. Hyperlipidemia in coronary heart disease 11. Genetic analysis of lipid levels in 176 families and delineation of a new inherited disorder, combined hyperlipidemia. J Clin Invest 1973; 52: 1544-1568.
17. Keys A. Coronary heart disease, the global picture. Artherosclerosis 1975; 22: 149-192.
18. Lipid Research Clinics Program. The lipid research clinics coronary primary prevention trial results 1. Reduction in incidence of coronary heart disease. JAMA 1984a; 251: 251 - 364.
19. Lipid Research Clinics Program. The lipid research clinics coronary primary prevention trial results II. The relationship of reduction in incidence of coronary heart disease to cholesterol lowering. JAMA 1984b; 251: 365-374.
20. Helsinki Heart Study. Primary prevention trial with gemfibrozil in middle-aged men with dyslipidemia. New Engl J Med 1987; 317: 1237-1245.
21. Brown SB, Goldstein JL. Drugs used in the treatment of hyperlipoproteinemias in: Gilman AG, Rall TW, Nies AS, Taylor P (Eds.), Goodman and Gilman's Pharmacological Basis of the therapeutics 1992 Vol 1, 8th ed. McGraw-Hill Inc New York PP 874-894.
22. Filkins JP. Comparison of in vivo and in vitro effects of chloroquine on hepatic lysosomes. Biochemical Pharmacology 1969; 18: 2655-2660
23. Stein Y, Ebin V, Baron H, Stein O. Chloroquine induced interference with degradation of serum lipoproteins in rat liver studied in vivo and in vitro. Biochimica Biophysica Acta 1977; 486-497.

Correspondence:

Dr. A.A. Ngokere
Department of Morbid Anatomy
University of Nigeria Teaching Hospital
Enugu, Nigeria

e-mail: ngokereaa@yahoo.com

Biomedical Research 2004; 15 (2): 128-133

Exposure of thermophilic actinomycetes and development of hypersensitivity pneumonitis in agro-workers

Asif Hasan and Mohd. Saghir Khan*

Department of Medicine, Jawaharlal Nehru Medical College, Aligarh Muslim University, Aligarh, India
*Department of Agricultural Microbiology, Faculty of Agricultural Sciences, Aligarh Muslim University, Aligarh, India

Key words: hypersensitivity pneumonitis, thermophilic actinomycetes, agro-industrial workers, Ig, sera

Accepted March 24 2004

Abstract

Hypersensitivity pneumonitis associated with Thermophilic actinoimycetes in the agro -industrial workers was investigated. Our objective was to detect precipitin reaction and estimation of specific IgG antibodies in the sera of exposed agro-mill workers, using antigens of clinically important Thermophilic actinomycetes.

Preparation of culture filtrate antigens of *Thermoactinomyces vulgaris*, *T. thalpophilus*, *T. sacchari* , Saccaropolyspora viridis and *S. rectivirgula*. Antigens were purified by ammonium sulphate precipitation and gel filtration on sephadex G200. Blood samples were collected from workers of cotton spinning and sugar mill located in Northern India. The precipitation antibodies in the sera of workers were detected by double immunodiffusion (DID) test and IgG antibodies were estimated by ELISA.

Workers showing symptoms of Hypersensitivity pneumonitis (HP) as well as asymptomatic, showed maximum precipitin positive against *S. rectivirgula* antigen in the sera of cotton spinning mill workers, followed by *T. thalpophilus* and *T. vulgaris*. Whereas, *T. sacchari* antigen yielded higher number of precipitin positive in the sera of sugar mill workers. All the symptomatic sera showed high ELISA mean absorbance value for IgG antibodies against respective test antigens. The ELISA absorbance value varied from subject to subject and significantly higher values were found in the sera of precipitin positive symptomatic and asymptomatic subjects as compared to their respective precipitin negative and unexposed healthy control subject's sear ($P<0.05$).

ELISA is more sensitive and rapid assay as compared to DID, where elevated IgG antibodies level in the sera of workers exposed to bioallergens could be detected and help in monitoring hypersensitivity patients. The exposed workers can be suggested for the protective measures by the clinician before allergic reactions could damage their lungs.

Introduction

The occupational lung disease has been a challenge over the past few decades. It mainly present as asthma, bronchitis and other forms of lungs allergic reactions and is believed that agro-based industries harbour different types of microorganism[1,2] and organic allergens[3] which causes hypersensitivity pneumonitis (HP). One such example is Bagassosis which results from prolonged inhalation of dried sugarcane fiber dust (bagasse) which harbour actinomycetes[4]. In a similar study thermophilic actinomycetes (TAS) causing HP have also been recovered from cotton mill environment by Lockwood and Attwell [5]. The aerial prevalence of thermophilic actinomycetes like *T. vulgaris*, *S. rectivirgula* and *S. viridis* has also been reported to occur in cotton mill [6,7,8] and earlier also it was found in different sections of cotton spinning mill located in district of U.P., India. Chronic exposure leads to intensive irreversible lung damage [9]. The diagnosis of the allergic response depends on the demonstration of precipitating antibodies to one or more TAS which are easily detected by double immunodiffusion (DID) test [10] or ELISA (Bouretal [11,12]. The clinical symptoms appear to be correlated with the level of antibodies, which may lead to permanent fibrosis of the lungs and irreversible lung damage [13].

In this study, we used the double immunodiffusion (DID) test and highly sensitive ELISA to determine the level of antibody in the sera of cotton spinning mill and sugar mill workers exposed to bioallergens. A comparison of a simple, sensitive and inexpensive ELISA capable of detecting low level of antibody to a panel of TAS was also made with the classic DID.

Materials and Methods

I. Preparation of antigens

The standard strains of S. *rectivirgula* (MTCC1547), *T. vulgaris* (MTCC 1757) and *T..thalpophilus* (A64) were grown in tryptic soya broth, whereas *T. sacchari* (MTCC 1753) was grown in malt yeast extract broth and were incubated at 50°C for two weeks [14].

II. Production of hyperimmune sera

III. Subject and Sera

On the basis of history, symptoms, examination and investigations the sera from subjects and volunteers was collected. Sera was harvested and stored with 1% merthiolate solution at 4°C.

IV. Double immunodiffusion (DID) test (Khan et al [15]

V. Enzyme linked Immunosorbent Assay (ELISA) as suggested by Fasani et al [16]

Results

Clinically important TAs prevalent aerially in cotton spinning mill, Hardoi and Saatha sugar mill, Aligarh were surveyed to find out their effect on the workers exposed to these bioallergens. The workers (115) were examined for the symptoms, on the basis of which HP can be recognized (Table 1). The cotton spinning mill workers showed cough with expectoration, wheezing dysnoea and loss of appetite and weight. Whereas, 43.6% of sugar mill subjects showed dry cough, 34.5% wheezing dyspnoea and 25.5% malaise. However, chill with fever, chest tightness and chest pains were less frequent in the workers of both the mills. Precipitin reactions against selected TAs in the sera of smoker and non-smoker of two mills is presented in Table 2.

Majority of the symptomatic subjects of cotton spinning mill were precipitin positive in the age group of 26-35 years including 23% smokers and 29.4% non-smokers. However, three non-smokers were precipitin positive among asymptomatic subjects as well. No precipitin positive case was detected among asymptomatic smokers. The sera of sugar mill symptomatic subjects (26-35 years) were more precipitin positive (>30%) in both smokers and non-smokers as compared to other age groups. Of the thirty-three sera of asymptomatic subjects (26-37y), 21% were precipitin positive among non-smokers. In general, the subjects above 35 years of age were less precipitin positive. Further the double immunodiffusion test was employed using the antigens prepared from *S. rectivirgula*, *T. thalpophilus*, *T. vulagris* and *T. sacchari* to detect the precipitin reactions in the sera of workers exposed to mill environment. Precipitin reactions varied from organism to organism (Table 3). *S. rectivirgula* was more precipitin positive among both symptomatic (30%) and asymptomatic subjects (10%) followed by *T. thalpophilus* (16.6) and *T. vulgaris* (6.6%) among cotton mill workers. However, all the sera were precipitin negative against *T. sacchari*. One of the symptomatic subject (16-25y) serum was precipitin positive for both *S. rectivirgula* and *T. vulgaris*. Similarly, one of the serum collected from symptomatic sugar mill workers (26-35) was precipitin positive against both *S. rectivirgula* and *T. thalpophilus*. The sera sample of 22 symptomatic workers showed maximum precipitin reactions against *T.* sacchari followed by *S. rectivirgula*, *T. thalpophilus*, and least number of subjects of sugar mill were precipitin positive against *T. vulgaris*.

Determination of Immunoglobulin G using ELISA

Specific IgG antibodies in the sera of cotton spinning mill and sugar mill workers were detected using indirect ELISA. A comparative data of precipitin positive and ELISA values (mean OD/SD) for IgG determination in the sera of workers of both the mills is presented in Table 4. Of the 60 cotton mills workers, 9 precipitin positive of symptomatic sera against *S. rectivirgula* antigen were ELISA positive. Interestingly, of the 21 precipitin negative subjects, 3 were ELISA positive. The sera of five symptomatic subjects were also positive for both precipitin and ELISA reaction (0.036/0.13) against *T. thalpophilus* antigen.

Table 1: Clinical symptoms among cotton spinning mill (n=60) and sugar mill workers (n=55)

Symptoms	No. of cases studies		Symptoms (%)	
	Cotton mill	Sugar mill	Cotton mill	Sugar mill
Dry cough	20	24	33.3	43.6
Cough with expectorations	32	10	53.3	18.2
Wheezing	46	19	76.7	34.5
Chill with fever	12	5	20	9.1
Dyspnoea	20	19	33.3	34.5
Malaise	10	14	16.7	25.5
Chest pain	2	0	3.33	
Chest tightness	7	5	11.7	9.1
Lost of appetite and weight	28	12	46.7	21.8

Table 2: Distribution of precipitin reaction against Thermophilic actinomycetes in the sera of smoker and non-smoker of cotton spinning mill and sugar mill workers *(n=115)*

Category	Precipitin positive cases		
	Age group (Years)	Smokers	Non-smokers
	Cotton spinning mill		
Symptomatic	16-25	0/5	3/5 (17.6)
	26-35	3/6 (23.7)	(5/8 29.41)
	46-52	2/2 (15.4)	2/4 (11.7)
Asymptomatic	13-25	0/4	2/2 (11.1)
	26-35	0/8	1/12 (55.5)
	36-50	0	0/4
Total		5/25 (20)	13/35 (37.1)
Sugar mill			
Symptomatic	20-25	1/3 (11.1)	3/5 (23.1)
	26-35	3/6 (33.3)	5/6 (38.5)
	37-48	0	2/2 (15.3)
Asymptomatic	15-25	2/7 (14.2)	3/7 (15.7)
	26-37	1/5 (7.1)	4/8 (21.0)
Total	40-50	0/2	0/4
		7/23(30.4)	17/32 (53.1)

Figure in parenthesis represents the percent precipitin reactions against Thermophilic actinomycetes.

Table 3: Antibody activity in the sera of cotton and sugar mill workers exposed to Thermophilic actinomycetes as detected by DID

Category	No. of Workers tested Age group (years)		Precipitin positive				
			Sr	Tt		Tv	Ts
Cotton mill workers							
Symptomatic	10		16-25	2	1	1	0
	14		26-35	5	2	1	0
	6		45-52	2	2	0	0
Total	30			9 (30)	5 (16.6)	2 (6.6)	0
Asymptomatic	10		13-25	2	0	0	0
	17		26-35	1	0	0	0
	3		46-48	0	0	0	0
Total	30			3 (10)			
Sugar mill workers							
Symptomatic	8	20-25	1	0		1	2
	12	26-35	2	1		0	5
	2	37-48	1	1		0	0
Total			4 (28.5)	2 (14)		1 (7.1)	7 (50)
Asymptomatic	14	15.25	0	2		2	1
	13	26.37	3	0		0	2
	6	40.50	0	0		0	0
Total			3 (9)	2 (6)		2 (6)	3 (9)

Table 4: Detection of antibodies in the sera of cotton mill workers (n=60) and Sugar mill workers

Species	Symptomatic		Asymptomatic		Control
	Precipitin +ve	Precipitin –ve	Precipitin +ve	Precipitin –ve	Subject
Cotton mill workers					
S. rectivirgula	9	21	3	37	10
ELISA values	(0.35/0.07)	(0.19/0.08)	0.34/0.03)	(0.15/0.07)	0.11/0.047)
ELISA positive	9	3	3	3	
T. thalpophilus	5	25	0	30	10
ELISA values	(0.36/0.12)	(0.14/0.06)		(0.14/0.07)	(0.08/0.047)
ELISA positive	5	2		3	
T. sacchari	0	30	0	30	10
ELISA values		(0.115/0.36)		(0.104/0.019)	(0.89/0.025)
ELISA positive	0	0	0	0	
T. vulgaris	2	28	0	30	10
ELISA values	(0.499/0.025)	(0.14/0.067)		(0.14/0.038)	(0.94/0.03)
ELISA positive	2	2	0	0	
Sugar mill workers					
T thalpophilus	2	20	2	31	10
ELISA values	(0.47/0.13)	(0.162/0.046)	(0.338/0.076)	(0.15/0.062)	(0.08/0.046)
ELISA positive	2	0	2	0	
T. vulgaris	3	19	2	31	10
ELISA values	(0.459/0.89)	(0.131/0.037)	(0.452/0.053)	(0.113/0.035)	(0.094/0.055)
ELISA positive	3	0	2	0	
S. rectivirgula	4	8	3	30	10
ELISA values	(0.458/0.056)	(0.221/0.11)	(0.452/0.0412)	(0.19/0.096)	(0.157/0.039)
ELISA positive	4	5	3	6	
T. sacchari	7	15	3	30	10
ELISA values	(0.447/0.109)	(0.295/0.081)	(0.408/0.013)	(0.22/0.075)	(0.152/0.04)
ELISA positive	7	3	3	4	

(n=55) using DID and ELISA (mean ± S.D., DD at 492)

The sera samples of two symptomatic workers were precipitin and ELISA positive against *T. vulgaris* antigen, 2 out of 28 precipitin negative sera were also ELISA positive. The antigen of *T. sacchari* did not react in precipitin test to any of the subject's sera of cotton spinning mill.

The sera of sugar mill workers were also tested for IgG antibodies using ELISA test. Of the 55 sugar mill workers, *T. sacchari* antigens exhibited both precipitin and ELISA positive reactions in the sera of 7 symptomatic and 3 asymptomatic subjects (Table 4). Whereas, among the 15 precipitin negative symptomatic group, 3 were ELISA positive and among 30 asymptomatic sera, 4 were ELISA positive. The ELISA mean absorbance values against *S. rectivirgula* antigen were higher in the precipitin positive sera of symptomatic (0.45/ 0.056) and asymptomtaic sera (0.45/0.41) as compared to their respective precipitin negative sera and healthy control group. The precipitin negative sera were also ELISA negative against the antigen of *T. thalpophilus*. Two symptomatic cases were positive for precipitin and ELISA reactions against *T. vulgaris*. The ELISA absorbance values varied from subject to subject and the sensitivity was subjects dependent. The mean absorbance value of ELISA in the sera of symptomatic and asymptomatic precipitin positive against 4 selected antigens of thermophilic actinomycetes were found to be significantly higher than respective precipitin negative subject or the unexposed healthy control ($P<0.05$).

Discussion

The agro-based industries are continuously polluting the environment through transportation of the agro-products which contain airborne microflora [9]. In the present study, the allergic respiratory response or symptoms of HP among the workers of the two agro-based mills were surveyed. The subjects showing few or more of the respiratory symptoms were selected for further serological studies. Most of the cotton spinning mill workers reported cough with expectoration, wheezing, dyspnoea, where as dry cough and wheezing were frequent among sugar mill workers after a few hours of re-exposure to the mill environment. Similar symptoms of acute HP have also been observed by Moreno et al. [17]. The farming populations of Western Austria also had chills with fevers, chest pain and dyspnoea, 4-6 hours after working in the farms [18]. It is suggested that the HP should be detected earlier before it reaches the irreversible diffuse interstitial lung fibrosis and respiratory insufficiency, which may lead to cardiac failure [9]. In our study, the most common sensitizing agents noted were air borne actinomycetes prevalent in the environment of the cotton and sugar mill as reported earlier [7,8]. Similarly, Reponen et al [19] have also reported the prevalence of spores of actinomycetes in the agro-environment. Further, the sera of the subjects were analysed for the presence of precipitating antibodies against the aerially prevalent TAS. In general, the subject of the two mills above 35 years of age were less precipitin positive compared to younger age group subjects. The result indi-

cates that the formation of precipitating antibodies against airborne TAs in susceptible individuals occur predominantly at young age. Therefore, we suggest an early antibody screening to identify young farm workers at risk. Our results indicate that the smoking habit of the individual may prevent exposed workers to become affected with HP due to certain protective mechanism against allergens. The possible explanation could be the increased number of macrophages in the upper respiratory tract of smokers which provide a high rate of antigen clearance and therefore the protection to the smokers against TAS can be one of the possible mechanisms.

Demonstration of precipitating antibodies to TAS were considered as a prerequisite for the diagnosis of farmer's lung disease. The precipitin reactions among the sera of exposed symptomatic workers of the cotton mill were more against *S. rectivirgula* followed by *T .thalpophilus* and *T. .vulgaris*. The difference in precipitin reactions in the sera of workers and the aerial prevalence pattern of surveyed TAS is possible due to the differences in the antigenic properties of the actinomycetes. The sections containing bagasse in the sugar mill resulted in maximum count of *T. thalpophilus* and *S. rectivirgula* [8]. The prevalence of *T. sacchari* in bagasse resulted in maximum precipitin positive subjects and therefore led to bagassosis in sugar mill workers [4]. Though, the aerial prevalence of *S. rectivirgula* in sugar mill was quite low, but the precipitin positive cases were determined in symptomatic as well as asymptomatic subjects.

A comparative data of precipitin positive and ELISA values (mean±S.D.) for IgG determination in the sera of 115 subjects of cotton spinning mill and sugar mill were investigated (Table 4). The sera of cotton spinning mill workers were accounted for maximum precipitin positive against *S. rectivirgula* subjects. Nine precipitin positive symptomatic subject sera were ELISA positive and from rest of the 21 precipitin negative sera, 3 were also ELISA positive against *S. rectivirgula*. However, symptomatic precipitin positive cases against *T. thalpophilus* and *T.vulgaris* were ELISA positive with a significantly higher ELISA value as compared to their symptomatic and healthy control group ($P<0.05$). The enhanced ELISA observance values of IgG antibody in symptomatic subjects against *S. rectivirula* antigen was probably due to the greater sensitivity of these subjects towards specific antigen prepared from *S. rectivirgula*. Similar observations were recorded by Iranitalab et al. [20] where they observed substantially weaker immune response in healthy farmers as compared to the patients of hypersensitivity pneumonitis.

The sera of sugar mill workers demonstrated the precipitin reaction mostly against *T. sacchari* and *S. rectivirgula*. Though the environmental prevalence of *S. rectivirgula* was comparatively low than *T. thaphophilus* and *T. vulgaris* as observed in our earlier with study, yet the minute antigenic stimulus was found sufficient to trigger a detectable immunse response [21]. The elevated level of specific IgG antibodies against the tested antigens TAS in precipitin positive symptomatic and asymptomatic cases were all ELISA positive, whereas, in their respective negative group, few of the subjects were also ELISA positive.

The thermophilic actinomycetes laden bagasse considered to be the main cause of bagassosis. Six symptomatic and three asymptoamtic sera were positive for both precipitin and ELISA against *T. sacchari* (0.447/0.10, 0.408/0.011). Of the 15 precipitin negative sera of symptomatic group, 3 were ELISA positive (0.295/0.181). However, among the 30 asymtomatic precipitin negative cases, only 4 sera were ELISA positive. The mean absorbance value for IgG antibody activity against *T. sacchari* and *S. rectivirgula* was found to be elevated significantly in the symptomatic worker's sera than in the asymptotic workers ($P>0.05$) or unexposed control ($P<0.05$)). This is in conformity with the observation of Cornelia et al. [22], who demonstrated a specific binding of IgG in the sera of the farmer's lung patient to *S. rectivirgula* purified antigens. However, no such antibody response was found in exposed and unaffected subject. The antibody response and symptoms suggests that the environmental exposure may lead to pulmonary fibrosis in certain instance [23] it was suggested by Erkinjuntti et al [24] that the high antibody levels in farmer's lung patients were due not only to high exposure level but also to individual sensitivity to environmental microbes. Before the irreversible fibrosis develops in the lung and create airflow obstructions, the present study may enable us to warn the patient or farmers form further damage by the re-exposure to the *Thermophilic actinomycetes* acting as bio-allergens in the agro-environment which can be detected through ELISA.

In summary, formation of precipitating antibodies in the sera of susceptible individuals were detected. The elevated IgG antibodies specific against *Thermophilic actinomycetes* in the sera of symptomatic subjects were correlated with the intensity of exposure. Asymptomatic cases with no pulmonary impairment were found precipitin positive for *T. actinomycetes* but a few cases of symptomatic were precipitin negative. ELISA used in the present study presented a reasonable simple and rapid tool with which the clinicians could monitor HP patients for continued exposure. Which might be encouraged to take measures against allergens exposure. The smoking factor among the exposed workers possibly acted as a protective mechanism. However, the additional comprehensive studies is required to determine the impact of smoking, if any, on the protection of Hypersensitivity pneumonitis.

References

1. Pickering CAC, Newman TAJ. Extrinsic allergic bronchiolo alveolitis (hypersensitivity pneumonitis). In: occupational lung disorders (ed. Parkers, WR) 1995; pp667-709. Oxford butterworth-Heinemann.
2. Krasnik JHJ, Meuwissen MA, Nakao A, Patterson R. Hypersensitivity pneumonitis: Problems in diagnosis. J Allergy Clin Immunol 1996; 97: 1027-1031.
3. dO Pico GA. Hazardous exposure and lung disease among farm workers. Clin Chest Med 1992; 13: 311-316.
4. Khan ZU, Gangwar M, Gaur SN, Randhawa. Thermophilic actinomycetes in cane sugar mills, an aeromicrobiologic and seropidemiologic study. Antonie Van leeuwenhock 1995; 67: 339-337.

5. Lockwood MG, Attwell RW. Thermophilic actinomycetes in the air of cotton mills. Lancet 1997, ii: 45-46.
6. Lacey J, Lacey M. Microorganisms in the air of cotton mills. Ann. Occupt Hyg 1987; 31: 1-19.
7. Jabeen M, KHAN MS. Prevalence of thermophilic actinomycetes among Agro-Industrial workers J Microb World 2000; 2: 35-41.
8. Jabeen M, Khan MS, Khan MW. Thermophilic actinomycetes causing bagassosis in sugar mill workers. National symposium on Microbes and Human welfare 2000; Oct. 14-16, Ch. Charan Singh University Meerut. India.
9. Salvaggio JE. Extrinsic allergic alveolits (hypersensitivity pneumonitis): past, present and future. Clin Expt Allergy 1997; 27:18-25.
10. Marx JJ, Robert, Gray BS. Comparison of the enzyme linkedimmunosorbant assay and double immunodiffusion test for the detection and quantitation of antibodies in farmer's lung disease. J Allergy Clin Immunol 1982; 70: 109-113.
11. Bour X, EHR J, Dewar M, Ehret W, Fruhmann G, Vogelmeier C, Weiss W, Zinkernagel V. Humidifier lung and humidifier fever lung. J Allergy Clin. Immuno. 19980; 166: 113-124.
12. Baur X, Richter G, Pethran A, Czuppon AB, SCHWAIBLMair M. Increased prevalence of IgG-induced sensitization and hypersensitivity pneumonitis (humidifier lung) in nonsmokers exposed to aerosols of a contaminated Airconditioner. Respiration 1992; 59: 211-214.
13. Fink JN. Hypersensitivity pneumonitis. J Allergy Clin Immunol 1984; 74: 1-9.
14. Kurup VP, Barboriak JJ, Fink JN, Scribner G. Immunologic cross reaction among thermophilic acctinomycetes associated with hypersensitivity pnumonitis. J Allergy Clin Immunol 1976; 57: 417-421.
15. Khan ZU, Misra VC, Ranhawa HS. Precipitating antibodies against Micropolyspora faent in Equines in North-Western India. Antonie Van Leeuwenhock 1985; 51: 313-319.
16. Fasani F, Bossi A, Garmia V. Double diffusion and ELISA for the detection of IgG and IgM antibodies against Micropolyspora faeni. Ann Allergy. 1987; 59: 451-454.
17. Moreno-Ancillo A, Vicente J, Gomez et al. Hypersensitivity pneumonitis related to a covered heated swimming pool environment. In Arch Allergy Immunol 1997; 144: 205-206.
18. Prior C, Falk M, Frank A. Early sensitization to farming related antigens among farmers: analysis of risk factors. Int Arch Allergy Immunol 1996; 111: 1018-2438.
19. Reponen TA, Gazenko SV, Grinshpun SA, Willeke K, Cole EC. Characteristic of airborne actinomycetes spore. App Env Microbil 1998; 64: 3807-3812.
20. Iranitalab M, Jarolim E, Rumpold H, Steiner R, Ebner H, Feldner H, Scheiner O, Kraft D Characterization of *Micropolyspora faeni* antigens by human antibodies and immunoblot analysis. Allergy 1989; 47: 314-321.
21. Reiss E. Thermophilic actinomycetes. In: Molecular immunology of mycotic and actinomycetic infections. Elsevier. New York 1986; 321-336.
22. Cornelia M., Backer W, Schaak M. Farmer's lung patent's IgG_2 antibodies specifically recognize Saccharopolyspora rectivirgula proteins and carbohydrate structures. J Allergy Cli Inmmunol 1996; 98: 441-450.
23. Sutinen S. Reijula K, Huhti E, Karkola P. Extrinsic allergy bronchiolo-alveolitis: Serology and biopsy findings Eur J Resp Dis 1983; 64: 271-282.
24. Erkinjuntti-Pekkanen RM, Reiman JI, Kokkainen HO, Tero EO. IgG antibodies, Chronic bronchitis and pulmonary function values in farmer's lung patients and matched controls. Allergy 1999; 54: 1181-1187.

Correspondence:

Dr. Asif Hasan
4/1176-H, New Sir Syed Nagar
Aligarh 202 002
India

Phone: 0571-2501877
Mobile: 09837323382
e-mail : asif_8796@rediffmail.com

Biomedical Research 2004; 15 (2): 134-137

Prevention of garlic induced haemolytic anaemia by some commonly consumed green leafy vegetables in Nigeria

Ganiyu Oboh

Biochemistry Department, Federal University of Technology, P.M.B. 704 Akure, Nigeria

Key words: Garlic, Aneamia, Haemolytic, Leafy Vegetables

Accepted April 4, 2004

Abstract

Garlic (*Allum sativum*) is popularly consumed in Nigeria because of its health benefits in management of several disease conditions. However, unregulated intake of garlic can cause haemolytic anaemia. This study sought to investigate the ability of some commonly consumed tropical green leafy vegetables namely *Amaranthus cruentus*, *Baselia alba*, *Solanum macrocarpon*, *Ocimum gratissimum*, *Corchorus olitorius* to prevent garlic induced haemolytic anaemia. Wistar strain albino rats were fed diet containing 4% garlic with or without 40% leafy vegetable supplement. The result of the study shows that there was a decrease in daily feed intake (6.7-7.2), daily weight gain (0.7-1.5) and digestibility (70.4 - 91.5) of rats fed diet with garlic (4%), with or without vegetable (40%) supplement when compared with those rats fed the basal diet without garlic (4%) and vegetable (40%) supplement [digestibility (95.5), daily feed intake (7.5), daily weight gain (2.0)]. However, there was a significant decrease ($P<0.05$) in the PCV (31.0), Hb (10.2), RBC (4.3) and WBC (3.5) of rats fed diet with garlic (4%) but without vegetable; when compared to those rats fed diet without garlic (4%) and vegetable (40%) supplements [PCV (38.2), Hb (13.0), RBC (5.5), WBC (4.0)]. Conversely, there was a significant increase in the PCV (33.5 - 35.6), Hb (12.0 -12.5) and RBC (4.9-5.3) of rats fed diet with garlic (4%) and vegetable (40%) supplement when compare to rat fed diet with 4% garlic supplement alone (except *Solanum macrocarpon* and *Corchorus olitorius*). Futhermore, there was a significant decrease ($P<0.05$) in MCV (69.2-72.0) of rats fed the basal and those fed diet with garlic and vegetable (except *Corchorus olitorius* and *Solanum macrocarpon*) supplement, when compared to the rats fed diet with garlic, but without vegetable supplement (74.5). This therefore implies that garlic could induce haemolytic anaemia in rats. However, such anaemia could be prevented by some tropical green leafy vegetable such as *Amaranthus Cruentus*, *Baselia alba* and *Ocimum gratissimum*

Introduction

The potency of garlic or its products in the treatment or management of several disease conditions has been extensively investigated and reviewed [1-2]. However, chronic and unregulated intake of garlic causes some other less desirable effects the Chief amongst which is anaemia [1]. The anaemia caused by garlic is apparently haemolytic [2]. Recently, an additional factor was introduced into the aetiology of garlic induced anaemia. A correlation was reported [2] between the degree of anaemia caused by garlic intake and the level of garlic induced decreases in erythrocyte GSH and plasma ascorbic acid. It was suggested that garlic depleting the body's content of GSH, ascorbic acid and perhaps other important endogenous antioxidants, in conjunction with garlic's ability to increase the body's free radical load: caused a reduction in the degree of protection given to the erythrocyte membrane against oxidative damage. The oxidation of membrane lipids causes alterations in membrane structure leading to haemolysis. Consequently haemolysis would increase, leading to the observed anaemia.

Recent report by Umar *et.al* [1] revealed that supplementation of garlic-intake with ascorbic acid or vitamin E prevented decrease in GSH and plasma ascorbic acid, thereby giving greater protection to erythrocyte membrane lipids against oxidative damage by peroxides and free radicals generated in the body. The erythrocytes hence became more resistant to oxidative damage and consequently garlic-induced anaemia was prevented. Many phenolics, such as flavonoids, have antioxidant capacities that are much stronger than those of vitamins C and E. Flavonols and flavones are flavonoids of particular importance because they have been found to possess antioxidant and free radical scavenging activity in foods [3]. Some evidence showed that flavonoids could protect membrane lipids from oxidation. A major

source of flavonoids is vegetables and fruits [3]. Recently, phytochemicals in food materials and their effects on health, especially the suppression of active oxygen species by natural antioxidants from teas, spices and herbs, have been extensively studied. Chinese herbs have been used for diet therapy for several millennia. Some of them are alleged to exhibit significant antioxidant activity [3-5]. This study therefore sought to investigate the ability of some popularly consumed tropical green leafy vegetables to prevent garlic induced haemolytic anaemia.

Materials and Methods

Materials

The vegetables used were obtained from the research farm of the Federal University of Technology, Akure, Nigeria. These vegetables include: *Amaranthus cruentus* (Atetedaye), *Baselia alba* (Amunu tutu), *Solanum macrocarpon* (Igbagba), *Corchorus olitorus* (Ewedu), and *Ocimum gratissimum* (Efinrin). The chemicals were analytical grades, while the water used was glass distilled water.

Methods

Sample Preparation:

The vegetables were rinsed in water, and the edible portions were separated from the inedible portion. The edible portions were chopped into small pieces (500g) and sundried for further analysis.

Bioassay

Wistar strain albino rats weighing 120 – 200g were purchased from Biochemistry Department, University of Ilorin, Nigeria. And acclamatized for 2 weeks during which period they were maintained *ad libitum* on commercial diet. The rats were subsequently divided into seven treatment groups. Animals in group 1 were fed the basal diet without garlic and vegetable supplement, while animals in group 2 were fed the basal diet containing garlic supplement (4%), animals in groups 3 – 7 were fed the basal diet containing garlic (4%) and the vegetable (40%), as shown in table 1. The feed and water were given *ad libitum* through out the duration of the experiment. Daily feed-intake, weekly changes in body weight and digestibility of the feed were monitored throughout the experiment. The experiment last two weeks, at the end of which the rats were sacrificed by decapitation after an 18-hour fast and the blood were collected into EDTA-tubes. The haematological tests, Packed cell volume (PCV), Red blood cell counts (RBC), white blood cell counts (WBC), Haemoglogin (Hb) and Mean corpuscular volume (MCV) were conducted according to the conventional methods reported by Aning *et.al.* [6].

Analysis of data

The result of the three replicates were pooled and expressed as mean±standard error (S.E.). A one-way analysis of variance (ANOVA) and the Least Significance Difference (LSD) were carried out [7]. Significance was accepted at $P \leq 0.05$.

Results and Discussion

Oxidative stress is considered to be associated with many diseases including haemolytic anaemia, but diet plays an important role in human health and in the prevention of certain diseases [3, 8]. The result of the feed performance and growth of albino rats fed diet containing 4% garlic and 40% vegetables supplement is shown in table 2. The result revealed that there was a significant decrease ($P<0.05$) in daily feed intake (6.2 – 7.2), daily weight gain (0.7 - 1.5) and digestibility

There was a significant decrease ($P<0.05$) in the PCV (31.0), Hb (10.2), RBC (4.3) and WBC (3.5) of the fats fed diet with garlic, but without vegetable supplement when compare to the rats fed diet without garlic and vegetable supplement [PCV (38.0), Hb (13.0), RBC(5.5), WBC (4.0)] (table 3). This reduction in haematological parameters could be attributed to the ability of the garlic to induce the production of free radicals, which result in oxidative damage on the erythrocyte membrane [1]. This garlic induced-oxidative damage on rat erythrocytes ultimately results in haemolytic anaemia [9]. This result also agrees with earlier report by Younghong [10] to the extent that over consumption of garlic induces haemolytic anaemia in hk phenotype dogs. The decrease in white blood cell count also confirms that the anaemia caused by garlic is haemolytic anaemia [11].

Table 1: The feed formulation with or without garlic and vegetable supplement

Basal	Treatment 1	Treatment 2	
Casein	10g	10g	-
Soyabeans Oil	10g	10g	10g
Vitamin/Mineral Premix	4g	4g	4g
Corn Starch	76g	72g	42g
Vegetable	-	-	40g
Garlic	-	4g	4g
Total	**100**	**100**	**100**

Table 2: Nutrient utilization and Growth Performances rats fed diet with garlic and vegetable supplement

Sample	Daily feed intake (g/rat/day)	Daily weight gain (g/rat/day)	Dry matter digestibility (%)
BSF	7.5±0.1[a]	2.0±0.1[a]	95.5±0.4[a]
COWG	6.7±0.2[c]	1.5±0.1[b]	91.5±0.2[b]
EDWG	7.2±0.1[b]	0.7±0.0[d]	70.4±0.3[f]
IGWG	7.2±0.1[b]	1.2±0.1[c]	74.7±0.4[e]
ATWG	6.5±0.0[c]	1.0±0.2[c]	84.2±0.6[c]
ADWG	6.2±0.2[d]	0.7±0.1[d]	80.9±0.1[d]
EFWG	6.6±0.3[c]	1.1±0.2[c]	76.3±0.2[e]

Values are mean±S.E (n =3)
Means with the same superscript letter(s) along the same row are not significantly different (P>0.05)
BSF: Basal
COWG: Diet with garlic (4%) supplement;
EDWG: Diet with garlic (4%) and *Corchorus olitorius* (40%) supplement
IGWG: Diet with garlic (4%) and *Solanum macrocarpon* (40%) supplement
ATWG: Diet with garlic (4%) and *Amaranthus cruentus* (40%) supplement
ADWG: Diet with garlic (4%) and *Baselia alba*(40%) supplement
EFWG: Diet with garlic (4%) and *Ocimum gratissimum* (40%) supplement

Table 3: Haematological changes in rats fed diet with garlic and vegetable supplement

Sample	PCV (%)	RBC(10^6/µl)	Hb(g/dl)	WBC(10^6/µl)	MCV (fl)
BSF	38.2±0.2[a]	5.5±0.3[a]	13.0±0.6[a]	4.0±0.2[a]	71.0±1.2[b]
COWG	31.0±0.5[c]	4.3±0.3[c]	10.2±0.2[c]	3.5±0.2[b]	74.0±0.5[a]
EDWG	30.8±0.3[c]	4.1±0.1[c]	10.1±0.3[c]	3.0±0.1[b]	75.0±0.6[a]
IGWG	30.9±0.2[c]	4.2±0.0[c]	10.2±0.5[c]	2.9±0.2[b]	77.0±0.2[a]
ATWG	33.5±0.4[b]	5.3±0.2[a]	12.0±0.5[ab]	4.3±0.1[a]	70.8±0.7[b]
ADWG	35.6±0.6[b]	5.0±0.1[b]	12.5±0.4[ab]	4.0±0.3[a]	69.2±1.5[b]
EFWG	34.2±0.2[b]	4.9±0.2[b]	11.8±0.2[b]	4.2±0.2[a]	72.0±0.3[b]

Values are mean ± S.E (n =3)
Means with the same superscript letter(s) along the same row are not significantly different (P>0.05)

BSF: Basal diet
COWG: Diet with garlic (4%) supplement;
EDWG: Diet with garlic (4%) and *Corchorus olitorius* (40%) supplement
IGWG: Diet with garlic (4%) and *Solanum macrocarpon* (40%) supplement
ATWG: Diet with garlic (4%) and *Amaranthus cruentus* (40%) supplement
ADWG: Diet with garlic (4%) and *Baselia alba*(40%) supplement
EFWG: Diet with garlic (4%) and *Ocimum gratissimum* (40%) supplement

However, supplementation of the garlic diet with vegetables (40%) cause a significant increase (P < 0.05) in the PCV (33.5 - 35.6), Hb (11.8 -12.5) and RBC (4.0 - 4.3) in the rats, except in those rats whose diet are supplemented with *Solanum macrocarpon* and *Corchorus olitorius*. This possible indicate that tropical green vegetables are capable of preventing garlic induced haemolytic anaemia. Furthermore, there was a significant decease (P<0.05) in MCV (71.0) of albino rats fed diet without garlic and vegetable supplement when compared to the rats fed diet with garlic, but no vegetable supplement [MCV (74.0)], which is an indication of the presence of haemolytic anaemia in animals consuming diet with garlic only [9]. However there was a significant increase (P< 0.05) in MCV of rat fed garlic with *Corchorus Olitorius* (75.0) and *Solanum macrocarpon* (77.0) when compared to those fed diet with garlic but without vegetable (74.0), which is an indication that *Corchorus olitorius* and *Solanum macrocarpon* can not prevent the haemolytic anaemia unlike other green leafy vegetables used in the study.

The mechanisms of prevention of the haemolytic anaemia can not be categorically stated. However, it could be attributed to the high antioxidant properties of green leafy vegetables which serve

as an extracellular neutralizer of free radical [12]. In addition, vegetables had been reported to be rich in vitamin C [13] and many phenolics, such as flavonoids [3, 5]. Flavonoids have antioxidants capacities that are much stronger than those of vitamins C and E, which are reportedly used to prevent haemolytic anaemia by Umar *et.al.* [1]. Reports have shown that flavonoids could protect membrane lipids from oxidation [3], a major source of flavonoids are vegetables and fruits [3].

Conclusion

The results obtained from these studies revealed that some tropical green leafy vegetables such as *Amaranthus cruentus*, *Baselia alba* and *Ocimum gratissimum* could prevent garlic induced haemolytic anaemia in rats. Therefore, the most likely and practical way to fight against degenerative diseases is to improve body antioxidant status which could be achieved by higher consumption of green leafy vegetables [8].

Acknowledgement

This work was done within the framework of the Associateship Scheme of The Abdus Salam International Centre for Theoretical Physics, Trieste, Italy. Financial support from the Swedish International Development Cooperation Agency is acknowledged.

References

1. Umar IA, Arjinoma ZG, Gidado A, Hamza HH. Prevention of garlic (*Allium sativumlinn*)-induced anaemia in rats by supplementation with ascorbic acid and vitamin E Nig J Biochem & Mol Biol 1998; 13, 31-40.
2. UmarIA, Otukenyong EE, Igbokwe IO, Omage JJ, Buralai IB: Garlic Induced Haemolytic anaemia in garlic-fed rats may be associated with decreased levels of erythrocyte. West Africal J Biol Sc 1996; 4: 73-81.
3. Amic D, Davidovic-Amic D, Beslo D, Trinajstic N. Structure-Radical Scavenging Activity Relationship of Flavonoids, Croatia Chemica Acta 2003; 76: 55-61.
4. Yang J, Lin H, Mau J: Antioxidant properties of several commercial mushrooms. Food Chemistry 2002; 77; 229-235.
5. Alia M, Horcajo C, Bravo L, Goya L. Effect of grape antioxidant dietary fiber on the total antioxidant capacity and the activity of liver antioxidant enzymes in rats. Nutrition Research 2003; 23: 1251-1267.
6. Aning KG, Ologun AG, Onifade A, Alokan JA, Adekola AI, Aletor VA. Effects of replacing dried brewer's grains with sorghum rootlets on growth, nutrient utilization and some blood constituents in the rat. Animal Feed Science Technology 1998; 71: 185-190.
7. Zar J. H.: Biostatistical Analysis. USA. Prentice-Hall. 1984.
8. Zhang Z, Chnag Q, Zhu M, Huang Y, Ho WKK, Chen Z. Characterization of antioxidants present in hawthorn fruits. Journal of Nutritional Biochemistry 2001; 12: 144-152
9. Baker FJ, Silverton RE. Haematology, Introduction to Medical Laboratory Technology 6th Edition, Butterworth & Co, Publishers Ltd, UK. 1985; 303-346.
10. YoungHon Y, Maede Y, Lee K, Chang WS: Garlic induced heamatologic effect in small dogs. Korean-journal of veterinary clinical medicine 1999; 16: 270-280.
11. Jin-Taewon, Kim-Hong Tae, chang-wooseok, Oh-Tacho, Song-Jaechan, Jeong-Kyushik, Park-Seungchun, Leekeunwoo. The effect of short-term administration of excessive amount of garlic on haematology in Hk Phenotype jindo-dog. Journal of Veterinary-Clinics 2001;18: 232-236.
12. son R, Theron AJ. Antioxidant and tissue Protective function of ascorbic acid.In: World Review of Nutrition and Dietetics 1990, 62; 37-38.
13. Achinewhu SC. Ascorbic-Acid Content of Some Nigerian, Local Fruits and Vegetables. Qualitas Plantanum Plant Food and Human Nutrition 1983; 33: 261-266.

Correspondence:

Dr. Ganiyu Oboh
Department of Biochemistry
Federal University of Technology
P.M.B. 704 Akure
Nigeria

e-mail: goboh2001@yahoo.com

Biomedical Research 2004; 15 (2): 138-141

99mTC-DTPA ventriculocisternography for postoperative evaluation of endoscopic third ventriculostomy: A preliminary study model.

Flávio Nigri*, Mario Bernardo-Filho, Carlos Telles*, Jorge W. E Silva*** and Edson M. Boasquevisque*****

*Disciplina de Neurocirurgia, **Departamento de Radiofarmácia, ***Disciplina de Medicina Nuclear, Hospital Universitário Pedro Ernesto. Av. 28 de Setembro 87, Rio de Janeiro, RJ, BRASIL, Zip Code : 20551-030. Phone/fax: 55 21 22543532.

Key words: Endoscopy, hydrocephalus, Technetium, Third ventriculostomy, aqueductal stenosis

Accepted May 12 2004

Abstract

Postoperative evaluation of endoscopic third ventriculostomy is based mainly on clinical analysis, computerized tomography and nuclear magnetic resonance images. However, these methods are unable to provide a clear view of whole circulation pattern of the cerebrospinal fluid, and specifically the absorption capability of the arachnoid villi. We performed a preliminary study with postoperative ^{99m}Tc-DTPA ventriculocisternography to try to overcome this handicap. A 13 year old boy with obstructive hydrocephalus and signs and symptoms of intracranial hypertension underwent an endoscopic third ventriculostomy. On the next postoperative day a ^{99m}Tc-DTPA ventriculocisternography was performed and peripheral blood taken for radioactivity evaluation. As seen on scintigraphic images, the radioisotope first injected into the right lateral ventricle, diffused to the left lateral ventricle, spinal subarachnoid space and convexity. The blood activity curved sharply upwards.

Signs and symptoms of intracranial hypertension disappeared and after six months a new CT scan revealed a lower ventricular volume. Net correlation between the clinical and tomographic evolution and the ventriculocisternography was observed. This method seems to be a promising tool for fast postoperative determination of the cerebrospinal fluid circulation.

Introduction

The choroid plexus produces approximately 480 ml of cerebrospinal fluid (CSF) in 24 hours. The total system capacity is 150 ml, which means that CSF may be cleared out completely three times a day. The choroid plexus is mainly situated in the lateral ventricles and produces almost all CSF. From the lateral ventricles the CSF follow a pathway inside and outside the brain [1-3]. The obstruction of the aqueduct of Sylvius causes enlargement of the lateral and third ventricle. By endoscopy it is possible to perform a communication between the third ventricle and the interpeduncular cistern, allowing the CSF to reach subarachnoid space and then be absorbed by the arachnoid villi to the blood stream [4]. Endoscopic third ventriculostomy (ETV) is the treatment of choice for obstructive hydrocephalus [5,6]. The standard methods of evaluation after surgery are: (a) clinical and neurological examination, (b) computerized tomography scan (CT) and (c) magnetic resonance imaging (MRI) with flow study [5-9]. Neither of these methods show CSF circulation and its absorption capability together. The purpose of the present work was to perform a nuclear medicine ventriculography model for postoperative evaluation of ETV using ^{99m}Tc-DTPA.

Material and Methods

A 13 year old male was admitted to the hospital with headache, vomiting and somnolence. CT scan revealed an obstructive hydrocephalus with a ventricular-inner table ratio (FH/ID) of 51% (Figure 1B). An ETV was performed without complications. After the ETV a 22 gauge catheter was introduced into the right lateral ventricle. On the next postoperative day, 10mCi (37 x 10^7 Bq) of ^{99m}Tc-DTPA was injected into the ventricle. Scintigraphic images were obtained with a gamma camera with low energy high resolution collimator. (E.Cam, Siemens, USA) at 5 minutes, 1, 2 and 24 h post injection. The radionuclide activity was obtained drawing ROIs in lateral ventricles, spinal subarachnoid space and

cerebral convexity (Fig. 2). Post injection peripheral blood samples were taken from the patient at 0, 30, 60 and 90 min. The

plasma was separated and radioactivity was measured. Count Levenberg-Marquardt algorithm on Matlab 6.5R13 (The Math rates were corrected for radioactive decay and then compartmental analyses were done, considering the lateral ventricles as the injection one, subarachnoid space as the second and vascular space as the opened compartment. The curve fitting was done using the Linear Least Square method with the application of the Works, Inc., USA). Curves were adjusted applying first order kinetic model [10] assuming that the transfer rates between compartments were proportional to the material concentration between compartments, where the curve slope (m of the lateral ventricle and subarachnoid space are: - 0,5 and – 34,4 . The patient was discharged from the hospital on the fourth postoperative day without the previous symptoms.

Results

Ventricular size measured on CT scan by the FH/ID ratio, where FH is the largest width of the frontal horns and ID is the internal diameter from inner table to inner table at this level, showed a decrease from 0,51 to 0,43 mm ((Fig 1B and 1D, respectively) after six months. The CSF dynamic process measured by radiopharmaceutical washout from ventricular system (Figure 2) demonstrates a very rapid interventricular equilibrium and flow to subarachnoid space where the transient influx (Fig 3B) happens early, demonstrated by the first part of the curve, and decreases immediately, as can be seen by a very steep second phase of the time activity curve. A slow third part curve (Fig 3C) shows the transfer velocity of the radiopharmaceutical to the vascular compartment.

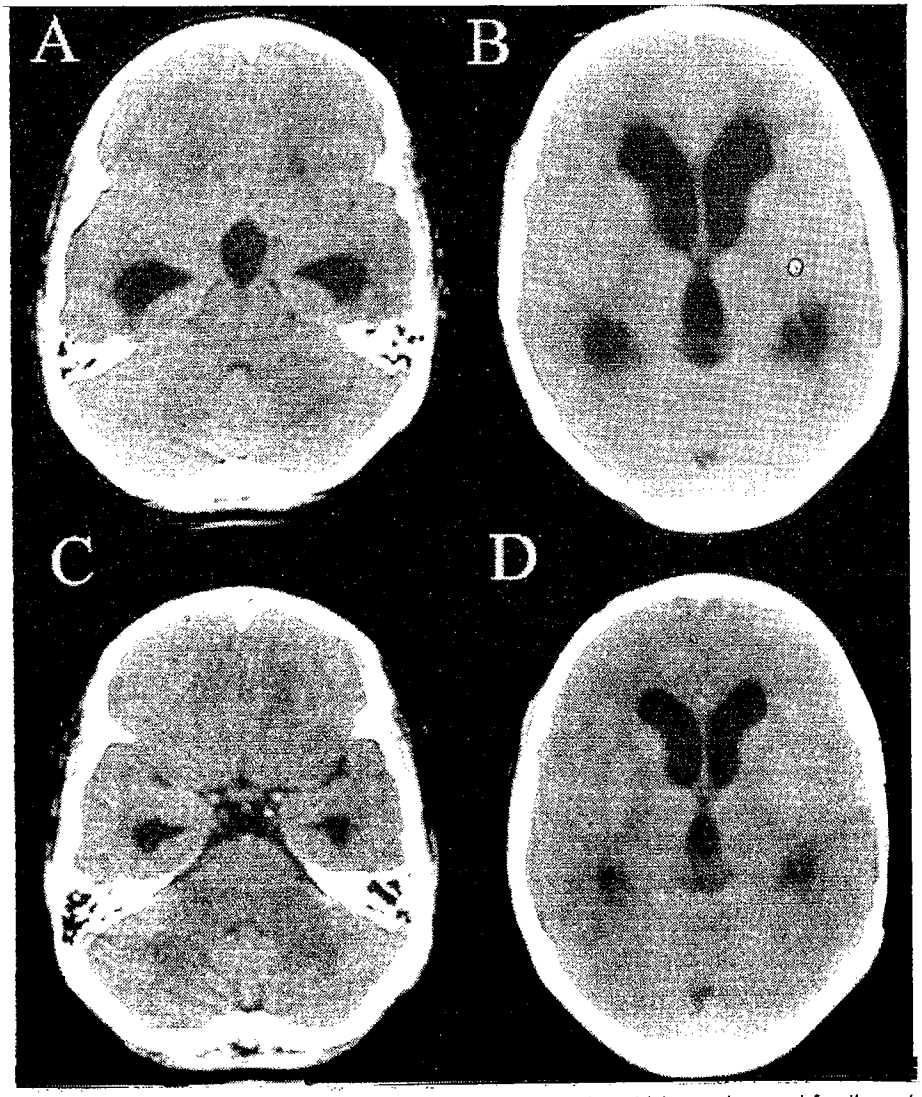

Fig.1: (A-B), Preoperative ct images showing dilated supratentorial ventricles and normal fourth ventricle. (C-D), posoperative 6 monthsct scan images revealing decrease ventricular size

FIGURE 2

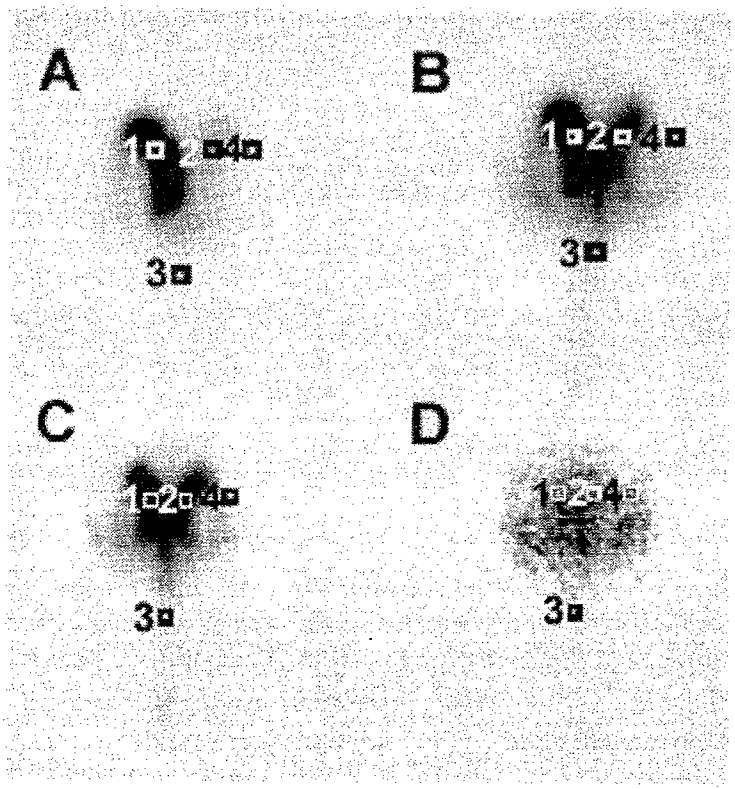

Fig. 2: (A-)-scinitigraphic images at 15 minutes, 1,2 and 24 hours showing values of rois drown at different sites: 1-right lateral ventricle, 2-left lateral ventricle, 3-spinal subarachnoid space and 4-convexity.

FIGURE 3

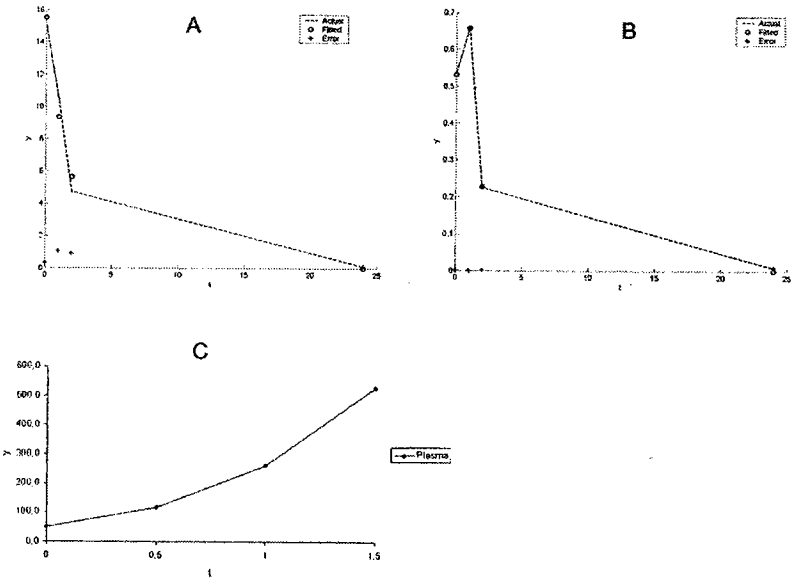

Fig. 3: Time-activity curves, A-Lateral ventricles, B- Subarachnoid space and C- blood (t= time in hour, y= count rates)

Discussion

The CSF circulation was separated in three main compartments: the ventricular system, the subarachnoid space and the vascular compartment. The tendency of the first two compartments is to equilibrate both the CSF pressure and the radiopharmaceutical concentration, once connected. The rapid initial decrease observed in the lateral ventricles and the initial increase in the subarachnoid space represent the diffusion of the radiotracer through a well connected system. The overall radiopharmaceutical decreasing may represent the CSF diffusion to the subarachnoid space plus absorption to the vascular bed. The radioactivity appeared in the blood at 30 minutes. The slow third part of the ventricular and subarachnoid space activity curve may represent the capability of the whole system to transfer the radiotracer from the ventricular-SAS to the vascular compartment, which is an exponential curve.

The evaluation of ETV with intraventricular injection of radionuclide has already been performed [11]. New methods like CT and MRI are far from offering the answer to cases of failed ETVs [5-7]. The advantages of using the radiotracer model are: (a) evaluate the complete CSF pathway, (b) measure directly the vascular absorption process and (c) obtain a functional evaluation of the procedure. A future development of a bedside diagnostic tool with intraventricular injection and blood samples is desired. In conclusion, present case shows a good correlation between the neurological improvement and the CSF kinetic. Additional studies are necessary to define the limits of the normal pattern of CSF circulation and its absorption to the blood stream, in this type of patients.

This work was supported by a grant from the School of Medicine and the Pedro Ernesto Universitary Hospital, State University of Rio de Janeiro and FAPERJ, Brazil.

References

1. Adams RD, Victor M. Disturbances of cerebrospinal fluid circulation, including hydrocephalus and meningeal reaction. In: Principles of Neurology, Adams RD, Victor M (eds.), McGraw-Hill Inc., New York, 1989, pp. 501-515.
2. McComb JG, Zlocovic BV. Cerebrospinal fluid and blood-brain interface. In: Pediatric Neurosurgery, Cheek WR (eds.), WB Saunders Company, Philadelphia, 1994, pp167-184.
3. Sainte-Rose C. Hydrocephalus in childhood. In: Neurological Surgery, Youmans JR(ed.), WB Saunders Company, Philadelphia 1996, pp. 890-926.
4. Decq Ph, Yepes C, Anno Y, Djindjian M, Nguyen JP, Kéravel Y. L´endoscopie neurochirurgicale. Indications diagnostiques et thérapeutiques. Neurochirurgie 1994; 14:313-321.
5. Drake JM. Ventriculostomy for treatment of hydrocephalus. In: Neurosurgery Clinics of North America, Butler AB, McLone DG (eds.), WB Saunders Company, Philadelphia 1993, pp. 657-666.
6. Sainte-Rose C. Third ventriculostomy. In: Neuroendoscopy, Manwaring, K.H., Crone KR (eds.); Mary Ann Liebert Inc., New York 1992, pp. 47-61.
7. Hoffmann KT, Lehmann TN, Baumann C, Felix R. CSF flow imaging in the management of third ventriculostomy with a reversed fast imaging with steady-state precession sequence. Eur Radiol 2003; 13: 1432-1437..
8. Jones RFC, Teo C, Stening WA, Kwok BCT. Neuroendoscopic third ventriculostomy. In: Neuroendoscopy, Manwaring KH, Crone KR (eds.); Mary Ann Liebert Inc., New York 1992, pp. 63-77..
9. Sainte-Rose C, Cinalli G, Roux FE, Maixner W, Chumas PD, Mansour M, Carpentier A, Bourgeois M, Zerah M, Pierre-Kahn A, Renier D. Management of hydrocephalus in pediatric patients with posterior fossa tumors: The role of endoscopic third ventriculostomy. J Neurosurg 2001; 95:791-797.
10. Coxson PG, Salmeron EM, Huesman RH, Mazoyer BM. Simulation of compartmental models for kinetic data from a positron emission tomography. Comput Methods Programs Biomed 1992; 37: 205-214.
11. Vries JK, Friedman WA. Postoperative evaluation of third ventriculostomy patients using 111 In-DTPA. Childs Brain 1980; 6:200-205.

Correspondence to:

Dr. Flávio Nigri .
Disciplina de Neurocirurgia
Hospital Universitário Pedro Ernesto.
Av. 28 de Setembro 87
Rio de Janeiro, RJ
BRASIL 20551-030

Phone/fax: 55 21 22543532.
e-mail: flavionigri@aol.com

Biomedical Research 2004; 15 (2): 142-149

Analysis of seroreactivity of different endemic populations of bancroftian filariasis with field MF isolates and B*rugia malayi* antigens

Yashodhar.P. Bhandary, K.N.Krithika, Sandeep Kulkarni, M.V.R. Reddy*, B.C.Harinath

Jamnalal Bajaj Tropical Disease Research centre and Department of Biochemistry, Mahatma Gandhi Institute of Medical Sciences, Wardha-442102, Maharashtra, India.

Key words: Filariasis, excretory-secretory antigen, phosphate buffer soluble antigen, circulating antigen, antibodies

Accepted June 14 2004

Abstract

Seroreactivity of bancroftian filarial cases of different endemic zones with different geogrophical isolates of *W.bancrofti* mf was checked by indirect fluorescent antibody test (IFAT). While the filarial sera of Calicut showed binding to the mf isolates of all four endemic zones studied (Calicut, Bhubaneshwar, Rourkela and Wardha), the sera of Bhubaneshwar and Rourkela were not reactive with mf of any of the four regions. The sera of microfilaraemics of Wardha did not bind to the mf from Rourkela region. Further analysis of antibody levels against *B.malayi* ES antigen in human sera from different endemic zones showed high GMT of filarial IgG antibody in microfilaraemic sera of Wardha region compared to Bhubaneshwar ($P<0.05$). The microfilaraemic and as well clinical filarial sera of Wardha also showed significantly high GMT of filarial IgG antibodies against *B.malayi* mfS antigen compared to the antibody levels in the respective categories of sera from Calicut region ($P<0.05$). These differences in the seroreactivity of filarial groups in different endemic zones to the mf isolates of different geogrophical regions and difference in filarial antibody responses in different host populations may reflect parasite specific variations in immunogenecity.

Introduction

Human lymphatic filariasis is a mosquito-borne disease of the tropics caused by infection with the nematode parasites *Wuchereria bancrofti* and *Brugia malayi*. According to the estimates available from National Institute of Communicable Diseases (NICD), Delhi, there are 412 million people exposed to the infection in India with 31 million people harboring microfilariae and another 21 million suffering from chronic manifestations of the disease like hydrocele, lymphoedema and elephantiasis [1]. Lymphatic filariasis is characterized by a wide spectrum of clinical manifestations. The nature of spread of infection and disease manifestations due to *W.bancrofti* infection have been noted to differ from country to country and also from one community to another within the country. Genital manifestations specially hydrocele are more prevalent in North, while swelling /elephantiasis of limbs was predominant in South [2]. Scrotal hydrocele is also reported to be quite common in Orissa [3]. There has also been considerable variability among the filarial cases in their response to antifilarial drugs [4,2]. Existence of such wide spread variability in the disease pattern and in chemotherapeutic response in the infected cases suggests the presence of different strains of the *W. bancrofti* parasite. This will have serious implications in the control /elimination programmes of this major tropical disease. The existence of different strains of a parasite may affect the application of immunodiagnostics and chemotherapeutics and may also influence the efficacy of vaccination.

Ravindran *et al* [5] provided the serological evidence for the existence of different strains of *W bancrofti* by demonstrating the differential reactivity of sera of mf carriers to mf sheath. This study also showed that mf carriers sera could be used as 'serotyping' reagents for differentiating the 'strains' of *W .bancrofti*. Analysis of morphological variations and isoenzyme patterns of a parasite and serotyping of infected people from different localities are the approaches that help in identification of different strains of the parasite. However no extensive and confirmatory studies have been conducted on the seroreactivity patterns among *W.bancrofti* infected individuals from different endemic areas . The present communication reports on the differential seroreactivity among the different groups of bancroftian filariasis of four endemic regions in India.

Materials and Methods

Study population:

The study population comprised of individuals residing in Calicut (Kerala), Wardha (Maharashtra), Trivendrum (Kerala), Bhubaneshwar (Orissa) and Rourkela (Orissa) which are endemic for bancroftian filariasis. Parasitological, clinical examination and blood withdrawal were done after taking the informed conscent from individuals.

Collection of blood samples:

Blood samples were collected from *W.bancrofti* infected microfilaraemic individuals from different endemic areas mentioned above. The presence of mf was checked in the finger prick blood samples collected at night between 21:00 and 24:00 h. About 10 ml of blood sample was collected from each individual during night hours. About 2ml of blood was transferred to a sterile plain vial (for serum separation). The rest was transferred into another sterile container with 2.5ml of Citrate dextrose solution (anticoagulant), mixed gently and was placed in an ice box or refrigerator.

Isolation of W.bancrofti microfilariae:

Microfilariae were isolated from blood samples as described by Davaney and Howell's [6] with few modifications. Blood samples were diluted with equal volume of normal saline and filtered through 5µ nucleopore membrane filter. After passing two more volumes of normal saline, the filter holder was inverted and the membrane was flushed with normal saline. The filter membrane was removed and transferred to a petridish, the membrane was washed thoroughly with normal saline, the washings were collected in a centrifuge tube and centrifuged at 2000 xg for 5-10 min. The supernatant was discarded and the mf pellet was collected in normal saline.

The mf was further purified in normal saline by percoll gradient separation. The microfilarial suspension was carefully layered on the top of the percoll gradient (0.6% to 100%) and centrifuged at 10000xg for 10min. The whitish band containing microfilariae at the interface between the 0.6% and the undiluted percoll layer was removed and washed several times in RPMI-1640 medium. Finally the pellet was resuspended in 200µl of Tris EDTA buffer and stored at -70°C.

Analysis of seroreactivity of filarial endemic populations with mf isolates from different endemic areas by Indirect Fluorescent Antibody Test (IFAT) :

IFAT was performed as described by Kaliraj *et al* (7) with few modifications. About 100 microfilariae were incubated with different test sera diluted optimally (1:10) in PBS (0.05M) in conical vials and incubated at room temperature for 2 hr. After washing twice with PBS in a microfuge, the mf were further incubated with 20µl of optimally diluted (1:10 in 0.05M PBS) anti human IgG-FITC conjugate at 4°C for 1hr. The mf were washed twice with PBS and further incubated with 0. 1% Evans blue for 5min at 4°C. The mf were taken on to a glass slide with 20 µl of mount solution (50% glycerol in 0.06M carbonate buffer, pH 9.6), placed a cover slip, the edges were sealed and observed under a fluorscene microscope (Nikon, Japan) using 10X objective lens. A positive result was recorded when yellow green fluorescence was observed on the surface of microfilariae . Intensity of fluorescence was expressed as +++ (high), ++(medium) and +(Low) or NR (Non-reactive) for each mf preparation.

B. malayi microfilarial Excretory-Secretory (ES) antigens :

Bm mf ES antigens were prepared as described by Chenthamarkshan *et al* (8) with few modifications. *B.malayi* mf were isolated from the peritoneal lavage of jirds with intra peritoneal infections of 4 months or more duration. Mf (15,000/ml) were maintained in RPMI-1640 supplemented with organic acids and sugars of Grace's culture medium and 0.1mM phenyl methyl sulphonyl floride (PMSF) at 28°C for 48 h. The supernatant was collected, concentrated by ultra membrane filtration and dialyzed against 0.01M sodium phosphate buffer (SPB) pH 7.2. The protein content was measured by Lowry's method (9) and the antigen was stored at –70°C with a cocktail of protease inhibitors, viz., ethylene diamine tetra acetic acid (EDTA), PMSF at 0.1mM concentration and tosyl-L-lysine chloromethyl ketone (TLCK) at 0.2 mM concentration

B. malayi microfilarial Phosphate Buffer Saline soluble (mfS) antigen:

B. malayi microfilarial soluble antigen was prepared as described by Kaliraj *et al* (10). About 10 Lakhs mf were washed twice with 0.05M Phosphate buffer saline (PBS) pH 7.2.The mf pellet was suspended in 2ml of 0.05M PBS containing 0.1mM EDTA,TPCK and PMSF and homogenized at 4°C for 30min.The homogenate was further sonicated at 4°C using vibronic sonicator ,10 times,each time for 30 sec at 1min intervals and further extracted overnight by gentle shaking at 4°C and supernatant collected was labelled as Bm mf S antigen. After estimation of protein the antigen was stored at –70°C until further use.

Stick Indirect Enzyme linked immunosorbant assay (ELISA):

The assay was done as described earlier [11] using cellulose acetate membrane fixed plastic sticks, coated with optimal concentration (100pg) of antigen fraction as sorbent material . Optimal dilution (1:300) and two fold dilutions of sera of different groups from different regions were analyzed for filarial antibodies. Anti-human IgG was conjugated to enzyme penicillinase (Sigma Chem.Co.,USA) following the method of Avrameas,(12) and used as a probe. The immune reaction was observed by incubating the stick each with 0.5 ml of starch-iodine penicillin substrate. The sera showing complete decolourisation of blue color substrate at least 3 minutes earlier than the referral negative control sample were considered positive.

Stick Inhibition Enzyme linked immunosorbant assay (ELISA):

Inhibiton ELISA was carried out as described by Ramprasad *et al* [13]. 5 µl volume of FSIgG (20µg/ml), sera dilution of 1:300 and penicillinase labeled excretory secretory antigen (1:1000) were used in the assay system. The persistent of blue color indicated a positive reaction.

Statistical Analysis:

Mann Whitney 'U' test was used to compare the GMT of various groups of sera from different regions.

Results

Seroreactivity of different filarial endemic populations with field mf isolates:

The results of the analysis of seroreactivity of different filarial groups from different endemic zones with *W.bancrofti* mf isolates in IFA are summarized in Table-1. The clinical filarial sera of Calicut and Wardha regions reacted strongly with the surface of mf collected from different zones . While the microfilaraemic sera of Bhubaneshwar and Rourkela showed no reactivity with mf isolates, the microfilaraemic sera from Calicut and Wardha samples showed medium to low reactivity with mf isolates of these two regions. The mf and clinical sera of Calicut also showed low reactivity with mf isolates of Rourkela and Wardha regions. Sera of endemic normals from all the endemic zones studied were non reactive with mf collected from all the zones.

Circulating filarial antibody and antigen levels in different endemic populations:

Filarial antibody levels against B.malayi mf ES antigen:

Sera samples were screened from four regions viz., Calicut, Bhubaneshwar, Trivendrum and Wardha and the results are summarized in Table 2 a,b,c. Among the microfilaraemic sera samples, 10 out of 11 (91%) from Calicut region, 14 out of 16(87.5%) from Wardha region and 28 out of 37(75.6%) from Bhubaneshwar were positive for filarial IgG antibody, while in clinical filariasis group 23 out of 26 (89%) from calicut region ,14 out of 16 (87.5%) from Wardha and 13 out of 16 (81.3%) from Trivendrum were positive for filarial IgG antibody. Among the endemic normal samples 1 out of 11 (9%) from Calicut; 2 out of 16(12%) from Wardha, 1 out of 10(10%) from Bhubaneshwar and 1 out of 9(11%) from Trivendrum were positive for filarial IgG antibodies. The microfilaraemic samples collected from Wardha region showed higher GMT (504) of filarial IgG antibodies when compared to microfilaraemic samples of Calicut (362) and Bhubaneshwar (336) but the difference was not statistically significant in case of Calicut microfilaraemic samples. However with Bhubaneshwar samples the difference was significant ($P<0.05$) The Clinical samples collected from calicut region showed somewhat higher Geometric Mean Titre of filarial IgG antibodies (511) compared to the GMT of antibodies in clinical samples of Wardha (483) and Trivendrum (372). But the difference was not significant (Fig. 1).

Filarial antibody levels against B.malayi mf S antigen:

Results of analysis of different groups of sera against Bm mf S antigen are shown in Table 3 a,b,c. Among the microfilaraemic sera samples, 8 out of 11 (73%) from Calicut region, 16 out of 16(100%) from Wardha region and 25 out of 37(68.5%) from Bhubaneshwar were positive for filarial IgG antibodies, While in case of clinical sera 15 out of 26 (57%) from Calicut region, 13 out of 16 (81%) from Wardha and 9 out of 16(56%) from Trivendrum were positive for filarial IgG antibodies. In the endemic normal group 1 out of 11 (9%) from Calicut, 2 out of 16(12%) from Wardha, 1 out of 10(10%) from Bhubaneshwar and 1 out of 9(11%) from Trivendrum were positive for filarial IgG antibodies. The Geometric Mean Titre of filarial IgG antibody in microfilaraemic sera of wardha region was higher (526) when compared to the antibody levels in microfilaraemic samples collected from Calicut (299) and Bhubaneshwar (226) and the difference was significant ($P<0.05$). In case of clinical samples the GMT of Wardha region was significantly higher (483) when compared to the GMT of antibody levels in samples from Calicut (242) and Trivendrum (203) ($P<0.05$)(Fig. 2).

Circulating filarial antigen levels against B.malayi mf ES antigen conjugate:

Bm mf ES penicillinase conjugate was used in inhibition ELISA for detection of circulating filarial antigen in bancroftian filarial sera of different regions. In mf positive cases, 9 out of 11 (81%) sera from Calicut, 11 out of 16 (68%) from Wardha and 26 out of 37 (70%) from Bhubaneshwar showed the presence of circulating filarial antigen. In clinical filarial group 19 out of 24 (79%) from Calicut, 5 out of 16(31%) from Wardha and 7 out of 16(43%) from Trivendrum were positive for filarial antigen. Among the endemic

Table 1: Analysis of seroreactivity of different endemic populations with field isolates of mf by Indirect Fluorescent Antibody Test

Region	Sera samples	Reactivity with microfilariae collected from endemic zones			
		Calicut	Bhubaneshwar	Rourkela	Wardha
Calicut	Mf	+	++	+	+
	Cl	+++	++	+	++
	En	NR	NR	NR	NR
Bhuban-	Mf	NR	NR	NR	NR
eshwar	En	NR	NR	NR	NR
Rourkela	Mf	NR	NR	NR	NR
Wardha	Mf	+	NR	NR	+
	Cl	++	+	NR	++
	En	NR	NR	NR	NR

Mf= Microfilaraemia ; Cl = Clinical filariasis ; En = Endemic normals ; NR = Non Reactive

Table 2a: Filarial IgG antibody levels in microfilaraemic sera collected from different endemic areas against B. malayi mf ES antigens

Group	Region	No Exam.	No +ve* (%+ve)	No of sera having filarial IgG antibody titre of 75	150	300	600	1200	GMT
	Calicut	11	10(91)	-	1	6	4	-	362 a
Mf	Wardha	16	14(87.5)	-	2	4	6	4	504 b
	Bhubaneshwar	37	28(75.6)	6	3	15	5	8	336 c

*sera showing filarial IgG antibody titre of ≥ 300
Mf= Microfilaraemic; GMT= Geometric Mean Titre
b Vs c P< 0.05

Table 2b: Filarial IgG antibody levels in Clinical filariasis sera collected from different endemic areas against B. malayi mf ES antigens

Group	Region	No Exam.	No +ve* (%+ve)	No of sera having filarial IgG antibody titre of 75	150	300	600	1200	GMT
	Calicut	26	23(89)	1	2	9	4	10	511 a
Cl	Wardha	16	14(87.5)	-	2	1	13	-	483 b
	Trivendrum	16	13(81.3)	2	1	6	4	3	372 c

*sera showing filarial IgG antibody titre of ≥ 300
Cl= Clinical filariasis; GMT= Geometric Mean Titre

Table2c: Filarial IgG antibody levels in endemic normal sera collected from different endemic areas against B. malayi mf ES antigens

Group	Region	No Exam.	No +ve* (%+ve)	No of sera having filarial IgG antibody titre of 75	150	300	600	1200	GMT
	Calicut	11	1 (9)	4	6	1	-	-	126a
En	Wardha	16	2(12)	7	7	2	-	-	120b
	Bhuba-neshwar	10	1(10)	3	6	1	-	-	130 c
	Trivendrum	9	1(11)	6	2	1	-	-	102 d

*sera showing filarial IgG antibody titre of ≥ 300
En = Endemic normal; GMT= Geometric Mean Titre

Table-3 a: Filarial IgG antibody levels in microfilaraemic sera collected from different endemic areas against B. malayi mf PBS(S) antigens

Group	Region	No Exam.	No +ve* (%+ve)	No of sera having filarial IgG antibody titre of 75	150	300	600	1200	GMT
	Calicut	11	8(73)	1	2	4	4	-	299 a
Mf	Wardha	16	16(100)	-	-	5	9	2	526 b
	Bhuba-neshwar	37	25(68.5)	6	6	22	3	-	226 c

*sera showing filarial IgG antibody titre of ≥ 300
Mf= Microfilaraemic; GMT= Geometric Mean Titre
a Vs b P<0.05 ; b Vs c P< 0.001

Table-3 b: Filarial IgG antibody levels in clinical filariasis sera collected from different endemic areas against B. malayi mf PBS(S) antigens

Group	Region	No Exam.	No +ve* (%+ve)	No of sera having filarial IgG antibody titre of 75	150	300	600	1200	GMT
	Calicut	26	15(57)	5	6	7	8	-	242 a
Cl	Wardha	16	13(81)	1	2	1	9	3	483 b
	Trivendrum	16	9(56)	3	4	8	1	-	203 c

**sera showing filarial IgG antibody titre of ≥ 300*
CL = Clinical filariasis ; GMT= Geometric Mean Titre
a Vs b P < 0.05 ; b Vs c P< 0.05

Table-3 c: Filarial IgG antibody levels in Endemic normal sera collected from different endemic areas against B. malayi mf PBS(S) antigens

Group	Region	No Exam.	No +ve* (%+ve)	No of sera having filarial IgG antibody titre of 75	150	300	600	1200	GMT
	Calicut	11	1(9)	5	5	1	-	-	116 a
En	Wardha	16	2(12)	3	11	2	-	-	143 b
	Bhuba-neshwar	10	1(10)	6	3	1	-	-	106 c
	Trivendrum	9	1(11)	6	2	1	-	-	102d

**sera showing filarial IgG antibody titre of ≥ 300*
En = Endemic normal ; GMT= Geometric Mean Titre

Table 4 a - *Filarial antigen levels in microfilaraemic sera collected from different endemic areas using Bm mf ES antigen conjugate*

Group	Region	No Exam.	No +ve* (%+ve)	No of sera having filarial IgG antibody titre of 150	300	600	1200	GMT
Mf	Calicut	11	9(81)	2	6	-	3	385 a
	Wardha	16	11(68)	5	6	-	5	372 b
	Bhubaneshwar	37	26(70)	11	11	2	13	412 c

**sera showing filarial IgG antibody titre of ≥ 300*
MF= Microfilaraemic; GMT= Geometric Mean Titre

Table 4b: Filarial antigen levels in Clinical filariasis sera collected from different endemic areas using Bm mf ES antigen conjugate

Group	Region	No Exam.	No +ve* (%+ve)	No of sera having filarial IgG antibody titre of 150	300	600	1200	GMT
	Calicut	24	19(79)	5	9	3	7	424 a
CL	Wardha	16	5(31)	11	-	2	3	300 b
	Trivendrum	16	7(43)	9	1	1	5	327 c

**sera showing filarial IgG antibody titre of ≥ 300*
CL= Clinical filariasis ; GMT= Geometric Mean Titre

Table 4c: Filarial antigen levels in Endemic normal sera collected from different endemic areas using Bm mf ES antigen conjugate

Group	Region	No Exam.	No +ve* (%+ve)	No of sera having filarial IgG antibody titre of				GMT
				150	300	600	1200	
	Calicut	11	2(18)	9	-	-	2	218 a
En	Wardha	16	3(18)	13	3	-	-	170 b
	Bhubaneshwar	10	1(10)	9	1	-	-	160 c
	Trivendrum	9	1(11)	8	-	1	-	174 d

**sera showing filarial IgG antibody titre of ≥ 300*
En = Endemic normal ; GMT= Geometric Mean Titre

Table-5 a: Filarial antigen levels in microfilaraemic sera collected from different endemic areas using Bm mf PBS(S) antigen conjugate

Group	Region	No Exam	No +ve* (%+ve)	No of sera having filarial IgG antibody titre of				GMT
				150	300	600	1200	
	Calicut	11	10(90)	1	6	1	2	438a
Mf	Wardha	16	13(81)	3	8	-	5	406b
	BhubaNeshwar	37	29(78)	8	12	8	9	420c

**sera showing filarial IgG antibody titre of ≥ 300*
MF= Microfilaraemic; GMT= Geometric Mean Titre

Table-5b: Filarial antigen levels in Clinical filariasis sera collected from different endemic areas using Bm mf PBS(S) antigen conjugate

Group	Region	No Exam.	No +ve* (%+ve)	No of sera having filarial IgG antibody titre of				GMT
				150	300	600	1200	
	Calicut	24	17(71)	7	11	3	3	318a
CL	Wardha	16	8(50)	8	-	5	3	342b
	Trivendrum	16	7(44)	9	2	1	4	300c

**sera showing filarial IgG antibody titre of ≥ 300*
CL= Clinical filariasis ; GMT= Geometric Mean Titre

Table 5c: Filarial antigen levels in Endemic normal sera collected from different endemic areas using Bm mf PBS(S) antigen conjugate

Group	Region	No Exam.	No +ve* (%+ve)	No of sera having filarial IgG antibody titre of				GMT
				150	300	600	1200	
	Calicut	11	1(9)	10	1	-	-	160a
En	Wardha	16	1(6)	15	1	-	-	157b
	Bhubaneshwar	10	1(10)	9	-	1	-	172c
	Trivendrum	9	1(11)	8	1	-	-	162d

**sera showing filarial IgG antibody titre of ≥ 300*
En= Endemic normal ; GMT= Geometric Mean Titre

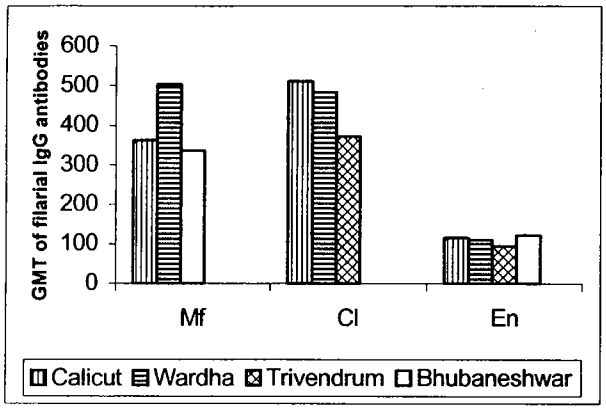

Fig.1: Geometric Mean Titres of Filarial IgG antibodies in sera of different groups collected from different endemic areas against B. malayi mf ES antigen (Mf= microfilaraemic; Cl = Clinical filariasis; En = Endemic normal)

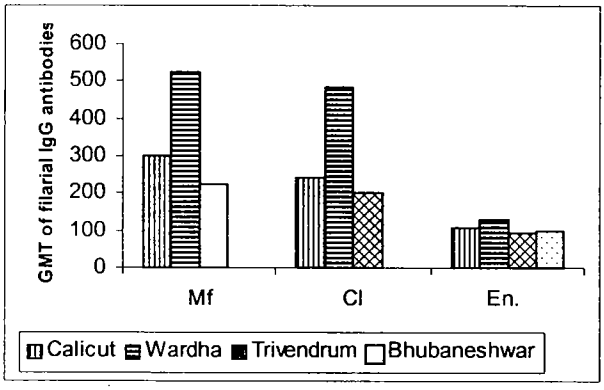

Fig.2: Geometric Mean Titres of Filarial IgG antibodies in sera of different groups collected from different endemic areas against B.malayi mf PBS (S) antigens. (Mf= microfilaraemic; Cl = Clinical filariasis; En = Endemic normal)

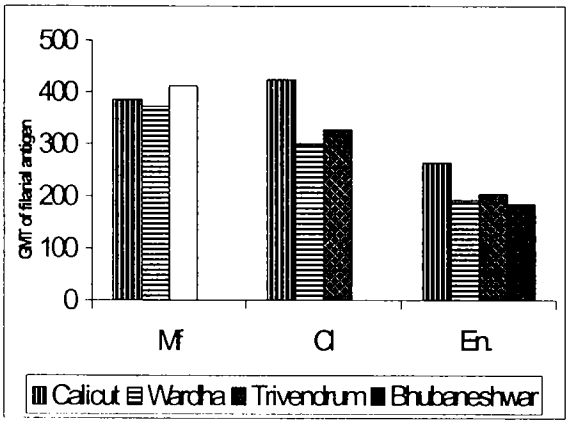

Fig.3: Geometric Mean Titres of Filarial antigen levels against Bm mf ES antigen conjugate in sera of different groups collected from different endemic areas. (Mf= microfilaraemic; Cl = Clinical filariasis;En=Endemic normal).

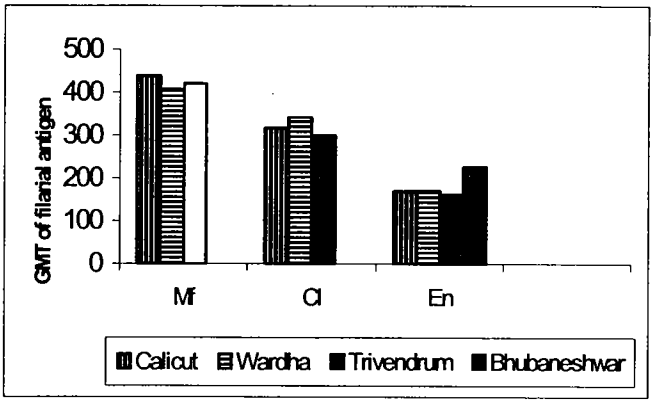

Fig.4: Geometric Mean Titres of Filarial antigen levels against Bm mf PBS (S) antigen conjugate in sera of different groups collected from different endemic areas. (Mf= microfilaraemic;Cl=Clinical filariasis; En= Endemic normal)

normal samples 2 out of 11 (18%) from Calicut, 3 out of 16(18%) from Wardha ,1 out of 10(10%) from Bhubaneshwar and 1 out of 9(11%) from Trivendrum were positive for filarial antigen (Table-4 a,b,c). There was no significant difference in GMTs for filarial antigen in microfilaraemic as well as clinical filarial sera samples collected from Bhubaneshwar, Wardha and Calicut (Fig.3).

Circulating filarial antigen levels using Bmalayi mf PBS(S) antigen conjugate:

Using PBS (S) antigen Penicillinase conjugate, in microfilaraemic group, 10 samples out of 11(90%) from Calicut, 13 out of 16 (81%) from Wardha and 29 out 37(78%) from Bhubaneshwar were positive for filarial antigen. While in clinical filarial group 17 out of 24 (71%) Calicut samples, 8 out of 16(50%) Wardha samples and 7 out of 16 (44%) Trivendrum samples showed positivity for filarial antigen (Table-5 a,b,c). In the endemic normal group 1 out of 11(9%) samples collected from Calicut region,1 out of 16(6%) from Wardha, 1 out of 10(10%) from Bhubaneshwar and 1 out of 9(11%) from Trivendrum showed positivity for filarial antigen. There was no significant difference in the GMTs of filarial antigen in both microfilaraemic and clinical filarial sera of different zones (Fig 4).

Discussion

Immunological criteria have also been used to study genetic variants of parasites. The differences in the antigenicity of the parasite and cellular and antibody responses in the host have been considered to correlate with different geographical isolates of *Trichinella* (14, 15, 16).

In the present study the immune responses of different filarial endemic populations were studied by analyzing their seroreactivity with different geographical isolates of *W.bancrofti* mf in indirect fluorescent antibody test and by assaying for filarial antibody and antigen levels by ELISA. In IFAT, microfilaraemic and as well clinical filarial sera from Calicut showed binding to the mf isolates of all the four endemic zones studied (Calicut, Bhubaneshwar,

Rourkela & Wardha). While clinical filarial sera from Wardha showed binding to mf of Calicut, Bhubaneshwar and Wardha regions, the microfilaraemic sera were reactive with the mf of Calicut and Wardha. Sera of Bhubaneshwar and Rourkela were not reactive with mf of any of the four regions (Table-1). These variations in host responses in different endemic zones to the mf isolates of different geographical regions presumably reflect mf isolate specific variations in immunogenicity.

Ravindran *et al* [5] reported on the differential reactivity of anti-sheath antibodies in *W.bancrofti* microfilariae carriers. Microfilariae of *W.bancrofti* purified from five different mf carriers were used separately as antigen to identify anti-sheath antibodies and the reactivity was found to be quite variable to the five different mf preparations suggesting the existence of polymorphic antigens on the sheath of *W.bancrofti* mf. This study also indicated the possible use of mf carrier sera as 'serotyping' reagents for differentiating the 'strains' of *W.bancrofti.*

The analysis of filarial antibody responses in samples of different endemic zones by ELISA also showed the existence of such variations in the host response to the parasite antigens. The microfilaraemic sera of Wardha compared to those of Bhubaneshwar showed significantly high GMT of filarial IgG antibodies against both *B.malayi* mfES and mfS antigens($P<0.05$). The microfilaraemic and as well clinical filarial sera of Wardha also showed significantly high GMT of filarial IgG antibodies against *B.malayi* mfS antigen compared to the antibody levels in the respective categories of sera from Calicut region (Fig.2) ($P<0.05$). However there were no significant differences in the circulating filarial antigen levels in different endemic populations (Fig. 3,4).

These observations validate the belief that distinct populations of parasite may show significant differences in immunogenicity. The variation in the antibody responses among the sera of different endemic zones provides indirect evidence on the possible existence of different strains among the filarial parasites. Further studies on genetic or isoenzyme analysis of the *W.bancrofti* collected from different endemic zones will be useful to confirm and characterize such strain variations.

Acknowledgement

This work was supported by the Dept of Biotechnology and the JBTDRC Research scheme of Mahatma Gandhi Institute of Medical Sciences, Sevagram. Our thanks Shri. Dhirubhai Mehta, President, KHS and Dr. (Mrs). P. Narang, Dean, Mahatma Gandhi Institute of Medical Sciences for their keen interest and encouragement in this work.

References

1. National Institute of Communicable Diseases Revised strategy for control of lymphatic filariasis in India (Recommendations of the WHO sponsored workshop) New Delhi 4-5 January. 1996
2. Rao CK, Sen T, Narasimhan MVVL, Krishna Rao CH, Sharma SP. Variation in clinical pattern of bancroftian filariasis in Kerala and Uttar Pradesh. J.Com.Dis. 1977; 9: 203-205.
3. Dandapat MC. Mahapatro SK ,Mohanty SS. The incidence of filaria as an aetiological factor for testicular hydrocele. Br.J.Surg. 1986; 73: 77-78.
4. Sasa M. Human filariasis- A global survey of epidemiology and control. University of Tokyo Press, Tokyo 1976; p.334.
5. Ravindran B. Satapathy AK, Sahoo PK. Bancroftian filariasis-differential reactivity of antisheath antibodies in microfilariae carriers. Parasite Immunology 1994; 16: 321-323.
6. Davaney E, Howells RE. The development of exsheathed microfilariae of *Brugia pahangi* and *Brugia malayi* in mosquito cell lines; Ann.Trop.Med.Parasitol., 1979; 73: 277.
7. Kaliraj P, Ghirnikar SN, Harinath BC. Indirect flourescent antibody technique using sonicated *W.bancrofti* mf for immunodiagnosis of bancroftian filariasis. Indian.J.Exp.Biol., 1979; 17, 1148-1149.
8. Chenthamarakshan V, Reddy MVR ,Harinath BC. Diagnostic potential of fractionated *Brugia malayi* microfilarial excretory-secretory antigen for bancroftian filariasis. Trans. Of Roy. Soc. Trop. Med. & Hyg. 1996a; 90: 250-254.
9. Lowry OH, Rosenbrough NJ, Farr AL, Randall RJ. Protein measurement with the Folin- Phenol reagent. J. Biol. Chem., 1951; 193: 265-275
10. Kaliraj P, Ghirnikar SN , Harinath BC. Fractionation and evaluation of Wuchereria bancrofti microfilarial antigens in Immunodiagnosis of bancroftian filariasis. Ind. J. Exptl. Biol. 1982; 20: 440-444.
11. Parkhe KA, Prasad GBKS, Das A, Harinath BC, Roebber M , Hamilton RG. Disc/Stick ELISA for diagnosis of bancroftian filariasis. Ind. J. Exptl. Biol 1986; 24: 437-439.
12. Avrameas S. Coupling of enzymes to proteins with glutaraldehyde- use of conjugates for the detection of antigen and antibody. Immunochem. 1969; 6: 43-52
13. Ramaprasad P, Reddy MVR, Kharat, Harinath.B.C). Comparison of radioimmunoassay and inhibition enzyme linked immunosorbant assay (ELISA) using 14c-labeled *W.bancrofti* microfilarial excretory- secretory antigen for the detection of filarial antigen. IRCS Med.Sci. 1985; 13: 1110-1111.
14. Goyal PK, Wakelin D. Influence of variation in host strain and parasite isolate on inflammatory and antibody responses to *Trichenella spiralis* in mice. Parasitology. 1993; 106: 371-378.
15. Bolas-Fernandez F, Wakelin D. Infectivity of *Trichenella* isolates in mice is determined by host immune responsiveness. Parasitology. 1989; 99: 381-388
16. Sukhdeo MVK and Meerovitch FA comparison of the antigenic characteristics of three geographical isolates of *Trichenella*. Int.J.of Parasitol. 1979; 9: 571-576.

Correspondence

Dr. M.V.R. Reddy
Department of Biochemistry
MGIMS, Sevagram
Wardha-442102
India
e-mail: mvreddymgims@rediffmail.com

Biomedical Research 2004; 15 (2): 150-152

A novel "no touch" saphenous vein harvesting technique for coronary artery bypass surgery: A new strategy to improve vein graft patency

Domingos S.R. Souza[1], Mikael Arbeus[1] and Derek Filbey[2]

Departments of Cardiothoracic Surgery[1], and Transfusion Medicine[2], Örebro University Hospital, Örebro, Sweden

Key words: CABG, saphenous vein, no-touch technique

Accepted February 17 2004

Abstract

This contribution briefly describes a technique for harvesting saphenous vein (SV) for coronary artery bypass graft surgery (CABG), which has been successfully applied to our patients at the Cardiothoracic Department, Örebro University Hospital, Sweden. This improved 'no-touch' harvesting technique is very beneficial to patients health as is indicated by the graft patency at mid-term and long-term follow-up studies.

Introduction

CABG that was developed in the late1960s utilizing the SV graft, has dramatically changed the management of patients with ischemic heart disease. There are three main reasons for CABG: a) to relieve ischemia resistant to medical treatment, b) to prevent myocardial infarction and c) to increase a productive life span [1]. Although coronary bypass surgery has achieved these goals, the degeneration of the venous graft with time is a major problem. All data indicate that the long-term outcome of venous bypass grafts is poor and that one should strive to use alternative methods. Virtually every synthetic and biologic alternative to arterial conduits or autologous fresh SV has proved disappointing. Nowadays the use of arterial conduits, which have a better long-term outcome, has become very common. Nevertheless, the SV is still an important conduit for CABG. However, for SV grafts to remain useful as stable and long-lasting coronary bypass conduits, graft thrombosis and atherosclerosis, which are the most important pathologic changes causing graft failure, must be delayed or prevented.

Vein graft failure

In the 1980s several studies published by Campeau 2], Bourassa [3] and Grondin [4] demonstrated that severe atherosclerotic deterioration of SV grafts occurs between 6 and 11 years. They proposed that aortocoronary surgery, with the use of SV grafts, should eventually be reconsidered and suggested that modifications of harvesting techniques and pharmacological intervention might improve the durability of aortocoronary vein grafts. At the same time Loop [5], in a great number of patients, showed a clear advantage of using the internal mammary artery (IMA) over the SV.

Despite the widespread use and superior patency of the IMA, the SV continues to be the most commonly used conduit for CABG. However, vein graft failure is associated with recurrence of angina [2] and is one of the primary reasons for re-operation. Early vein graft failure occurs in approximately 18% of SV grafts within the first month of implantation and approx 30% of SV grafts occlude within the first year [6]. At ten years, graft occlusion rates are more than 50% and the grafts that remain patent frequently show angiographic luminal irregularity or narrowing. Preparation of the graft is important, as there is direct evidence that surgical injury during vein preparation causes severe intimal loss as well as biochemical and functional changes of the graft [7].

Strategies of reducing vein graft failure

Many strategies have been used to prevent vein occlusion and to improve short- and long-term graft patency rate. Apart from established adjuvant medical therapy, new pharmacological agents [8] and gene therapy [9], also mechanical devices [10] are presently undergoing evaluation. Many of these strategies have shown promise in experimental vein bypass models, however few have successfully been transferred into clinical practice. In addition, an important point is the continued improvement of surgical techniques to prevent vein wall damage during its harvesting and implantation.

Routinely, vein graft is prepared with the *conventional harvesting technique*, which includes dissection of the vein from its bed, ligation of side branches, and flushing and distension of the lumen to overcome spasm and to identify leaks [11]. Endothelial injury results from direct mechanical trauma and stretching as a result of luminal distension [12].

A" no-touch" technique of harvesting SV has been described (13) which consists of retaining the cushion of surrounding tissue that both prevents venospasm, thereby obviating the need for distension, and protects the vein from direct handling by surgical instruments even during performing the anastomoses (Fig. 1). We showed that the "no-touch" technique results in well-maintained endothelial cell integrity, as revealed both by scanning and transmission electron microscopy [13,14]. With the conventional technique there was extensive damage to the endothelial layer [13]. We could also demonstrate [15] that the adventitia and the

Fig. 1: Anastomosis with the "no-touch" procedure. The cushion of surrounding tissue prevents direct contact between instrument and vein.

Fig. 2: A "No-touch" graft anastomosed to a small size coronary artery.

cushion of surrounding tissue that remains intact after harvesting by the "no-touch" technique has high collagen content. This may therefore act as a buffer against the pulsatile stresses the graft is exposed to, working in a similar manner as an external stent. There is evidence that even in the absence of intraluminal blood flow the vasa vasorum maintained endothelial integrity and that endothelium is very sensitive to the loss of the vasa vasorum [16]. Thus, the endothelial surface of an arterialized vein bypass is probably nourished by both the luminal blood and through the vasa vasorum blood supply. We found [17] that the vasa vasorum drains into the vein lumen, so it is possible that arterial blood from the lumen to some extent perfuses retrogradely through the vasa vasorum, thereby decreasing ischemic damage of the vein's medial layer.

The alterations in nitric oxide synthase (NOS) distribution in SV harvested by the "no-touch" technique was demonstrated and compared to that in conventionally harvested SV. In addition to the preservation of NOS associated with luminal endothelial cells, NOS in the media and adventitia of "no-touch" vessels were also preserved. This preservation of NOS sources suggests that nitric oxide (NO) availability, which is usually reduced by conventional surgical preparation, may be improved using the "no-touch" technique and that the NO pathway contributes to the improved results of SV harvested by this technique.

During surgery and in the immediate postoperative period, venospasm is often encountered and NO donors have been shown to reduce venospasm via their vasodilator action (18). Preservation of adequate

endogenous NO may provide protection against venospasm; indeed no significant venospasm occurs intraoperatively using the "no-touch" technique, abolishing the need for distension and any resultant vascular damage. This protective mechanism may be maintained during the early postoperative period and counteract any effects of endogenous vasoconstrictors to which the vein graft is highly sensitive [18].

The early patency rate of SV harvested with surrounding tissue is very high [19], even in SV grafts demonstrating low blood flow (Fig 2). Such a high patency rate has not been demonstrated when using other harvesting techniques. Furthermore, the preliminary results of the long term angiographic follow up, which will be reported in the near future, has also shown a high patency rate for the SV grafts that were prepared with the "no touch" technique.

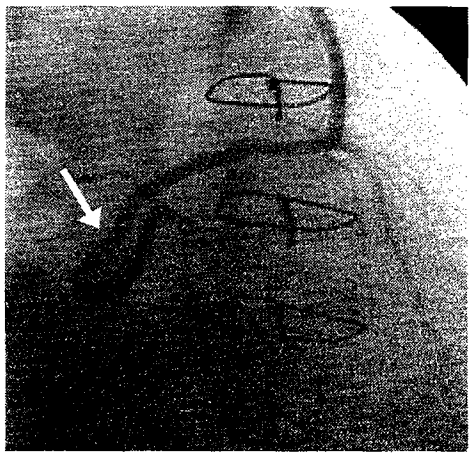

Fig. 3: Excessively long "no-touch" graft without kinking.

When the vein is stripped from its surrounding tissue, the accurate adjustment of the length of the graft is an important technical aspect as kinking will certainly occur if the graft is too long. Many techniques have been applied for dealing with aorto-coronary graft length to prevent kinks and twists in the grafts [20]. The preservation of the surrounding tissue when using the NT technique protects the vein graft and prevents the occurrence of such complications (Fig. 3).

In conclusion, the technique of harvesting the SV has a great influence on the fate of the venous graft and our study was based on a novel harvesting technique of SV preparation for CABG whereby the vein is protected by its cushion of surrounding tissue. The adventitial layer and the structures

contained within the cushion of surrounding tissue possess both mechanical and functional properties that protect the vein from spasm and ischemia. Endothelial integrity remained intact when using the "no-touch" technique. NOS activity was also preserved on the endothelium and on both neuronal and adventitial microvessel sources, suggesting that these grafts retain NO availability. The vasorelaxant and thromboresistant activities of NO may be responsible for the reduced venospasm and observed improved patency rates associated with the "no-touch" technique. In addition, the surrounding tissue supports excessively long vein grafts and prevents them from kinking.

Our results suggest that the "no touch" technique for harvesting the SV for CABG could be an additional strategy to improve both the short and the long-term patency rate of the venous graft.

References

1. Rahimtoola SH. Coronary bypass surgery - a perspective. In: Rahimtoola SH, Brest AN, editors. *Coronary Bypass Surgery.* Philadelphia: F A Davis, 1977: 11.
2. Campeau L, Enjalbert M, Lesperance J, Vaislic C, Grondin CM, Bourassa MG. Atherosclerosis and late closure of aortocoronary saphenous vein grafts: sequential angiographic studies at 2 weeks, 1 year, 5 to 7 years, and 10 to 12 years after surgery. *Circulation* 1983; 68: 1-7.
3. Bourassa MG, Enjalbert M, Campeau L, Lesperance J. Progression of atherosclerosis in coronary arteries and bypass grafts: ten years later. *Am J Cardiol* 1984; 53: 102C-107C.
4. Grondin CM, Campeau L, Lesperance J, Enjalbert M, Bourassa MG. Comparison of late changes in internal mammary artery and saphenous vein grafts in two consecutive series of patients 10 years after operation. *Circulation* 1984; 70: 208-212.
5. Loop FD, Lytle BW, Cosgrove DM, Stewart RW, Goormastic M, Williams GW, et al. Influence of the internal-mammary-artery graft on 10-year survival and other cardiac events. *N Engl J Med* 1986; 314: 1-6.
6. Mehta D, Izzat MB, Bryan AJ, Angelini GD. Towards the prevention of vein graft failure. *Int J Cardiol* 1997; 62 Suppl 1: S55-63.
7. Mills NL, Everson CT. Vein graft failure. *Curr Opin Cardiol* 1995; 10: 562- 568.
8. Sogo N, Campanella C, Webb DJ, Megson IL. S-nitrosothiols cause prolonged, nitric oxide-mediated relaxation in human saphenous vein and internal mammary artery: therapeutic potential in bypass surgery. *Br J Pharmacol* 2000; 131: 1236-1244.
9. Janssens S, Flaherty D, Nong Z, Varenne O, van Pelt N, Haustermans C, et al. Human endothelial nitric oxide synthase gene transfer inhibits vascular smooth muscle cell proliferation and neointima formation after balloon injury in rats. *Circulation* 1998; 97: 1274-1281.
10. Mehta D, George SJ, Jeremy JY, Basher Izzat M, Southgate KM, Bryan AJ, et al. External stenting reduces long-term medial and neointimal thickening and platelet derived growth factor expression in a pig model of arteriovenous bypass grafting. *Nature Medicine* 1998; 4: 235-239.
11. Hofer H, Mihatsch MJ, Guggenheim R, Amsler B, Hasse J, Graedel E. Morphologic studies in saphenous vein grafts for aorto-coronary bypass surgery. Part I: Morphology of the Graft using ordinary surgical preparation techniques. *Thorac Cardiovasc Surg* 1981; 29: 32-37.
12. Adcock OT, Adcock GLD, Wheeler JR, Gregory RT, Snyder SO, Gayle RG. Optimal techniques for harvesting and preparation of reversed autogenous vein grafts for use as arterial substitutes: A review. *Surgery* 1984; 96:886-94.
13. Souza D. A New No-touch Preparation Technique. Scand J Thorac Cardiovasc Surg 1996; 30: 41-44.
14. Ahmed SR, Johansson BL, Karlsson MG, Souza DSR, Dashwood MR, Loesch A. Human saphenous vein and coronary bypass surgery: ultrastructural aspects of conventional and 'no-touch' vein graft preparations. *Histol Histopathol* (2003) (in press)
15. Tsui JCS, Souza DR, Filbey D, Bomfim V, Dashwood MR. Preserved endothelial integrity and nitric oxide synthase in saphenous vein graft harvested by a "no-touch" technique. *Br J Surg* 2001;88:1209-1215.
16. Corson JD, Leather RP, Naraynsingh V, Karmody AM, Shah DM. Relationship between vasa vasorum and blood flow to vein bypass endothelial morphology. *Arch Surg* 1985; 120:386-388.
17. Souza DSR, Christofersson RHB, Bomfim V, Filbey D. "No-touch" technique by using saphenous vein harvested with its surrounding tissue for coronary artery bypass grafting maintains an intact endothelium. *Scand J Thorac Cardiovasc Surg* 1999; 33:323-9.
18. Cracowski JL, Stanke-Labesque F, Sessa C, Hunt M, Chavanon O, Devillier P, et al. Functional comparison of the human isolated femoral artery, internal mammary artery, gastroepiploic artery, and saphenous vein. *Can J Physiol Pharmacol* 1999; 77:770-6.
19. Souza D.S.R., Bomfim V, Skoglund H, Dashwood M.R., Borowiec J.W., Bodin L. and Filbey D. High early patency of saphenous vein graft for coronary artery bypass harvested with surrounding tissue. Ann Thorac Surg 2001; 71:797-800.
20. Durrani A, Sim EKW, Grignani RT. Accurate length adjustment of aortocoronary saphenous vein bypass grafts. *Ann Thorac Surg* 1998; 66:966-7.

Correspondence:

Dr. Domingos S R Souza
Department of Cardiothoracic Surgery
Örebro University Hospital
SE-701 85 Örebro
Sweden

Phone: +46 19 602 52 20
e-mail: domingos.souza@orebroll.se

Biomedical Research 2004; 15 (2): 153-156

The effect of surgical trauma on vein graft occlusion

Michael R Dashwood

Department of Clinical Biochemistry, Royal Free and University College Medical School, Pond Street, London NW3 2QG, UK

Key words: bypass surgery, saphenous vein, occlusion, vascular damage, endothelium

Accepted February 10 2004-07-03

Abstract

Although the saphenous vein is the most commonly used vessel for coronary artery disease graft failure is high. During harvesting this vein is exposed to considerable damage due to surgical trauma and high pressure distension. There is evidence of increased graft patency in veins that have been prepared using atraumatic surgery and that this improvement is mainly associated with the preservation of structures that are removed, or damaged, during conventional surgery. In this review we consider the importance of the endothelium and the tunica adventitia on the performance of saphenous veins used as coronary artery bypass grafts.

Introduction

Over the last 30 years coronary artery bypass surgery (CABG) has become a well-established means of revascularization in patients with coronary artery disease. The use of autologous grafts eliminates tissue rejection problems and the need of tissue typing and matching. The saphenous vein, in particular, has several practical advantages: it is expendable since lower limb venous drainage can rely solely on the deep venous system; its long length allows its use for multiple grafts and its superficial position renders it easily accessible, facilitating its exposure and harvest. The long saphenous vein has been the vessel of choice for autologous vein graft since its use was first described by Favaloro in 1969 [1] and is the most commonly used conduit in CABG in patients with coronary artery disease. Patency rates of venous conduits are generally poor, compared with those of arterial grafts such as the internal mammary, gastroepiploic and radial arteries, with early signs of graft occlusion appearing within months. However, suitable arterial conduits are not always available and the saphenous vein remains a commonly used conduit for CABG.

In this review the potential role of the adventitia and its associated structures on vein graft occlusion is considered and how their preservation during the surgical preparation and harvesting of veins may affect graft patency.

Pathophysiology of vein graft failure

Early vein graft failure occurs in up to 18% of saphenous vein grafts within the first month of implantation, and this is mainly due to thrombotic occlusion [2,3]. Within the first year up to 30% coronary saphenous vein grafts occlude, with subsequent occlusion rates of 2-3% per year [4,5]. At ten years, graft occlusion rates are more than 50% with the remaining patent grafts frequently showing angiographic lumenal irregularity or narrowing (see Fig. 1).

During vein harvest, a considerable degree of vascular trauma occurs, with consequent damage to the vessel wall (tunica media) and surrounding tissue (including the tunica adventitia). It has been suggested that vein graft occlusion may be largely due to the endothelial damage encountered during harvesting and clinical evidence and data from animal studies suggest that reduced graft patency is associated with endothelial damage and/or dysfunction. Recently, new observations indicate that adventitial remodelling and subsequent effects on microvessels (vasa vasorum) and vascular nerves may also be important in the pathophysiology of vein graft narrowing and occlusion.

Animal models of vein graft surgery have been used in an attempt to overcome certain problems encountered in patients following CABG. Experimental vein grafts in large animals have been developed such as the porcine carotid artery-saphenous vein interposition graft [6] and the canine femoral artery-internal jugular vein interposition graft [7]. Although such models may be relevant to the clinical situation, since the general anatomy and vascular histology of these species are close to those described in man, it is difficult to mimic the underlying lipid abnormalities and atherosclerotic vascular disease observed in humans, which contribute to vein graft occlusion. Another potential limitation of these models is that the type of graft and technique used are not the same as that used in man. For example, in the saphenous vein to carotid artery interposition graft model, the carotid artery does not have the same characteristics as the coronary arteries, which are exposed to quite different haemodynamic conditions following bypass surgery. This model generally uses end-to-end anastomoses that may not be a suitable model for the end-to-side anastomoses used in man.

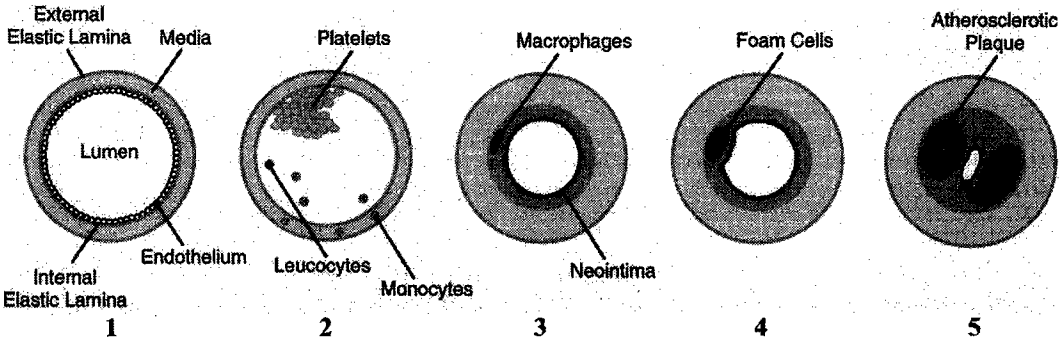

Fig. 1: Different stages of vascular remodelling after vein graft surgery

1a. At day zero there may appear a few nests of smooth muscle cells within the intima and some degree of medial fibrosis may be present. The lumenal endothelium will be continuous and the lumen patent.

1b. Up to 1 week following graft implantation the surgical preparation during vessel harvesting results in endothelial injury and denudation. Subsequent thrombus formation occurs at regions where the intima is exposed. Adhesion of neutrophils and monocytes leads to the release of a range of factors that can stimulate smooth muscle cell proliferation and migration.

1c. Between 1 week and 1 month medial thickening occurs as a results from VSMC proliferation. VSMCs also migrate through the internal elastic lamina and this leads to neointimal formation (independent of endothelial damage). Macrophages may appear within the neointima.

1d. Between 1 month and 3 years typical atheromatous lesions may appear which are rich in foam cells and smooth muscle cells (characteristic of early atherosclerotic plaque formation).

1e. Beyond 3 years progressive intimal thickening occurs with formation of superimposed atheromatous plaques, resulting in narrowing of the lumen. Plaque rupture may occur, leading to thrombotic graft occlusion.

(modified from Jeremy and Dashwood [27]).

Despite these limitations many of the models may still be useful in so far as the grafts exhibit many of the morphological changes seen in human vein graft failure and that surgical/pharmacological interventions may be studied over relatively short time periods.

Coronary Artery Bypass Surgery (CABG)

During conventional surgical preparation of the saphenous vein for grafting, the perivascular tissue is stripped from the vein resulting in venospasm that is overcome by distention with saline at pressures of up to 600mm Hg. This procedure results in significant denudation of the endothelium with subsequent effects on vascular reactivity, thrombus formation, cell proliferation [8,9] and damage to the media [10]. Whilst it is now recognised that careful handling to reduce vascular trauma is important during vein harvesting, adventitial damage still occurs due to the stripping of the perivascular tissue. This could significantly contribute to graft occlusion since the adventitia contains the majority of vascular nerves and the vasa vasorum, a microvessel network that provides the vessel wall with oxygen and nutrients. There is also recent evidence that vein graft adventitial mass is increased, mainly due to the proliferation of fibroblasts and it has been sug gested that these fibroblasts from the adventitia are the progeny-

In CABG, the importance of atraumatic preparation of the saphenous vein has been recognised for many years. Different 'atraumatic' or 'no-touch' techniques have been described to minimize vein graft damage [13]. These generally aim to reduce or avoid direct instrumentation of the vein during harvesting. As mentioned above, venospasm is common following dissection and isolation of the vein and is overcome by hydraulic distension. Various pharmacological agents have been used topically or intraluminally to reduce venospasm [14]. Papaverine in electrolyte solution or in blood or albumin [15] and glyceryl trinitrate-verapamil solution [16] have been found to reduce the pressures required to overcome spasm during vein harvesting. The harvested vein is generally stored in colloidal and/or vasodilating solutions with storage time kept to a minimum.

Recently a novel 'no-touch' technique for vein harvesting has been described where the saphenous vein is harvested together with a cushion of surrounding tissue, with minimal handling of the vessel [17]. Apart from avoiding direct instrumentation of the vein as in earlier 'no-touch' techniques, Souza's technique also preserves the perivascular tissue. Interestingly, no significant venospasm is encountered using this technique and therefore, no mechanical distension or pharmacological vasodilators are required. Using this technique a graft patency rate of 95% was found on angiographic follow-up at 18 months [18]. Although the patient numbers were small, these pilot results are encouraging when compared to patency rates reported for current methods of surgery. Souza's technique has several potential advantages that could impact favourably on graft patency. Scanning electron microscopy has demonstrated improved endothelial integrity of grafts harvested by this technique compared with those harvested conventionally [19]. It is also possible that the surrounding tissue that remains in place using this technique acts to reduce the effects of pulsatile pressure and shear flow once the vein is subjected to coronary arterial conditions. Another potential ad-

vantage of this new no-touch technique is the preservation of the adventitia that would generally be damaged or removed during conventional harvesting of the saphenous vein. There is also evidence that distension of the saphenous vein required by conventional techniques to overcome spasm causes endothelial denudation and damage with associated loss of endothelial nitric oxide synthase (eNOS) [20]. This is obviated using Souza's approach since venospasm is not observed. eNOS is also located within the adventitia of 'no-touch' vein grafts and is associated with microvessels (vasa vasorum) and nerves [21]. Preservation of these microvascular and neuronal sources of nitric oxide (NO) in the native vessel, which are destroyed during conventional vein harvesting, may contribute to improved graft patency.

Tunica adventitia in veins

The tunica adventitia is the outermost layer of blood vessels and is usually removed during conventional harvesting of saphenous veins for use as bypass conduits. It is composed of longitudinally arranged collagenous tissue and elastic fibres. The connective tissue elements gradually merge with the loose connective tissue surrounding the vessel. The adventitia is relatively thin in most arterial vessels, but much thicker in venules and veins.

Large and medium veins are comprised of three layers, the tunica intima, tunica media and tunica adventitia. In large veins the adventitia is the thickest layer of the vessel wall. In medium veins such as the saphenous vein, the adventitia is usually thicker than the tunica media and consists of longitudinally oriented bundles of smooth muscle cells, collagen fibres and networks of elastin fibres. Also within the adventitia of medium and large veins are fibroblasts, macrophages and unmyelinated nerves.

Veins are also supplied by a more extensive vasa vasorum than arteries. The vasa vasorum represent a network of adventitial microvessels that are responsible for providing oxygen and nutrients to the wall of large arteries and veins. In particular, venous blood is poorly oxygenated, therefore the vasa vasorum is important in supplying the oxygen requirements of the cells of the venous wall. Since venous pressure is low, the vasa vasorum can approach the intimal layer without being collapsed by the pressure within the vein. The vasa vasorum of veins penetrate much closer to the intima than the vasa vasorum of arteries and this is particularly evident in the saphenous vein [22].

Potential role of adventitial structures in vein graft occlusion.

Vasa vasorum: The vasa vasorum has been shown to be associated with the long-term development of neointimal hyperplasia in vein grafts [23] and also with wound healing around saphenous vein grafts [24]. Damage to vasa vasorum in vein grafts may result in vessel wall hypoxia with subsequent neointima formation, similar to the observation in arteries where occlusion of vasa vasorum led to neointima formation and atherosclerosis [25,26].
Adventitial nerves: The vascular nerves located within the tunica adventitia of blood vessels are disrupted during bypass surgery. The innervation of veins differs from that of arteries, consequently there will be major differences between the saphenous vein graft and the host artery with respect to neurogenic factors [27,28]. Arteries remain under a degree of vascular tone that is influenced by the autonomic nervous system. Apart from classical compounds, such as acetylcholine, noradrenaline and 5-hydroxytryptamine, there is an increasing list of vasoactive transmitters including NO, canabinnoids and peptides such as substance P, vasoactive intestinal polypeptide and calcitonin gene-related peptide which affect vasomotor tone of arteries and veins.

The (autonomic) vascular nerves within the adventitia penetrate the adjacent tunica media to release neurotransmitters that can regulate vasomotor tone. Apart from their vasoactive properties many neurotransmitters are pro-mitogenic for vascular smooth muscle (e.g. noradrenaline and 5-hydroxytryptamine) and also have trophic actions on nerves [29,30]. The potential for certain neurotransmitters to play a trophic role in neointimal hyperplasia has been reinforced using animal models and pharmacological intervention. For example, a reduction in [^{3}H]-thymidine incorporation (a measure of cell proliferation) in the ear artery of young rabbits has been reported following sympathetic denervation [31] and alpha-adrenoceptor antagonists have been shown to inhibit neointima formation induced by vascular injury [32].

Adventitial fibroblasts: It has been suggested that adventitial fibroblasts are involved in neointimal formation and vessel occlusion [11,33]. There is evidence for adventitial remodelling following vascular damage, such as that caused during vein graft surgery. An increase in adventitial mass, due principally to the proliferation of fibroblasts has been described. More recently, it has been suggested that (myo)fibroblasts from the adventitia are the progenitors of the neointima [33]. The neointima may then progress, resulting in atherosclerotic changes in the vein wall, causing the neointima to be called "soil for atheroma" [34].

Conclusions

Clearly, prevention is better than cure. Early identification of patients with atherosclerotic risk factors and aggressive modification of these risk factors are important in the management of atherosclerotic vascular diseases. Bypass surgery, when required for established disease, is hampered by a high incidence of vein graft failure. New strategies are being introduced, with early data suggesting that improved patency rates are possible. These include the use of adjuvant pharmacological agents and local gene transfer strategies. However, the most promising advances may be accomplished by the modification of vein harvesting techniques, particularly those aiming to reduce the degree of surgical trauma.

Acknowledgements

Much of the work described in this review was supported by a British Heart Foundation Project Grant to M.R. Dashwood and J.C.S. Tsui.

References

1. Favaloro RG. Saphenous vein graft in the surgical treatment of coronary artery disease. Operative technique. J Thorac Cardiovasc Surg. 1969; 58: 178-185.

2. Izzat MB, West RR, Bryan AJ, Angelini GD. Coronary artery bypass surgery: current practice in the United Kingdom. Br Heart J. 1994;71: 382-385.
3. Mehta D, Izzat MB, Bryan AJ, Angelini GD. Towards the prevention of vein graft failure. Int J Cardiol. 1997;62 Suppl 1: S55-S63.
4. Bryan AJ, Angelini GD. The biology of saphenous vein graft occlusion: etiology and strategies for prevention. Curr Opin Cardiol. 1994;9: 641-649.
5. Angelini GD, Bryan AJ, Williams HM, Soyombo AA, Williams A, Tovey J et al. Time-course of medial and intimal thickening in pig venous arterial grafts: relationship to endothelial injury and cholesterol accumulation. J Thorac Cardiovasc Surg. 1992;103: 1093-1103.
6. Dashwood MR, Mehta D, Izzat MB, Timm M, Bryan AJ, Angelini GD et al. Distribution of endothelin-1 (ET) receptors (ET(A) and ET(B)) and immunoreactive ET-1 in porcine saphenous vein-carotid artery interposition grafts. Atherosclerosis. 1998;137: 233-242.
7. Ulus AT, Tutun U, Zorlu F, Can C, Apaydin N, Karacagil S et al. Prevention of intimal hyperplasia by single-dose preinsertion external radiation in canine-vein interposition grafts. Eur J Vasc Endovasc Surg. 2000;19: 456-460.
8. Cambria RP, Megerman J, Abbott WM. Endothelial preservation in reversed and in situ autogenous vein grafts. A quantitative experimental study. Ann Surg. 1985; 202: 50-55.
9. Dries D, Mohammad SF, Woodward SC, Nelson RM. The influence of harvesting technique on endothelial preservation in saphenous veins. J Surg Res. 1992;52: 219-225.
10. Angelini GD, Passani SL, Breckenridge IM, Newby AC. Nature and pressure dependence of damage induced by distension of human saphenous vein coronary artery bypass grafts. Cardiovasc Res. 1987;21: 902-907.
11. Shi Y, Pieniek M, Fard A, O'Brien J, Mannion JD, Zalewski A. Adventitial remodeling after coronary arterial injury. Circulation. 1996;93: 340-348.
12. Shi Y, O'Brien JE, Mannion JD, Morrison RC, Chung W, Fard A et al. Remodeling of autologous saphenous vein grafts. The role of perivascular myofibroblasts. Circulation. 1997;95: 2684-2693.
13. Gottlob R. The preservation of the venous endothelium by "dissection without touchin" and by an atraumatic technique of vascular anastomosis. The importance for arterial and venous surgery. Minerva Chir. 1977;32: 693-700.
14. Rosenfeldt FL, He GW, Buxton BF, Angus JA. Pharmacology of coronary artery bypass grafts. Ann Thorac Surg. 1999;67: 878-888.
15. Hausmann H, Merker HJ, Hetzer R. Pressure controlled preparation of the saphenous vein with papaverine for aorto-coronary venous bypass. J Card Surg. 1996; 11: 155-162.
16. Roubos N, Rosenfeldt FL, Richards SM, Conyers RA, Davis BB. Improved preservation of saphenous vein grafts by the use of glyceryl trinitrate-verapamil solution during harvesting. Circulation. 1995; 92: II31-II36.
17. Souza D. A new no-touch preparation technique. Technical notes. Scand J Thorac Cardiovasc Surg. 1996;30: 41-44.
18. Souza, D.S.R., Bomfim, V., Skoglund, H., Dashwood, M.R., Bodin, L. and Filbey, D. High midterm patency of saphenous veingraft for coronary artery bypass harvested with surrounding tissue. Ann Thorac Surg 2001; 71: 797-800.
19. Souza DS, Christofferson RH, Bomfim V, Filbey D. 'No-touch' technique using saphenous vein harvested with its surrounding tissue for coronary artery bypass grafting maintains an intact endothelium. Scand Cardiovasc J. 1999; 33: 323-329.
20. Chester AH, Buttery LD, Borland JA, Springall DR, Rothery S, Severs NJ et al. Structural, biochemical and functional effects of distending pressure in the human saphenous vein: implications for bypass grafting. Coron Artery Dis. 1998;9: 143-151
21. Tsui J, Souza DS, Filbey D, Bomfim V, Dashwood MR. Preserved endothelial integrity and nitric oxide synthase in human saphenous vein harvested by a novel 'no-touch' technique. J Physiol (Lond). 2000;528.
22. Wheater PR, Burkitt HG, Daniels VG. Functional Histology, A text and colour atlas. Edinburgh, London, Melbourne, New York: Churchill Livingstone; 1987.
23. McGeachie JK, Meagher S, Prendergast FJ. Vein-to-artery grafts: the long-term development of neo-intimal hyperplasia and its relationship to vasa vasorum and sympathetic innervation. Aust N Z J Surg. 1989;59: 59-65.
24. O'Brien JE, Shi Y, Fard A, Bauer T, Zalewski A, Mannion JD. Wound healing around and within saphenous vein bypass grafts. J Thorac Cardiovasc Surg. 1997;114: 38-45.
25. Barker SG, Talbert A, Cottam S, Baskerville PA, Martin JF. Arterial intimal hyperplasia after occlusion of the adventitial vasa vasorum in the pig. Arterioscler Thromb. 1993;13: 70-77.
26. Martin JF, Booth RF, Moncada S. Arterial wall hypoxia following thrombosis of the vasa vasorum is an initial lesion in atherosclerosis. Eur J Clin Invest. 1991;21: 355-359.
27. Jeremy, J.Y. and Dashwood, M.R. Innervation of the pig vein graft: a potential role for vascular nerves on graft occlusion; Chapter 18 In: Vascular Protection: Molecular Mechanisms and Novel Therapeutic Principles and Clinical Application. 2002. Eds G.M. Rubanyi, V.J. Dzau and J.P. Cooke, Taylor & Francis, London and New York, pp 223-236.
28. Dashwood MR, Angelini GD, Mehta D, Jeremy JY, Muenter K, Kirchengast M. Effect of angioplasty and grafting on porcine vascular nerves: a potential neurotropic role for endothelin-1. J Anat. 1998;192: 5-7.
29. Gutman, E. Neurogenic relations in the regeneration process. Brain Res 𝕀, 72-112. 1964.
30. Guth L. Trophic influences of nerve on muscle. Physiol Rev. 1968;48: 645-687.
31. Bevan RD. Effect of sympathetic denervation on smooth muscle cell proliferation in the growing rabbit ear artery. Circ Res. 1975;37: 14-19.
32. Law MM, Moore WS. Pharmacological inhibition of intimal hyperplasia in intact organisms. In: Dobrin PB, ed. Intimal Hyperplasia. Austin, USA: RG Landes; 1994: 307-325.
33. Shi Y, O'Brien JE, Fard A, Mannion JD, Wang D, Zalewski A. Adventitial myofibroblasts contribute to neointimal formation in injured porcine coronary arteries. Circulation. 1996;94: 1655-1664.
34. Schwartz SM, deBlois D, O'Brien ER. The intima. Soil for atherosclerosis and restenosis. Circ Res. 1995;77: 445-465.

e-mail address: e-mail mdashwood@rfc.ucl.ac.uk

Biomedical Research 2004; 15 (2): 157-159

Endothelin in Schwann cells of middle cerebral artery in a case of multiple system atrophy with autonomic failure.

Andrzej Loesch[1], Linda Kilford[2] and Ann Kingsbury[2]

[1]Department of Anatomy and Developmental Biology and Centre for Neuroscience, University College London, Gower Street, London, WC1E 6BT, UK
[2]Queen Square Brain Bank for Neurological Disorders, Institute of Neurology, University College London, Wakefield Street, London WC1N 1PJ, UK

Key words: Schwann cells, endothelin, middle cerebral artery, multiple system atrophy

Accepted January 11 2004

Abstract

This study demonstrates an association of perivascular nerves with immunoreactive endothelin-1 (ET-1) in the middle cerebral artery (MCA) of a subject who suffered multiple system atrophy (MSA) with autonomic failure. Finding of ET-1-positive Schwann cells embracing perivascular nerve varicosities suggests that ET-1 from Schwann cells may be implicated in autonomic failure in MSA.

Introduction

Degeneration of the nervous system, and autonomic dysfunction are the general characteristics of MSA [1-8]. We have previously reported several locations of ET-1 in the wall of human MCA in MSA [9]. This study showed that immunoreactive ET-1 was detected in the endothelium, vascular smooth muscle, and macrophages as well as in perivascular axon varicosities at the adventitial-medial border. These findings suggest a major role for ET-1 in MCA in MSA [9]. In non-diseased human MCA, immunoreactive ET-1 has previously been revealed in the endothelium and the perivascular autonomic nerves/axons [10, 11]. The present report provides further finding of a relationship between ET-1 and cerebrovascular autonomic nerves in the MCA in a MSA case with autonomic failure.

Material and Methods

An autopsy specimen (19 hours delay) of the left middle segment of MCA from a 63 year-old male suffering from MSA was examined. (For more details see [9]). Family consent (donation to the Queen Square Brain Bank for Neurological Disorders, Institute of Neurology, University College London), and ethical approval were obtained for this study. The subject was diagnosed as having MSA with autonomic failure 6 years before death, showing postural hypotension, which was symptomatic and worsening considerably in the last few months of life. 12 months before death he developed generalised 'slurring' of speech, bradykinesia, tremor, unsteadiness of walking and frequent episodes of central apnoea. The patient was taking L-DOPA and ephedrine daily within the last month of life. The patient died of respiratory failure. Histopathology examination confirmed the diagnosis of MSA, e.g. severe loss of neurones of the substantia nigra in combination with the presence of typical glial α-synuclein-positive cytoplasmic inclusions (GCIs).

Electron-immunocytochemistry

For a detailed description of methods see [9]. In brief, the dissected out MCA (left middle segment) was fixed in 4% paraformaldehyde and 0.2% glutaraldehyde, washed in 0.1M phosphate buffer, infiltrated with 10-20% sucrose, rapidly frozen at -80°C, and cryostat cross-sectioned at 50μm. Sections were processed for the pre-embedding ExtrAvidin electron-immunocytochemical method. Main steps of the procedure included: (i) incubation in 10% normal horse serum (Jackson ImmunoResearch Laboratories, West-Grave, PA, USA), (ii) incubation in mouse monoclonal antibody against human ET-1 (diluted 1:500 = 2μg/ml), (iii) incubation in a biotin-conjugated donkey anti-mouse IgG serum (Jackson ImmunoResearch; diluted 1:500), (iv) incubation in ExtrAvidin-horseradish peroxidase conjugate (Sigma, Poole, UK; diluted 1:1500), (v) exposure to 3,3'-diaminobenzidine (Sigma, Dorset, UK) and H_2O_2, (vi) exposure to 1% osmium tetroxide, (vii) dehydration in ethanol and propylene oxide, and (viii) flat embedding in Araldite and polymerisation. Ultrathin sections were stained with uranyl acetate and lead citrate, and subsequently examined using a JEOL-1010 transmission electron microscope. *Controls*: the mouse monoclonal ET-1 antibody (MCE-6901-01; the antibody highly specific for human ET-1) used in the present study, was manufactured and characterised by Peninsula Laboratories (Bachem UK Limited, St Helens, UK).

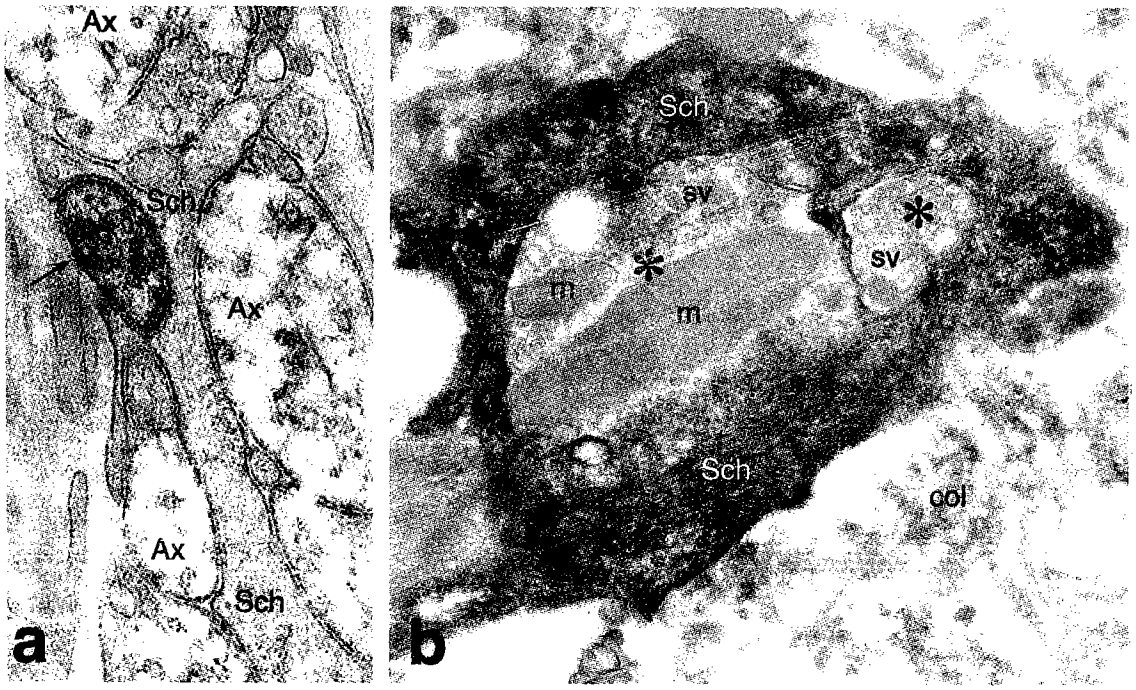

Fig. 1(a-b). ET-1 in perivascular nerves and Schwann cells in adventitia of MCA in a case of MSA with autonomic failure. (a) *Note immunoreactivity ('blackish' stain) for ET-1 in an axon varicosity (arrow) containing synaptic vesicles; Schwann cell (Sch) is immunonegative. Swollen axon profiles (Ax) displaying 'light' axoplasm scarce in synaptic vesicles are also seen. x 30,000.* ***(b)*** *Note that immunoreactivity for ET-1 is localised in a Schwann cell (Sch) embracing axon varicosities (asterisks); the varicosities are mostly immunonegative and display variety of synaptic vesicles (sv) and mitochondria (m); some labelling over varicosities is likely to belong to the immunoreactive Schwann cell; col=collagen. x 32,500.*

Results

Ultrastructural examination of the adventitial-media border of MCA showed the presence of perivascular autonomic nerve profiles and the associated immunoreactivity for ET-1. Immunoreactivity for ET-1 was localised in some axon profiles (Fig. 1a) and Schwann cells (Fig. 1b). ET-1-positive Schwann cells were closely associated with ET-1-negative axon varicosities (Fig. 1b).

Discussion

We showed that some of the adventitial Schwann cells of human MCA in MSA with autonomic failure immunoreact with a monoclonal antibody to human ET-1. Association of the ET-1-positive Schwann cells with ET-1-negative axon varicosities has been observed. The present study raises questions as to the nature of the relationship between ET-1, Schwann cell, nerve varicosity, and MSA.

Studies *in vivo* showed that ET-1 is implicated in the regulation of phenotype and proliferation of Schwann cells, suggesting an important role for ET-1 during nerve development and degeneration/regeneration [12, 13]. The regulation of Schwann cells proliferation and morphology is critical to nerve homeostasis [13]. The possibility cannot be excluded that during MSA this homeostasis is disturbed e.g. by ET-1 action deriving from Schwann cells. According to Pomonis et al. [14] there is a link between ET-1,

Schwann cells and nociception in peripheral nerves; endothelins (ETs) may have direct, nociceptive effects on the peripheral sensory nerves, whilst Schwann cells may be directly involved in signalling nociceptive events in peripheral tissues. On the other hand, ET-1 can promote the survival and differentiation of postganglionic sympathetic neurones, and can also both stimulate or inhibit the release of neurotransmitter(s) from postganglionic sympathetic neurones [15]. It has been found that the autonomic functions, at least of sympathetic nerves, may be preserved in MSA, but these nerves are not modulated efficiently [16]. Whether ET-1 deriving from Schwann cells influences nerve modulation in MSA is unknown at this stage.

ETs act in peripheral nerves and the ET_A and ET_B receptors are present on Schwann cells and neurones [14, 17, 18]. ET_B receptors are prevalent on Schwann cells, and can be coupled to phospholipase C and adenylyl cyclase [17]. Studies on diabetic neuropathy strongly support a view of the regulatory role of ETs in nerve physiology associated with proliferation and phenotype of Schwann cells [19]. This is in agreement with the fact that Schwann cells signal not only to themselves but also to the other cellular components within the nerve, particularly during nerve development [20].

A body of data has been collected on the oligodendrocytes and myalinated nerve fibres in the brain in MSA cases [see 5], whilst we know little about Schwann cells and ET-1 in autonomic nerves in MSA. Here we suggest that Schwann cells of cerebrovascular autonomic nerves may elaborate ET-1, which is likely to influence the autonomic function in MSA. Whether the ET-1 plays a beneficial or 'damaging' role needs to be determined. In this context, we are now examining more MSA cases in more detail.

Acknowledgements

The authors thank Ms Jane Pendjiky for assistance with the work with images.

References

1. Graham JG, Oppenheimer DR. Orthostatic hypotension and nicotine sensitivity in a case of multiple system atrophy. J Neurol Neurosurg Psychiat 1969; 32: 28-34.
2. Spokes EG, Bannister R, Oppenheimer DR. Multiple system atrophy with autonomic failure: clinical, histological and neurochemical observations on four cases. J Neurol Sci 1979; 43: 59-82.
3. Brooks DJ, Redmond S, Mathias CJ, Bannister R, Symon L. The effect of orthostatic hypotension on cerebral blood flow and middle cerebral artery velocity in autonomic failure, with observations on the action of ephedrine. J Neurol Neurosurg Psychiat 1989; 52: 962-966.
4. Mathias CJ. Autonomic disorders and their recognition. N Engl J Med 1997; 336: 721-724.
5. Castellani MD. Multiple system atrophy. Clues from inclusions. Am J Physiol 1998; 153: 671-676.
6. De Marinis M, Stocchi F, Gregori B, Accornero N. Sympathetic skin response and cardiovascular autonomic function tests in Parkinson's disease and multiple system atrophy with autonomic failure. Movement Disord 2000; 15: 1215-1220.
7. Horimoto Y, Aiba I, Yasuda T, Ohkawa Y, Katayama T, Yokokawa Y, Goto A, Ito Y. Cerebral atrophy in multiple system atrophy by MRI. J Neurol Sci 2000; 173: 109-112.
8. Rehman HU. Multiple system atrophy. Postgrad Med J 2001; 77: 379-382.
9. Mickey I, Kilford L, Kingsbury A, Loesch A. Endothelin in the middle cerebral artery: A case of multiple system atrophy. Histochem J 2002; 34: 469-477.
10. Gorelova E, Loesch A, Bodin L, Chadwick L, Hamlyn PJ, Burnstock G. Localization of immunoreactive Factor VIII, nitric oxide synthase, substance P, endothelin-1 and 5-hydroxytryptamine in human postmortem middle cerebral artery. J Anat 1996; 188: 97-107.
11. Loesch A, Burnstock G. Endothelin in human cerebrovascular nerves. Clin Sci 2002; 103 (Suppl. 48): 404S-407S.
12. Berti-Mattera LN, Wilkins PL Harwalkar S, Madhun S, Almhanna K, Mattera R. Endothelins regulate arachidonic acids and mitogen-activated protein kinase activity in Schwann cells. J Neurochem 2000; 75: 2316-2326.
13. Berti-Mattera LN, Harwalkar S, Hughes B, Wilkins PL, Almhanna K. Proliferative and morphological effects of endothelins in Schwann cells: roles of p38 mitogen-activated protein kinase and Ca^{2+}-independent phospholipase A_2. J Neurochem 2001; 79: 1136-1148.
14. Pomonis JD, Rogers SD, Peters CM, Ghilardi JR, Mantyh PW. Expression and localization of endothelin receptors: implications for the involvement of peripheral glia in nociception. J Neurosci 2001; 21: 999-1006.
15. Damon DH. Endothelin and post-ganglionic sympathetic neurons. Clin Exp Pharmacol Physiol 1999; 26: 1000-1003.
16. Robertson DA, Shannon JR, Jordan J, Davis TL, Diedrich A, Jacob G, Garland E, Tellioglu T, Biaggioni I. Multiple system atrophy: new developments in pathophysiology and therapy. Parkinsonism Relat Disord 2001; 7: 257-260.
16. Wilkins PL, Suchovsky D, Berti-Mattera LN. Immortalized Schwann cells express endothelin receptors coupled to adenylyl cyclase and phospholipidase C. Neurochem Res 1997; 22: 409-418.
17. Brennan A, Dean CH, Zhang AL, Cass DT, Mirsky R, Jessen KR. Endothelins control the timing of Schwann cell generation in vitro and in vivo. Dev Biol 2000; 227: 545-557.
18. Almhanna K, Wilkins PL, Bavis JR, Harwalkar S, Berti-Mattera LN. Hyperglycemia triggers abnormal signaling and proliferative responses in Schwann cells. Neurochem Res 2002; 11: 1341-1347.
19. Mirsky R, Jessen KR, Brennan A, Parkinson D, Dong Z, Meier C, Parmantier E, Lawson D. Schwann cells as regulators of nerve development J Physiol Paris 2002; 96: 17-24.

Correspondence

Dr. A. Loesch
Department of Anatomy and Developmental Biology
Royal Free and University College Medical School
University College London
Rowland Hill Street, London NW3 2PF
UK

e-mail: a.loesch@ucl.ac.uk

Biomedical Research 15 (2): 160-168

Are portal vessels present in the pituitary gland 'veins'? A histological study

Morihiro Yoshida[1], Richard J. Coombs[1], Masahiro Kuno[1], Ikuo Wada[2], Osamu Horiuchi[2], Damon C. Herbert[3], Tsuyoshi Soji[1], and Yoshio Mabuchi[1],

[1]Department of Functional Morphology, Nagoya City University, Graduate School of Medical Sciences, 1 Kawasumi, Mizuho-cho, Mizuho-ku, Nagoya City, Aichi, 467-8601, Japan

[2] Department of Orthopedic Surgery, Nagoya City University, Graduate School of Medical Sciences, 1 Kawasumi, Mizuho-cho, Mizuho-ku, Nagoya City, Aichi, 467-8601, Japan

[3] Department of Cellular and Structural Biology, Mail Code 7762, The University of Texas Health Science Center at San Antonio, San Antonio, Texas 78229-3900 USA (DCH)

Key Words: Rat, Anterior pituitary, Pars tuberalis, Portal vessel, Neuroendocrine

Accepted April 7, 2004

Abstract

Male Wistar-Imamichi rats were used for light and electron microscopic study. Prior to the appearance of the pars tuberalis (PT), a small cluster of arteries was found in the area where the gland would appear, while an array of capillaries was noted at the bottom of the median eminence (ME). The epithelial structure comprising the PT was first observed along with slender arteries approximately 1mm behind the optic chiasm on both sides of the ME. Although numerous thin capillaries were present in the hypothalamus, thick capillaries (thought to be portal vessels) showed unusually large luminal diameters and were noted attached to the ME, slightly posterior to the PT. In all specimens serially sectioned in the frontal plane, veins were not detected on either the ME or the pituitary stalk, nor was smooth muscle present in the wall of the thick capillaries. Where the pars tuberalis and the anterior lobe adjoined, clusters of agranular and a few granular cells were noted along with several thick capillaries located on the ventral side of the pituitary. Ultrastructurally, numerous capillaries, which were categorized into two groups, were observed between the agranular cells in the PT. One was thin-walled and randomly arranged while the other was thick-walled and contained fenestrations. At the inter-capillary space, connective tissue and interstitial cells were observed. In the PT, bundles of the neuroendocrine fibers, which contained many electron dense granules and mitochondria, were frequent around the capillaries. The cytoarchitecture of the portal vessels and their functional role are discussed in relation to that previously reported.

Introduction

Since the discovery of hypophyseal portal vessels by Popa and Fielding [1], their light and electron microscopic structure along with their function have been studied [2-5]. Ultrastructure of the vessels showed that a portion of the portal trunks was categorized as capillaries even though it had been accepted that these trunks were previously identified as 'veins'. On the other hand, the cast method combined with scanning electron microscopy (SEM) was employed to view the portal vasculature [3,4,6]. Only Satoh et al. [4] proposed that a part of the 'veins' were actually sinusoidal capillaries containing fenestrations. Concern was expressed that neither the cast SEM method nor transmission electron microscopy was suitable to observe the internal structure of the vessel walls. The present study uses serial sections in both the frontal and sagittal planes to study the 'venous' structures at the light microscopic level and electron microscopy as a means to examine the primary and secondary portal plexus areas.

Materials and Methods

Ten, 50 day-old intact male Wistar-Imamichi rats were used in this study and were separated into two groups. Five animals

were employed for light microscopic and the others for electron microscopic analyses. All were treated according to "The Guidelines for Animal Experimentation" of the Experimental Animal Science Center of the Nagoya City University and sacrificed under deep anesthetized with Nembutal (sodium pentobarbital).

For the light microscopic observations, pituitary glands with the median eminence area, the optic nerves, and trigeminal nerves attached were fixed overnight at 4ºC in Bouin's solution without acetic acid, dehydrated in an ethanol series and embedded in Paraplast embedding media (Sigma Chem. Co, St. Louis, MO, USA). Five µm thick sections were prepared in either the frontal or sagittal plane, mounted onto poly-L-lysine-coated glass slides and stained with hematoxylin and eosin (H&E). With the frontal, serial sections, a base line for onset of the observations was established as the point where the optic chiasm separated into the two optic nerves, while for the sagittal, serial sections, the base line from which the studies began was where the third ventricle was determined to be at its widest point.

For electron microscopic analyses, the animals were fixed by perfusion through the left ventricle of the heart for 10 min. with a fixative containing 2.5% glutaraldehyde and 2% sucrose buffered with 0.05M sodium cacodylate (pH 7.4). After perfusion, the pars tuberalis, the transitional zone of pars tuberalis, and the front half of the pituitary gland together with the hypothalamus were removed from the animals. Each specimen was then sectioned approximately 2mm in thickness along the sagittal center (SC) and refixed for an additional 20 min in the same fixative as used for perfusion. The specimens were then washed for half an hour with the same buffer solution used for fixation and postfixed for two hours with a 1% osmium tetroxide fixative containing 2% sucrose, buffered with 0.05M sodium cacodylate (pH 7.4). After postfixation, the tissues were subsequently dehydrated in a graded series of ethanol for 10 min. each, immersed twice in propylene oxide for 15 min. and embedded in epoxy resin [7]. Thin sections were then prepared parallel to the sagittal plane at 7 levels in increments of 50µm approximately 300µm from the SC and placed onto copper grids. All specimens were then stained with uranyl acetate and lead citrate and observed using a Hitachi H-7000 transmission electron microscope.

In identifying the vessels under study as capillaries rather than veins, an analysis was first made at the light microscopic level. It was found using serial sections that all vessels encountered consisted only of endothelial cells and pericytes through out their entire length. These observations were confirmed by ultrastructural analysis; additionally, the endothelial cells displayed fenestrations which are characteristic of capillaries.

Results

The median eminence was initially observed on the frontal, serial sections as a small protrusion of the floor of the third ventricle; numerous capillaries as well as one or two arteries were present adjacent to the protrusion (Fig 1a). A small glandular structure was observed on both sides of the median eminence approximately 1.5mm behind the optic chiasm. Prior to the appearance of the tips of the pars tuberalis, a small cluster of arteries was noted in the area where the tips were to first appear (Fig 1b). At this point, an array of capillaries appeared at the bottom of the median eminence of the dienceplalon; however; no capillary blood vessels of the so-called primary plexus of the hypophyseal portal vessels system were present (Fig. 1b). The ends of the epithelial structure of the pars tuberalis of the pituitary gland and slender arteries were first observed on both sides of the median eminence at approximately 1mm (200 sections) behind the optic chiasm (Fig. 1b).

Although numerous thin capillaries (approximately 30µm in diameter) were observed in the hypothalamus (Fig. 1c), thick capillary blood vessels (200µm or more in diameter) were attached to the median eminence, slightly behind the pars tuberalis (Fig. 1d). The latter along with the ends of the pars tuberalis then spread and intermingled over the median eminence (Fig. 1d); however, they did not enter the pars tuberalis but instead were wrapped around the gland (Figs. 1d-e). Thick capillaries showed an unusually large luminal diameter (approximately 200µm) compared to that of typical capillaries (30µm) and their number increased. Small arteries were observed throughout the course of the hypophyseal portal vessel system. At the point where the pituitary stalk separated from the median eminence, thick capillaries completely covered the adjacent pars tuberalis (Fig. 1e). As noted below, observations using sagittal sections confirmed these finding. It was particularly important to note that in all frontal serial sections, veins could not be observed in either the median eminence or the pituitary stalk (Fig. 1). It was interesting that the pars tuberalis did not completely encircled the pituitary stalk in any frontal plane, while within the brain and the stalk, a small amount of connective tissue and only a few arteries and capillaries were noted (Fig. 1e).

Large numbers of agranular, folliculo-stellate cells interposed by a few granular cells and numerous capillaries were identified by electron microscopy within the pars tuberalis (Fig. 4a). The capillaries were separated into two groups. One was composed of randomly arranged thin vessels located ventral to the stalk or to the floor of the third ventricle. The other, thick-walled capillaries, ran along a longitudinal axis between the pars tuberalis (Fig. 4a) and correspond to those seen in the frontal sections (Figs. 1d-e). On detailed observation, it appeared as though the thin capillaries flowed into the thick (Fig. 4a). Pericytes were associated with the latter but did not always completely encircled them; they were infrequently present around the thin capillaries (Fig. 4a). Next to the hypothalamus, thin capillaries within a small pericapillary space directly faced neuroendocrine fibers (Fig 4b). Fenestrations were more frequent on the dorsal (upper) as compared to the ventral (lower) side of the capillaries (Fig. 4a). At the intercapillary space, arrays of so-called pericapillary connective tissue or interstitial cells were present but were discontinuous (Fig. 4a). Bundles of neuroendocrine fibers containing dense granules and mitochondria were frequent around capillaries within the pericapillary space (Fig. 5a) and in the agranular cells of the pars tuberalis (Fig. 5b). Nonmyelinated nerve fibers were also present and fibroblasts were distributed around the bundles (Fig. 5b).

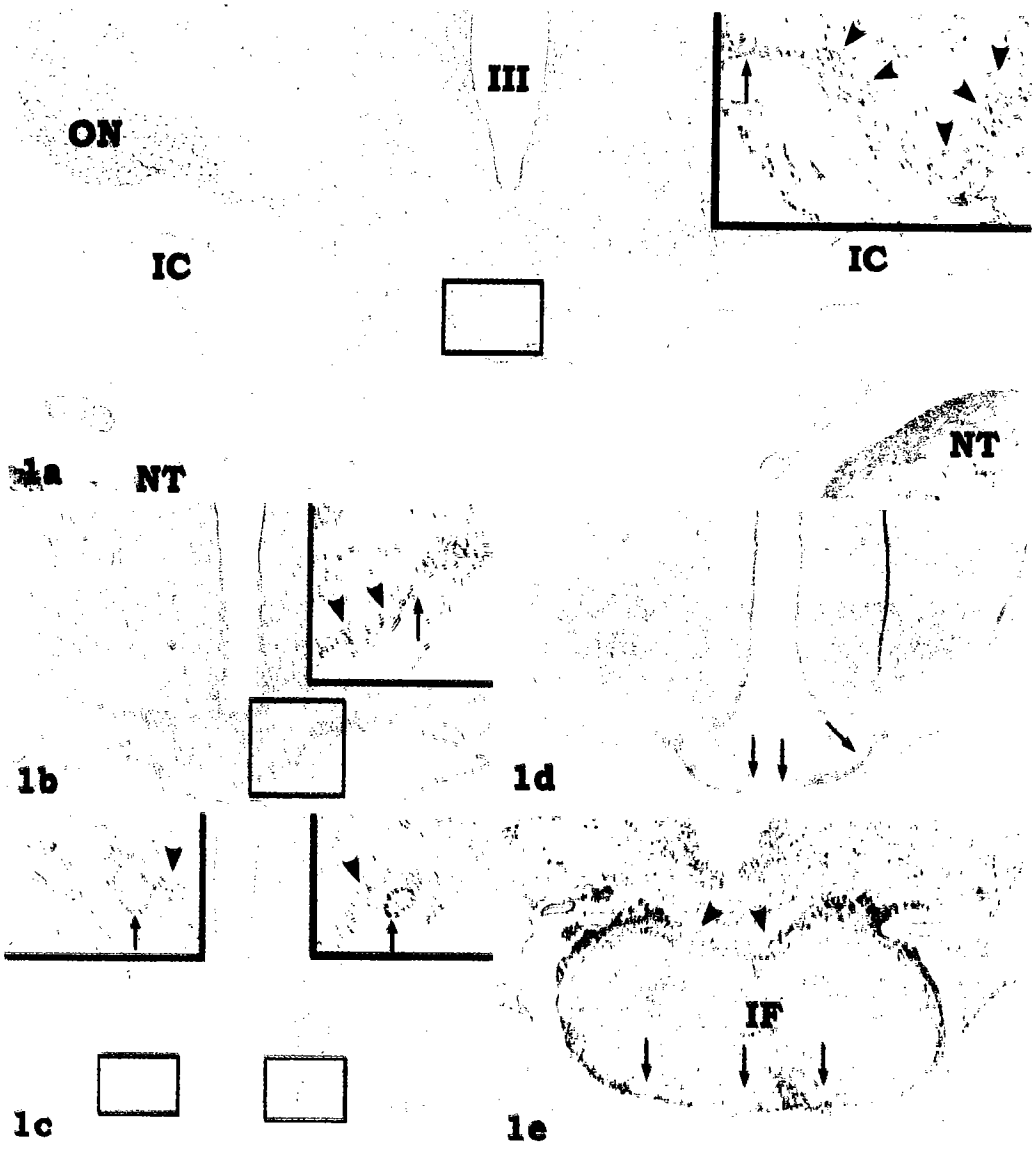

Fig. 1a: Frontal sections illustrating the optic (ON) and trigeminal nerves (NT). At beginning of the median eminence, a tiny protrusion on the floor of the third ventricle is present and shown as an enlargement in the inset. Inset: The protrusion contained numerous arrays of capillaries (arrowheads). Nearby, a few arteries considered to be the arteria hypophysis superior are clearly observed (arrow). III: Third ventricle, IC: Arteria carotis interna. X 30 inset X50

Fig. 1b: Slightly posterior to figure 1a, the protrusion becomes more apparent and the capillaries in the protrusion are in a regular order as they outline the median eminence. Glandular structures of the pars tuberalis are not observed and as noted in the inset, arteries present in figure 1a are again evident invading the median eminence (arrow). Arrowheads indicate capillaries in the median eminence. X 40 Inset X 60

Fig. 1c: Glandular structures are clearly observed beside both margins of the median eminence. Many capillaries are set within the median eminence beside the glandular structures. The glandular structures are tips of the pars tuberalis. Respective insets show enlargements of the rectangle. Glandular structures (arrows) surrounded by capillaries (arrowheads) are clear. X 40 Inset X 80

Fig. 1d: The pars tuberalis covers the median eminence in between which lie thick capillaries (arrows). Note no veins are observed. X 40

Fig. 1e: Numerous thick capillaries (arrows) are found on the ventral side of the infundibular stalk (IF). The pars tuberalis did not completely encircled the stalk and is not present on the dorsal side where a few connective tissue fibers and capillaries (arrowheads) can be found. X 80

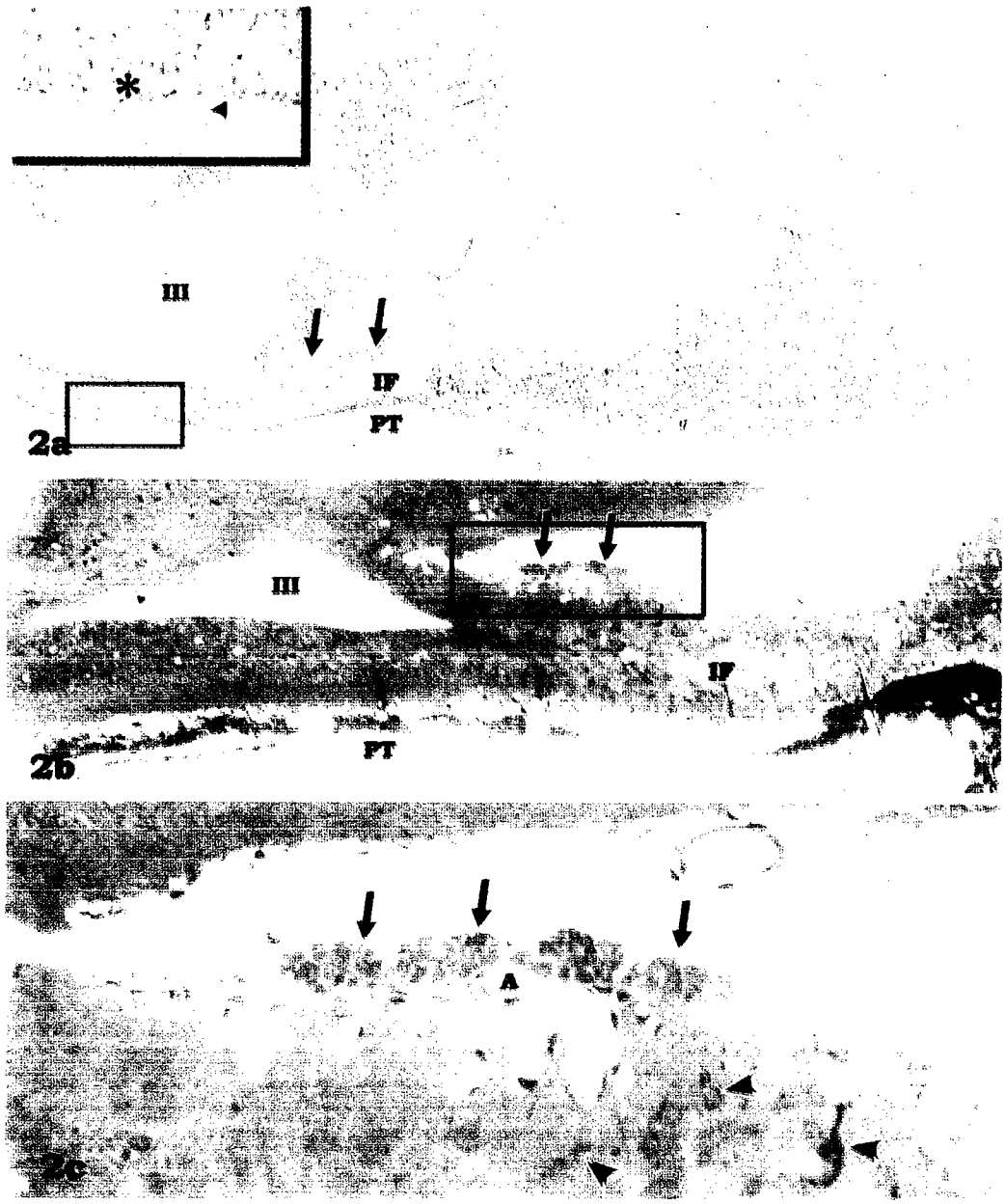

***Fig. 2**: Sagittal sections of the pituitary gland, infundibular stalk and brain. III: Third ventricle, IF: Infundibular stalk, PT: Pars tuberalis.*
***Figure 2a**: Midsagittal section. The third ventricle is relatively wide and the pituitary gland with its infundibular stalk are clearly observed. Arrows indicated that no glandular structures are observed in the infundibular fold. The inset illustrates the demarcated rectangle. The glandular structure of the pars tuberalis on the ventral side of the brain suddenly disappeared (arrowhead) where thick capillaries (asterisk) are found. X 30 Inset X60*
***Figures 2b and c**: This section was taken approximately 200µm from the sagittal center. The third ventricle narrows and in the fold of the infundibular stalk, glandular structures of the pars tuberalis are clearly observed (arrows in Figs. 2b-c). In the stalk, small capillaries, an artery (A) and pituicytes (arrowheads) are present (Fig. 2c). b: X100 c: X 300*

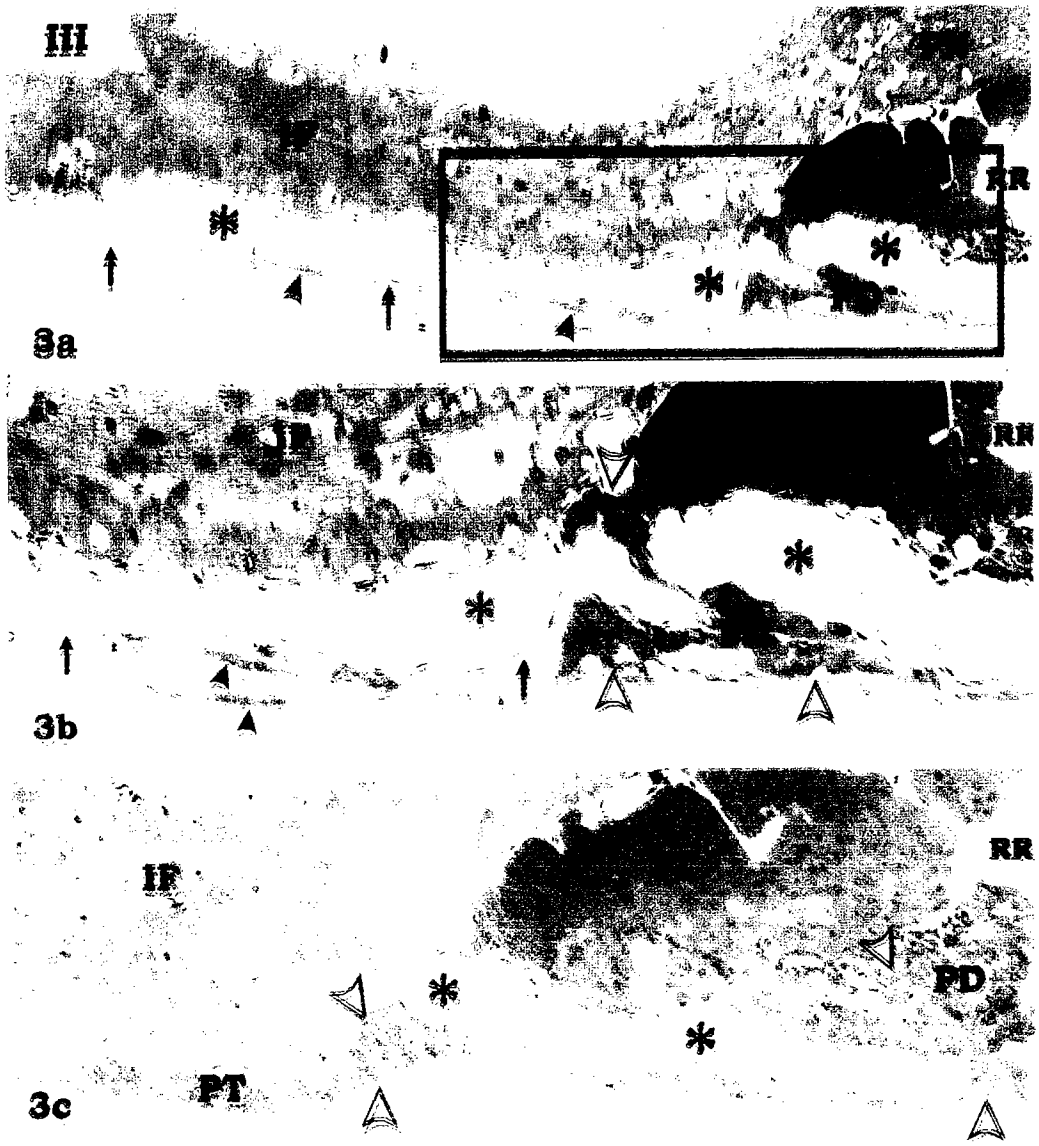

***Fig. 3**: The sections are approximately at the level of the sagittal center. Thick-walled blood vessels (asterisks) were observed on the ventral surface of the pars tuberalis. PD: Anterior lobe (Pars distalis), PI: Intermediate lobe (Pars intermedia), PN: Posterior lobe (Pars nervosa), PT: Pars tuberalis, IF: Infundibular stalk, RR: Rathke's residual pouch, III: Third ventricle.*

***Fig. 3a and b**: The rectangular part of Fig. 3a is enlarged in Fig. 3b. On the wall of the vessels, pericytes (black arrowheads) are observed but smooth muscle cells are absent. This absence of smooth muscle indicates that the vessels are capillaries. No pars tuberalis tissue is seen covering the capillary wall (black arrows). The capillaries are distributed along the ventral side of the anterior pituitary (white arrowheads in Fig. 3b). On the dorsal surface, both thick-walled and thin capillaries are numerous in the stalk (IF). a: X100: b: X250*

***Figure 3c**: At the transitional zone between the anterior lobe and the pars tuberalis, clusters of agranular cells (white arrowheads, also see Fig. 3b) with few granular cells are observed on the ventral sides of the pars tuberalis and the anterior pituitary. Note no veins are present. X250*

Fig 4: Electron micrographs of thick-walled capillaries on the ventral side of the pars tuberalis and anterior lobe.
***Figure 4a**: Insets a and b correspond to the respective rectangles (a dorsal and b ventral part). The pars tuberalis consists of a large number of agranular folliculo-stellate and a few granular cells (PT). Between the pars tuberalis and the pituitary stalk, numerous randomly arranged thin capillaries and longitudinally arranged thick-walled capillaries are observed. The latter correspond to the thick-walled capillaries shown in Fig. 1. Between the thick-walled capillaries (asterisk), tissues of the pars tuberalis (PT) are located. These vessels are encircled not only by smooth muscle but also by pericytes (white arrows) and collagen. The capillary walls differed with their position. Some are approximately 60nm in diameter (inset a) and their endothelial cells had numerous fenestrations. Others (inset b) showed fewer fenestrations and were thicker walled. The thin capillaries flowed into those that were thick-walled (arrowhead). A discontinuous distribution of the array of pericapillary connective tissue is observed between the capillaries (thick arrows). X 1,400: inset a: X 10,000: inset b:X 14,500*
***Fig. 4b**: Along the upper side of the thin capillaries facing towards the neuroendocrine elements, no pericapillary tissue is present (arrows). In contrast, a wide pericapillary space with pericytes and collagen fibers is apparent around the thick capillary (asterisk). Note around the thin capillaries, a few pericytes are present. X 7,000*

***Fig. 5a**: In the pericapillary spaces indicated by the thick arrows in Fig. 4a, a bundle of the neuroendocrine fibers is found. Within the bundle, profiles of non-myelinated neurons containing electron dense granules and elongated mitochondria can be seen (asterisks). X15,000*

Discussion

Since the discovery of hypophyseal portal vessels by Popa and Fielding [1], these structures and their function have been studied by both light and electron microscopy [2-4]. It had been accepted that the vascular system was composed of a primary plexus found in the foremost part of pituitary gland which received the releasing hormones, a secondary plexus situated within the anterior pituitary gland from which the releasing hormones are discharged, and 'veins' which connect the primary and secondly were actually sinusoidal capillaries with fenestrations. According To them [4], the portal trunk was 100-150μm in length and was surrounded by flattened pericytes. Concern was expressed that cast specimens were not suitable to observe the inner structure of the vessel walls. Also the electron microscopic study did not allow a complete survey of the tissue. The present study showed that no venous structures containing smooth muscle were found in either frontal or sagittal sections taken from the primary to the secondary plexus areas. Almost all of the portal trunks in the rat consisted of sinusoidal capillaries. Capillaries of the primary plexus met and separated to form portal trunks; then, the trunks entered the anterior pituitary. Trunks which invaded into the an-

terior gland continued to run down along its ventral side, and then branched to form the secondary plexus. Along their course, small capillaries from the hypothalamus joined the trunks even at the infundibular stalk. It was clear that the trunks may have the ability to accept certain releasing hormones, because they communicated with the pericapillary space via fenestrated endothelial cells. It was rather interesting that the frequency of fenestrations and the thickness of the endothelial cells differed depending upon their location in the trunk. The frequency of the fenestrations was more conspicuous on the dorsal side where the trunks faced the hypothalamus or the stalk than on the ventral side. Also the thickness of the endothelial cells was more evident ventrally than dorsally.

The present study clearly showed neuroendocrine fibers entering into the agranular cells of the pars tuberalis which supports our earlier work [8]. The occurrence of an array of interstitial cells between the trunks was also shown which may have provided an avenue for the neuroendocrine fibers to enter the pars tuberalis and subsequently into the agranular cells.

Recently the pars tuberalis has been described as being associated with the photoperiodic regulation of the anterior pituitary hormones via melatonin receptors [9-12]. Although the majority of previous investigators noted a relationship between LH-RH fibers and ependymal cell layers or tanycytes of the third ventricle, they ignored the association between neuroendocrine fibers and the pars tuberalis.

While there are numerous reports pertaining to the localization, morphological characteristics, gene expression, and/or regulation of the gonadal-pituitary axis by LH-RH and LH-RH neurons [13-24], only Naik [16] observed LH-RH immunoreactivity in the area around the pituitary gland. According to him, the LH-RH positive reactions were mainly found near the primary portal plexus, while some were detected in the pars tuberalis of the rat pituitary gland.

The present results have led us to postulate that two parallel routes exist for the releasing hormone "message" to reach the pituitary gland from the hypothalamus. One is the well known portal vessel system and the other is the network system of folliculo-stellate cells. In the latter system, the LH-RH "message" is first conducted to the agranular cells that are arranged around neuroendocrine varicosities in the pars tuberalis. The "message" can then be transmitted through a network of gap junctions to the folliculo-stellate cells which then affect the biosynthetic secretory cycle and release of hormones from secretory cells. Additional physiological studies are underway to lend further support to this premise.

References

1. Popa GT, Fielding U. A portal circulation from the pituitary to the hypothalamic region. J Anat 1930, 65: 88-91.
2. Murakami T. Pliable methacrylate cast of blood vessel: use a scanning electron microscope study of the microcirculation in the rat hypophysis. Arch Histo Jap 1975, 38: 151-168.
3. Page RB, Leure-Dupree AE, Bergland RM. The neurohypophyseal capillary bed. Part II Specializations within median eminence. Am J Anat 1978, 153: 33-66.
4. Satoh H, Inokuchi T, Shimizu M, Obayashi H, Nakashima Y. Ultrastructure of the hypophyseal portal vessel in mature rats – SEM and TEM observations. Kurume Med J 1989, 36: 91-94.
5. Wislocki GB, King LS. The permeability of the hypophysis and hypothalamus to vital dyes, with a study of the hypophyseal vascular supply. Am J Anat 1936, 58: 421-472.
6. Page RB, Bergland RM. The neurohypophyseal capillary bed. Part 1. Anatomy and arterial supply. Am J Anat 1977, 148: 345-358.
7. Luft JH Improvement in epoxy resin embedding methods. J Biophys Biochem Cytol 1961, 9: 409-414.
8. Mabuchi Y, Shirasawa N, Sakuma E, Hashimoto Y, Kuno M, Coombs RJ, Herbert DC, Soji T. Intercellular communication within the rat anterior pituitary gland: Relationship between LH-RH neurons and folliculo-stellate cells in the pars tuberalis. Cell Tissue Res 2004, in press.
9. Barett P, Morris M, Choi W-S, Ross A, Morgan PJ. Melatonin receptors and signal transduction mechanisms. Biol Signals Recept 1999, 8: 6-14.
10. Morgan PJ The pars tuberalis: the missing link in the photoperiodic regulation of the prolactin secretion? J Neuroendocrinol 2000, 12: 287-295.
11. Morgan PJ, Williams LM. The pars tuberalis of the pituitary: a gateway for neuroendocrine output. Rev Reprod 1996, 1: 153-161.
12. Morgan PJ, King TP, Lawson W, Slater D, Davidson G. Ultrastructure of melatonin-responsive cells in the ovine pars tuberalis. Cell Tissue Res 1991, 263: 529-534.
13. Barry J, Carette B. Immunofluorescence study of LRF neurons in primates. Cell Tissue Res 1975, 164: 163-178.
14. D'Este L, Kulaksiz H, Rausch U, Vaccaro R, Wenger T, Tokunaga Y, Renda TG, Cetin Y. Expression of guanylin in "pars tuberalis-specific cells" and gonadotrophs of rat adenohypophysis. Proc Natl Acad Sci USA 2000, 97: 1131-1136.
15. Foster WG, Youngai EV. An immunohistochemical study of the GnRH neuron morphology and topography in the adult female rabbit hypothalamus. Am J Anat 1991, 191: 293-300.
16. Kelly MJ, Condon TP, Levine JE, Ronnekleiv OK. Combined electrophysiological, immunocytochemical and peptide release measurements in the hypothalamic slice. Brain Res 1985, 345: 264-270
17. Naik DV. Immunoreactive LH-RH neurons in the hypothalamus identified by light and fluoresent microscopy. Cell Tissue Res 1975, 157: 423-436.
18. Naik DV. Immuno-electron microscopic localization of luteinizing hormone-releasing hormone in the arcuate nucleus and median eminence of the rat. Cell Tissue Res 1975, 157: 437-455.
19. Naik DV. Immuno-histochemical localization of LH-RH during different phases of estrus cycle of rat, with reference to the preoptic and arcuate neurons, and the ependymal cells. Cell Tissue Res 1976, 173: 143-166.
20. Nakazawa K, Marubayashi U, McCann SM. Mediation of the short-loop negative feedback of luteinizing hormone (LH) on LH-releasing hormone release by melatonin-induced inhibition of LH release from the pars tuberalis. Proc Natl Acad Sci USA 1991, 88: 7576-7579.
21. Oka Y, Ichikawa M. Ultrastructural characterization of gonadotropin-releasing hormone (Gn-RH)-immunoreactive terminal nerve cells in the dwarf gourami. Neurosci Lett 1992, 140: 200-202.

22. Rethelyi MS, Vigh S, Sétáló G, Merchenthaler I, Flerko B, Petrusz P. The luteinizing hormone releasing hormone-containing pathways and their co-termination with tanycyte processes in and around the median eminence and pituitary stalk of the rat. Acta Morphol Acad Sci Hung 1981, 29: 259-283.
23. Sétáló G, Vigh S, Schally AV, Arimura A, Flerko B. LH-RH-containing neural elements in the rat hypothalamus. Endocrinology 1975, 96: 135-142.
24. Siverman AJ, Krey LC. The luteinizing hormone-releasing hormone (LH-RH) neuronal networks of the guinea pig brain. I. Intra- and extra-hypothalamic projections. Brain Res 1978, 157: 233-246.
25. Soji T, Yashiro T, Herbert DC. Intercellular communication within the rat anterior pituitary gland. I. Postnatal development and changes after injection of luteinizing hormone-releasing hormone (LH-RH) or testosterone. Anat Rec 1990, 226: 337-341.
26. Kurono, C. Intercellular communication within the rat anterior pituitary gland. VI. Development of gap junctions between folliculo-stellate cells under the influence of ovariectomy and sex steroids in the female rat. Anat Rec 1996, 244: 366-373.
27. Soji T, Nishizono H, Yashiro T, Herbert DC. Intercellular communication within the rat anterior pituitary gland. III. Postnatal development and periodic changes of cell-to-cell communications in female rats. Anat Rec 1991, 231: 351-357.
28. Soji T, Yashiro T, Herbert DC. Intercellular communication within the rat anterior pituitary gland. IV. Changes in cell-to-cell communications during pregnancy. Anat. Rec. 1992, 233: 97-102.
29. Nishizono H, Soji T, Herbert DC. Intercellular communication within the rat anterior pituitary gland. V. Changes in cell-to-cell communications as a function of timing of castration in male rats. Anat. Rec. 1993, 235: 577-582.

Correspondence:

Dr. Morihiro Yoshida
Department of Functional Morphology
Nagoya City University
Graduate School of Medical Sciences
1Kawasumi, Mizuho-cho, Mizuho-ku
Nagoya City, Aichi, 467-8607
Japan

Phone: 052-853-8121
FAX: 052-842-3210
e-mail: yoshio@med.nagoya-cu.ac.jp

Biomedical Research 2004; 15 (2): 169-175

The effects of Leukemia Inhibitory Factor (LIF) on neointimal formation in injured arteries

World CJ, [1]Merrilees MJ, [1]Beaumont B, Campbell JH, Campbell GR, Rolfe, BE

Centre for Research in Vascular Biology, School of Biomedical Sciences, University of Queensland, Queensland, Australia, and [1]Department of Anatomy with Radiology, School of Medical Sciences, The University of Auckland, New Zealand.

Accepted August 6, 2004

Abstract

Continuous infusion of the pleiotropic cytokine leukaemia inhibitory factor (LIF) inhibits the formation of fatty streaks and neointimal thickening following vascular injury. LIF also prevents further development of pre-formed atherosclerotic lesions where lesion progression is associated with matrix accumulation rather than increased cell number. Since LIF is known to play a role in regulating matrix synthesis and degradation in other cell types, the present study investigated whether LIF inhibits the deposition of pro-atherogenic extracellular matrix proteoglycans biglycan and versican. Possible downstream consequences of changes to matrix composition were also investigated.

Rabbit carotid arteries were subjected to balloon catheter injury, and animals immediately placed on a cholesterol-enriched diet. After 4 weeks, by which time lesions with a fibrous cap overlying a central core of macrophages had developed, osmotic minipumps were inserted into the peritoneal cavity to deliver LIF (30μg/kg/day) or saline for a further 4 weeks. Immunohistochemical analysis of the carotid arteries showed that LIF treatment resulted in a marked reduction in versican and biglycan immunostaining, inhibition of vascular cell apoptosis, and a smaller and more compact neointima. LIF also dose-dependently inhibited VSMC migration in an *in vitro* scratch wound assay.

These results extend the pleiotropic actions of LIF in the vasculature to include changes to the extracellular matrix of the vessel wall, and further strengthen the evidence that LIF is an effective anti-atherogenic / anti restenotic agent.

Introduction

The cytokine leukaemia inhibitory factor (LIF) has a diverse range of biological effects in a variety of tissue systems, including the ability to act as an anti-atherogenic/anti-restenotic agent. Previous studies in our laboratory have shown that LIF decreases plasma and vessel wall cholesterol and prevents the development of a vascular smooth muscle cell (VSMC)-rich neointima after arterial injury [1]. LIF also retards the progression of preformed atherosclerotic lesions, reducing macrophage infiltration into fatty streaks, modulating iNOS expression and normalizing smooth muscle-dependent reactivity [2]. However in injured arteries, where lesion progression is associated with matrix accumulation rather than increased cell number, the neointimae of LIF-treated vessels were more ordered and cell densities were higher. Since LIF is known to play a role in regulating matrix synthesis and degradation in other cell types [3], we hypothesized that LIF may act to regulate extracellular matrix synthesis in the artery wall.

The extracellular matrix (ECM) proteins of the three layers of a healthy artery, notably collagen, proteoglycans and elastin, impart various properties that promote homeostasis within the vessel wall. Studies in experimental models of disease, as well as advanced human disease, have shown that formation of a neointima is associated with demonstrable changes to the ECM [4,5]. Observed changes include disruption or loss of elastic fibres [6] coupled with increased expression of collagens IV and VIII, with diffuse distribution found in the intimal space both beneath the endothelium and surrounding VSMC in lesions [7,8]. Changes in proteoglycan expression also occur in lesions from various stages of development. In human disease, the sulphated proteoglycans versican, biglycan and decorin are evident in thickened coronary arteries [9] and within restenotic lesions [10,11], with the expression of versican in the early lesion and biglycan predominantly in the more established lesion [12]. Biglycan is also present within the intermediate and advanced lesions of the ApoE-/- and LDLR-/- genetic mouse models of atherosclerosis [13]. Decorin is more predominant in macrophage-rich areas and versican more prevalent in VSMC-rich areas [14].

Changes in expression of ECM components in response to injury of healthy and diseased arteries are regulated by pro-atherogenic cytokines such as platelet-derived growth factor [15,16]. These changes have various pathological consequences. Versican, the largest of the matrix proteoglycans, is implicated in several atherogenic processes [17], including a major contribution to increased intimal volume due to water binding and space occupy-

ing properties. Both versican and biglycan co-localize with retained lipoprotein epitopes in human lesions [18] and both are associated with the retention of atherogenic lipid within the vessel wall. These proteoglycans also promote the migration and proliferation of VSMC [14,19] and regulate VSMC phenotype and growth factor availability within the vessel wall [5]. Decorin has largely been demonstrated to co-localize with transforming growth factor-β (TGF-β) [14] and to inhibit TGF-β-induced ECM accumulation in rat glomerulonephritis [20]. When VSMC retrovirally transfected with the decorin gene were seeded into balloon catheter-injured carotid arteries, the resultant neointima was reduced in size, more compact, and more fibrous due to increased collagen I expression and reduced versican and fibronectin production [21].

Our previous study, showing that LIF administration to preformed experimental atherosclerotic lesions results in a more compact neointima with higher cell density [2], led us to hypothesise that LIF may be regulating processes involved in matrix remodelling. Given the important role of proteoglycans in regulating lesion development, the present study investigated the influence of LIF treatment on versican, biglycan and decorin in a rabbit model of atherosclerosis. In addition the effects of LIF on apoptosis and vascular smooth muscle migration were investigated.

Methods

LIF

Recombinant human LIF (hLIF) was a gift from the Australian Medical Research and Development (AMRAD) Corp. (Victoria, Australia).

Animal Studies

Eighteen male 18-week-old New Zealand White rabbits weighing approximately 2.5 kg were obtained from commercial colonies. They were caged individually, maintained on a 12-hour day/night cycle, and fed *ad libitum* with standard rabbit chow (with or without 1% cholesterol) and small quantities of fruit and vegetables.

Experimental Protocol

At time 0, six rabbits were placed on normal rabbit chow (untreated controls). The remaining 12 rabbits were subjected to balloon catheter denudation injury of the right carotid artery as previously described [22] and immediately placed on a 1% cholesterol diet. At 4 weeks, by which time lesions with a central core of lipid-laden foam cells and a fibrous cap had developed [2] an Alzet osmotic minipump (Model 2ML4) containing saline or hLIF was inserted into the peritoneal cavity of each of the 12 rabbits (6/group). The dose of LIF was 30 μg/kg/day for 28 days, which from earlier studies is known to be effective in lowering plasma cholesterol and inhibiting the development of fatty lesions [23]. At the same time, the cholesterol in the chow of these 12 rabbits was reduced to 0.5% as continued consumption of 1% cholesterol can result in liver failure after 3-6 months. After 4 weeks of LIF (or saline) infusion, rabbits were sacrificed with an overdose of sodium pentobarbitone.

Immediately following sacrifice, arterial segments were removed and fixed in 4% paraformaldehyde, and then each piece cut into four 5.0-mm segments and embedded in paraffin for immunochemistry and TUNEL. Several sections (5 μm) were cut at intervals of 500 μm, yielding six sampling sites per artery.

The investigation was approved by the University of Queensland Animal Experimentation Ethics Committee and conforms with the *Guide for the Care and Use of Laboratory Animals* published by the US National Institutes of Health (NIH Publication No 88-23, revised 1996).

Immunohistochemical staining

Immunostaining was carried out using the DAKO Envision™ rabbit HRP [DAB] system. Sections were deparaffinized, then hydrated in TBS, incubated with 0.03% peroxidase block for 10 min, and washed (3 x 5min) in TBS. Sections were incubated for 60 min with the primary antibodies (rabbit anti-human versican, biglycan or decorin (all 1:500); kind gifts from Dr Larry Fisher at the NIH, Bethesda, Maryland USA) at room temperature. Following incubation, sections were washed in TBS, incubated with HRP polymer for 30 min, washed again, and antibodies visualised by incubation with DAB solution for 8 min. Sections were then washed twice in distilled water, counterstained in Harris' Haematoxylin and rapidly dehydrated and mounted.

Terminal Deoxynucleotidyl Transferase End-Labeling (TUNEL)

After deparaffinization and rehydration, tissue sections were incubated with 3% EDTA to remove all small calcium-containing vesicles that can be responsible for non-specific binding of nucleotides [24]. Following incubation of tissue with proteinase K (20 μg/ml), TUNEL analysis was performed using the ApopTag® kit (Chemicon International, Aust). The enzyme terminal deoxynucleotidyl transferase (TdT), which catalyzes a template-independent addition of deoxyribonucleotide to 3′-OH ends of DNA, was used to incorporate digoxigenin-conjugated dUTP to the ends of DNA fragments. The TUNEL signal was then detected by rhodamine-conjugated anti-digoxigenin antibody. Consecutive sections were counter-stained with the nuclear stain propidium iodide, washed and mounted in gelvatol containing polyvinylalcohol/glycerol n-propyl gallate (5 mg/ml) as anti-fade agent and visualised by confocal laser scanning microscopy. For each artery, a minimum of four sections were examined at high power and for each section, 400 cells were counted in random fields. The cells with clear nuclear labelling were defined as TUNEL positive ($TUNEL^+$) cells. The apoptotic index (AI) was calculated as percentage of $TUNEL^+$ cells using the following formula: AI = 100 x (No $TUNEL^+$ cell nuclei/No of total cell nuclei).

Isolation and culture of vascular SMC

Vascular SMC from the aortic media of New Zealand White rabbits (9-12 weeks old) were isolated by enzyme digestion [25]. Cells were maintained in Medium 199 (M199; Life Technologies, Australia) containing 5% FCS (Trace Biosciences, Australia) at 37°C in a humid atmosphere of 4% CO_2 in air. For the experiments described below, cells in primary culture or at passage 2-4

were seeded at moderate density ($4.7x10^4$ cells/cm^2) into 90 mm dishes or onto coverslips contained within 24 well plates. All experiments were repeated 3 times.

Cell Migration Assay

The effect of LIF on VSMC migration was determined by using a scratch wound assay. Rabbit aortic VSMC were grown to confluency in a 24-well dish, serum-starved overnight, then the cell monolayer disrupted with a sterile 10 µl pipette tip to create a cell-free zone. The cells were washed with serum-free medium to remove non-adherent cells and the wounded monolayer overlaid with M199 supplemented with 0.05% low melt agarose alone or containing various concentrations of LIF. At 24, 48 and 72 hours after treatment, cells were visualised on an inverted microscope and photographed with an Olympus digital camera at six distinct positions. Cell migration was quantified by measuring the width of the cell-free zone (distance between the edges of the injured monolayer) and expressing the change as percent recovery (%*R*). (%*R* = [1 – (wound distance at T_t/ wound distance at T_0) x 100%, where T_t is time (hours) post-injury and T_0 is immediately post-injury.)

Results

Effect of LIF on Vascular ECM

A previous study demonstrated that LIF treatment resulted in a more uniform and densely packed neointima of smaller size [2]. It was proposed that this may be due to changes in the ECM composition of the vessel wall. Immunostaining of uninjured control arteries showed that the proteoglycans versican, biglycan and decorin were largely absent from the media (data not shown). However 8 weeks after balloon catheter injury, staining for versican and biglycan was markedly increased in the neointima of the cholesterol-fed rabbits; decorin staining, although detectable, was much weaker (Fig. 1A-C). The administration of LIF for the final 4 weeks resulted in a marked reduction in the staining of both versican and biglycan and a more compact neointima (Fig. 1A'-C'). In contrast, immunostaining for decorin was pronounced and distributed uniformly throughout the neointima (Fig. 1C').

LIF Inhibits Vascular Apoptosis In Vivo

Previous studies have demonstrated the ability of decorin to promote cell survival in a variety of tissues [26, 27]. Thus the extent of apoptosis within the vessel wall was investigated by the TUNEL technique (Fig. 2). Eight weeks after injury, the proportion of apoptotic cells within the neointima of the PBS-treated control group was 3.09 ± 0.52%. In the LIF-treated group the proportion of apoptotic cells was significantly reduced (0.41 ± 0.03%; $P<0.05$), demonstrating the ability of LIF to act as a survival factor for vascular cells *in vivo*.

LIF Retards VSMC Migration

The pro-atherogenic proteoglycans versican and biglycan are known regulators of VSMC migration [28,29], a key step in the early stages of atherogenesis [30]. The ability of LIF to retard the migration of VSMC was investigated in a scratch wound assay. In the absence of LIF, cells migrated in a time-dependent manner into the cell-free zone created by disruption of the cell monolayer with a sterile 10 µl pipette tip. As demonstrated in Fig. 3, VSMC grown in M199 alone showed significant VSMC migration within the first 24 hours after wounding (VSMC having migrated 34.5 ± 2.1% into the cell-free zone; $P<0.001$) and after 72 hours (%*R* = 53.3 ± 1.5%, $P<0.005$). Although the rate of wound closure was reduced in comparison to cells in medium alone, LIF at a concentration of 10 ng/ml had no significant effect on VSMC migration, with migration into the cell-free wound evident after 24, 48 and 72 hours (Fig. 3A). However at a concentration of 50 ng/ml, LIF inhibited VSMC migration, with no significant reduction in the width of the cell-free zone up to 48 hours. The inhibition of VSMC migration by 50 ng/ml LIF was observed after 24 (%*R* = 4.5 ± 3.9%) and 48 hours (%*R* = 13.8 ± 4.5%), which was no longer evident after 72 hours (Fig. 3B). LIF at 100 ng/ml was found to inhibit VSMC migration after 24 (%*R* = 5.0 ± 4.9%) and 48 hours (%*R* = 7.9 ± 3.6%), but not after 72 hours (%*R* = 32.2 ± 1.8%, $P<0.001$) (Fig. 3C). Similar to that observed at 10 ng/ml, LIF at 200 ng/ml did not inhibit VSMC migration at any time-point investigated. Thus these experiments demonstrate the ability of LIF to inhibit VSMC migration in a scratch wound assay in both a dose- and time-dependent fashion.

Discussion

We previously demonstrated that LIF treatment prevents the progression of pre-existing atherosclerotic lesions in a rabbit model of disease, without reducing cell number [2]. The present study demonstrates, using the same animal model, a role for LIF in regulation of extracellular matrix composition, specifically its ability to inhibit expression of pro-atherogenic proteoglycans versican and biglycan, and promote expression of the anti-atherogenic decorin within the vessel wall. The ability of LIF to inhibit apoptosis within the vessel wall and VSMC migration within an *in vitro* wound assay is also demonstrated. The results extend our knowledge of how LIF acts as an anti-atherogenic/-restenotic agent, and highlight the potential of LIF as a multi-faceted treatment for vascular disease.

Although the mechanism by which LIF regulates expression of these proteoglycans was not determined, recent studies in a model of mesangioproliferative glomerulonephritis suggest that reduction of biglycan expression is dependent upon nitric oxide (NO) produced by inducible nitric oxide synthase (iNOS) [31]. Since LIF induces iNOS expression and activity [2, 32] and the actions of LIF are ameliorated by the NOS inhibitor L-NAME [22] a similar mechanism may be acting within the vessel wall in response to LIF administration.

The ECM component decorin is thought to possess anti-atherogenic properties. Evidence for this is provided by the demonstration that decorin inhibits cell proliferation via the induction of p21, an inhibitor of cyclin-dependent kinases [33]. Within the vessel wall, decorin [14] binds TGF-β [34] and interferes with binding to its cognate receptor; this in turn interferes with the ability of TGF-β to exert its effects both *in vitro* and *in vivo* [35], including the stimulation of biglycan expression [36] and versican core protein synthesis [15]. In addition, decorin protein binds C1q, the initial

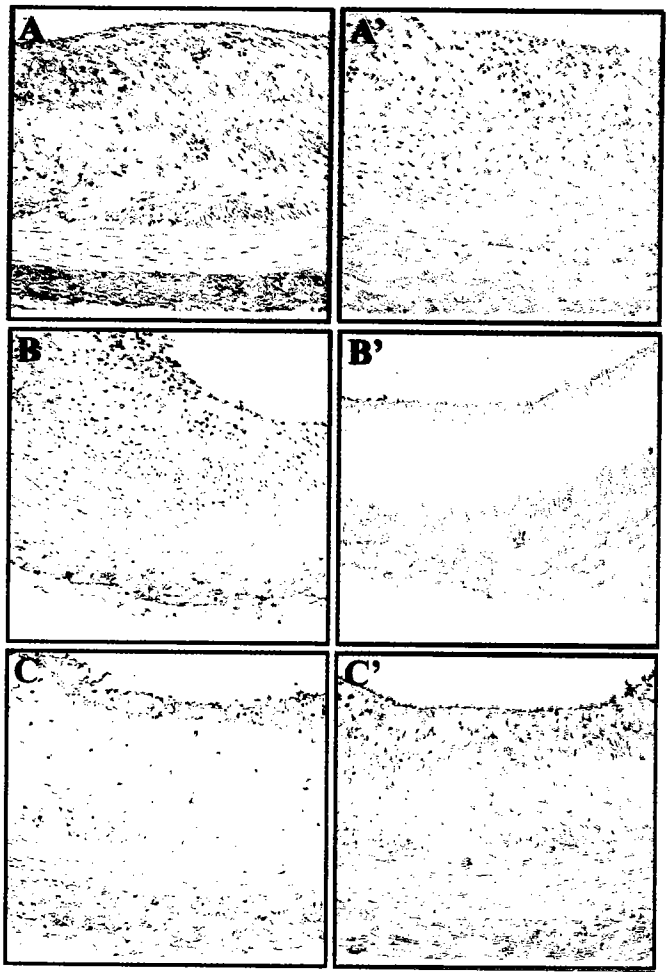

Fig. 1. Expression of ECM components in injured carotid arteries after 8 weeks cholesterol diet, treated with either saline (A-C) or LIF (A'-C') for the final 4 weeks. Sections are immunostained for versican (A and A'), biglycan (B and B') and decorin (C and C').

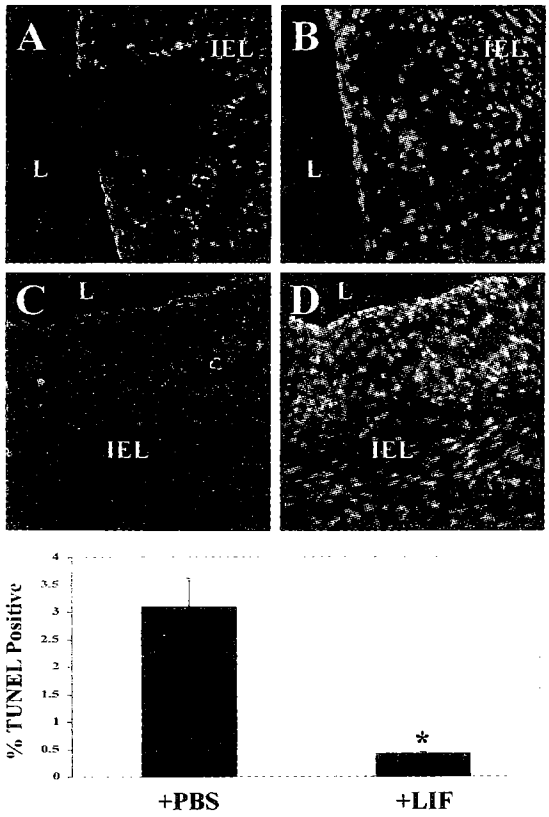

*Fig. 2. LIF inhibits vascular cell apoptosis in vivo. TUNEL staining (A and C) of apoptotic cells compared with propidium iodide staining (B and D) for total cells, in injured carotid arteries after 8 weeks cholesterol-rich diet, with either saline (A and B) or LIF (C and D) treatment for the final 4 weeks. Staining was performed on consecutive sections. Histogram: The extent of apoptosis (AI) was expressed as a percentage of TUNEL⁺ cells, using the formula: AI = 100 x (# TUNEL⁺ nuclei/total nuclei). A representative histogram, of three independent experiments, is shown. *P<0.05 compared with PBS-treated control. L = lumen; IEL = internal elastic lamina.*

component in the classical pathway of complement activation and inhibits the complement cascade [37]. Finally, decorin core protein binds fibrillar collagen and promotes collagen fibrillogenesis [38]. Thus the ability of decorin to promote an anti-atherogenic effect in early vascular lesions is facilitated by its capacity to inhibit TGF-β, and consequently reduce both versican and biglycan expression. The reduced expression of these proteoglycans would in turn result in reduced retention of atherogenic lipids in the vessel wall [17]. Asthe lesion develops, the inhibition of cell proliferation and complement activation would further limit vascular hyperplasia. In the advanced lesion it is expected decorin would facilitate the proper assembly of collagen fibrils and promote lesion stability by strengthening the connective tissue cap that contains lipid-rich, rupture-prone vulnerable plaques The composition of the ECM not only contributes directly to the physical properties of the vessel wall. •It also regulates vascular cell responses including survival, miggration and proliferation, all of which contribute significantly to the structure and functional properties of the vascular wall [5,17]. Thus in addition to alterations in lipid retention and growth factor activity, changes in ECM composition may lead to other biological effects. The present study shows that LIF also reduces apoptosis within the atherosclerotic lesion. While decorin has been shown to promote cell survival in several cell types, including macrophages and endothelial cells [27,39], LIF may act directly to inhibit apoptosis as previous shown in various other cell types [40,41]. The identity of the TUNEL positive cells in this study was not elucidated although they are likely to be VSMC. Apoptotic VSMC within the neointima participate in the recruitment of macrophages to the lesion via upregulation of the chemoattractant MCP-1 [42] and, once recruited, macrophages and foam cells secrete pro-death factors that contribute to VSMC apoptosis [43]. Thus the actions of LIF on lesion composition may be due either to its capacity to inhibit macro

phage infiltration into the vessel wall [2] or, as suggested in the present study, by the promotion of VSMC survival.

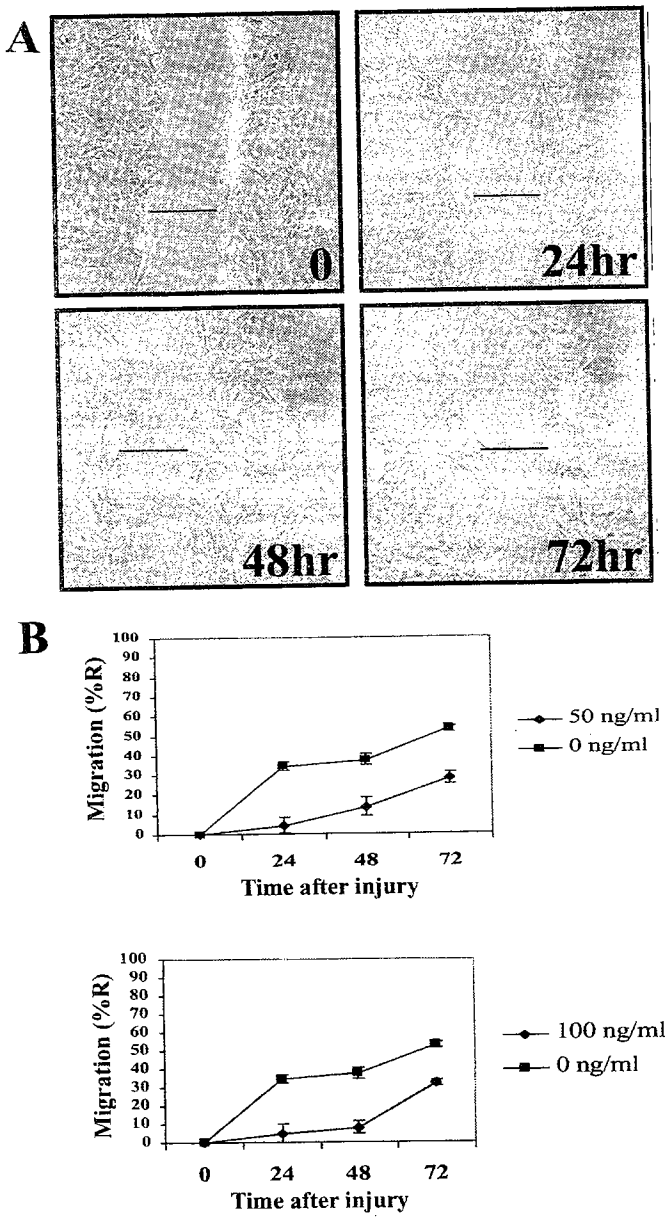

Fig. 3. The inhibition of VSMC migration following monolayer injury is dose-dependent. Growth-arrested VSMC were injured with a sterile 10 μl pipette tip and treated with media alone (0 ng/ml) or medium containing LIF at 50 ng/ml or 100 ng/ml. ***A.*** *Representative images of cells in medium alone taken with a C4040 digital camera mounted on an Olympus IMT2 inverted microscope. The distance between the edges of the cell-free zone was measured and the extent of VSMC migration (% Recovery) was quantified by using the equation: %R = [1 – (wound distance at T_t/wound distance at T_0) x 100%, where T_t is the time post-injury and T_0 is immediately post-injury. *P<0.05 compared with injury at time 0.* ***B.*** *Effect of LIF on migration over 72 hours post-injury.*

Instability of the atherosclerotic plaque is now well established as the underlying cause of most clinical events. Investigations of human lesions indicate that breakdown of the fibrous cap is associated with a low density of VSMC and collagen, increased frequency of inflammatory cells and increased tissue-degrading activity [44]. The loss of smooth muscle cells can be detrimental for plaque stability since they produce the majority if not all of the collagen fibrils necessary for tensile strength of the fibrous cap [45]. Once the matrix becomes devoid of smooth muscle cells, the balance shifts towards degradation. The present study suggests LIF treatment of pre-existing atheroma may not only retard lesion progression, but help stabilize the plaque. In line with our previous demonstration that LIF treatment of pre-existing lesions maintains the cellular content of the artery wall, the present study shows that LIF promotes cell survival within the vascular wall and inhibits smooth muscle migration. LIF also regulates composition of the extracellular matrix, reducing ECM volume, inhibiting synthesis of pro-atherogenic proteoglycans versican and biglycan, and promoting synthesis of the anti-atherogenic proteoglycan decorin. Although beyond the scope of the present study, previous *in vitro* studies showing that LIF induces TIMP-1 expression by VSMC [32] suggest that LIF may also stabilize plaques by reducing matrix degradation.

In summary, our previous studies have shown that LIF prevents the development of hyperplastic intimal thickenings after arterial injury and retards the progression of pre-formed atherosclerotic lesions. A number of mechanisms have been identified by which LIF exerts these effects, including the capacity to decrease plasma and vessel wall cholesterol, reduce VSMC proliferation and macrophage accumulation, normalise smooth muscle-dependent vasoreactivity, and regulate iNOS expression. The present study extends our knowledge of how LIF acts as an anti-atherogenic/-restenotic agent, demonstrating its ability to regulate the ECM, inhibit apoptosis within the vessel wall and inhibit VSMC migration *in vitro*. The results highlight the pleiotropic nature of LIF and indicate that LIF may be particularly effective in inhibiting atherogenic changes to the vessel wall.

Acknowledgements

This work was supported by NHF and NHMRC of Australia, and the NHF of New Zealand. We also acknowledge the assistance of Mr Alasdair Dyne with the cell culture, and Mr Anthony Chan with tissue processing.

References

1. Moran CS, Campbell JH, Simmons DL, Campbell GR. Human leukemia inhibitory factor inhibits development of experimental atherosclerosis. Arterioscler Thromb 1994; 14: 1356-1363.
2. Rolfe BE, Stamatiou S, World CJ, Brown L, Thomas AC, Bingley JA, et al. Leukaemia inhibitory factor retards the progression of atherosclerosis. Cardiovasc Res 2003; 58: 222-230.
3. White JD, Davies M, Grounds MD. Leukaemia inhibitory factor increases myoblast replication and survival and affects extracellular matrix production: combined in vivo and in vitro studies in post-natal skeletal muscle. Cell Tissue Res 2001; 306: 129-141.

4. Wight TN. Arterial Wall. In: W.D. C, editor. Extracellular Matrix Vol 1. Amsterdam: Harwood Academic Publishers; 1996.
5. Raines EW. The extracellular matrix can regulate vascular cell migration, proliferation, and survival: relationships to vascular disease. Int J Exp Pathol 2000; 81: 173-182.
6. Fulop T, Jr., Jacob MP, Khalil A, Wallach J, Robert L. Biological effects of elastin peptides. Pathol Biol (Paris) 1998; 46: 497-506.
7. Katsuda S, Okada Y, Minamoto T, Oda Y, Matsui Y, Nakanishi I. Collagens in human atherosclerosis. Immunohistochemical analysis using collagen type-specific antibodies. Arterioscler Thromb 1992; 12: 494-502.
8. Plenz G, Reichenberg S, Koenig C, Rauterberg J, Deng MC, Baba HA, et al. Granulocyte-macrophage colony-stimulating factor (GM-CSF) modulates the expression of type VIII collagen mRNA in vascular smooth muscle cells and both are codistributed during atherogenesis. Arterioscler Thromb Vasc Biol 1999; 19: 1658-1668.
9. Merrilees MJ, Beaumont B, Scott LJ. Comparison of deposits of versican, biglycan and decorin in saphenous vein and internal thoracic, radial and coronary arteries: correlation to patency. Coron Artery Dis 2001; 12: 7-16.
10. Wight TN, Lara S, Riessen R, Le Baron R, Isner J. Selective deposits of versican in the extracellular matrix of restenotic lesions from human peripheral arteries. Am J Pathol 1997; 151: 963-973.
11. Riessen R, Isner JM, Blessing E, Loushin C, Nikol S, Wight TN. Regional differences in the distribution of the proteoglycans biglycan and decorin in the extracellular matrix of atherosclerotic and restenotic human coronary arteries. Am J Pathol 1994; 144: 962-974.
12. Lin H, Wilson JE, Roberts CR, Horley KJ, Winters GL, Costanzo MR, et al. Biglycan, decorin, and versican protein expression patterns in coronary arteriopathy of human cardiac allograft: distinctness as compared to native atherosclerosis. J Heart Lung Transplant 1996; 15: 1233-1247.
13. Kunjathoor VV, Chiu DS, O'Brien KD, LeBoeuf RC. Accumulation of biglycan and perlecan, but not versican, in lesions of murine models of atherosclerosis. Arterioscler Thromb Vasc Biol 2002; 22: 462-468.
14. Evanko SP, Raines EW, Ross R, Gold LI, Wight TN. Proteoglycan distribution in lesions of atherosclerosis depends on lesion severity, structural characteristics, and the proximity of platelet-derived growth factor and transforming growth factor-beta. Am J Pathol 1998; 152: 533-546.
15. Schonherr E, Jarvelainen HT, Sandell LJ, Wight TN. Effects of platelet-derived growth factor and transforming growth factor-beta 1 on the synthesis of a large versican-like chondroitin sulfate proteoglycan by arterial smooth muscle cells. J Biol Chem 1991; 266: 17640-17647.
16. Schonherr E, Jarvelainen HT, Kinsella MG, Sandell LJ, Wight TN. Platelet-derived growth factor and transforming growth factor-beta 1 differentially affect the synthesis of biglycan and decorin by monkey arterial smooth muscle cells. Arterioscler Thromb 1993; 13: 1026-1036.
17. Wight TN, Merrilees MJ. Proteoglycans in atherosclerosis and restenosis: key roles for versican. Circ Res 2004; 94: 1158-1167.
18. O'Brien KD, Olin KL, Alpers CE, Chiu W, Ferguson M, Hudkins K, et al. Comparison of apolipoprotein and proteoglycan deposits in human coronary atherosclerotic plaques: colocalization of biglycan with apolipoproteins. Circulation 1998; 98: 519-527.
19. Wight TN, Kinsella MG, Qwarnstrom EE. The role of proteoglycans in cell adhesion, migration and proliferation. Curr Opin Cell Biol 1992; 4: 793-801.
20. Border WA, Noble NA, Yamamoto T, Harper JR, Yamaguchi Y, Pierschbacher MD, et al. Natural inhibitor of transforming growth factor-beta protects against scarring in experimental kidney disease. Nature 1992; 360: 361-364.
21. Fischer JW, Kinsella MG, Clowes MM, Lara S, Clowes AW, Wight TN. Local expression of bovine decorin by cell-mediated gene transfer reduces neointimal formation after balloon injury in rats. Circ Res 2000; 86: 676-683.
22. Moran CS, Campbell JH, Campbell GR. Induction of smooth muscle cell nitric oxide synthase by human leukaemia inhibitory factor: effects in vitro and in vivo. J Vasc Res 1997; 34: 378-385.
23. Moran CS, Campbell JH, Campbell GR. Human leukemia inhibitory factor upregulates LDL receptors on liver cells and decreases serum cholesterol in the cholesterol-fed rabbit. Arterioscler Thromb Vasc Biol 1997; 17: 1267-1273.
24. Kockx MM, Muhring J, Bortier H, De Meyer GR, Jacob W. Biotin- or digoxigenin-conjugated nucleotides bind to matrix vesicles in atherosclerotic plaques. Am J Pathol 1996; 148: 1771-1777.
25. Campbell JH, Campbell GR. Culture techniques and their applications to studies of vascular smooth muscle. Clin Sci (Lond) 1993; 85: 501-513.
26. Schonherr E, O'Connell BC, Schittny J, Robenek H, Fastermann D, Fisher LW, et al. Paracrine or virus-mediated induction of decorin expression by endothelial cells contributes to tube formation and prevention of apoptosis in collagen lattices. Eur J Cell Biol 1999; 78: 44-55.
27. Xaus J, Comalada M, Cardo M, Valledor AF, Celada A. Decorin inhibits macrophage colony-stimulating factor proliferation of macrophages and enhances cell survival through induction of p27(Kip1) and p21(Waf1). Blood 2001; 98: 2124-2133.
28. Wight TN. Versican: a versatile extracellular matrix proteoglycan in cell biology. Curr Opin Cell Biol 2002; 14: 617-623.
29. Shimizu-Hirota R, Sasamura H, Kuroda M, Kobayashi E, Hayashi M, Saruta T. Extracellular matrix glycoprotein biglycan enhances vascular smooth muscle cell proliferation and migration. Circ Res 2004; 94: 1067-1074.
30. Schwartz SM. Smooth muscle migration in vascular development and pathogenesis. Transpl Immunol 1997; 5: 255-260.
31. Schaefer L, Beck KF, Raslik I, Walpen S, Mihalik D, Micegova M, et al. Biglycan, a nitric oxide-regulated gene, affects adhesion, growth, and survival of mesangial cells. J Biol Chem 2003; 278:26227-37.
32. World CJ, Rolfe BE, Campbell JH. Regulation of LIF receptor expression in vascular smooth muscle. Ann N Y Acad Sci 2001; 947: 323-328.
33. De Luca A, Santra M, Baldi A, Giordano A, Iozzo RV. Decorin-induced growth suppression is associated with up-regulation of p21, an inhibitor of cyclin-dependent kinases. J Biol Chem 1996; 271: 18961-18965.
34. Hildebrand A, Romaris M, Rasmussen LM, Heinegard D, Twardzik DR, Border WA, et al. Interaction of the small interstitial proteoglycans biglycan, decorin and fibromodulin with transforming growth factor beta. Biochem J 1994; 302 : 527-534.
35. Schonherr E, Broszat M, Brandan E, Bruckner P, Kresse H. Decorin core protein fragment Leu155-Val260 interacts with TGF-beta but does not compete for decorin binding to type I collagen. Arch Biochem Biophys 1998; 355: 241-248.

36. Hausser H, Groning A, Hasilik A, Schonherr E, Kresse H. Selective inactivity of TGF-beta/decorin complexes. FEBS Lett 1994; 353: 243-24.
37. Krumdieck R, Hook M, Rosenberg LC, Volanakis JE. The proteoglycan decorin binds C1q and inhibits the activity of the C1 complex. J Immunol 1992; 149: 3695-3701.
38. Danielson KG, Baribault H, Holmes DF, Graham H, Kadler KE, Iozzo RV. Targeted disruption of decorin leads to abnormal collagen fibril morphology and skin fragility. J Cell Biol 1997; 136: 729-743.
39. Schonherr E, Levkau B, Schaefer L, Kresse H, Walsh K. Decorin affects endothelial cells by Akt-dependent and -independent pathways. Ann N Y Acad Sci 2002; 973: 149-152.
40. Negoro S, Oh H, Tone E, Kunisada K, Fujio Y, Walsh K, et al. Glycoprotein 130 regulates cardiac myocyte survival in doxorubicin-induced apoptosis through phosphatidylinositol 3-kinase/Akt phosphorylation and Bcl-xL/caspase-3 interaction. Circulation 2001; 103: 555-561.
41. Butzkueven H, Zhang JG, Soilu-Hanninen M, Hochrein H, Chionh F, Shipham KA, et al. LIF receptor signaling limits immune-mediated demyelination by enhancing oligodendrocyte survival. Nat Med 2002; 8: 613-619.
42. Schaub FJ, Han DK, Liles WC, Adams LD, Coats SA, Ramachandran RK, et al. Fas/FADD-mediated activation of a specific program of inflammatory gene expression in vascular smooth muscle cells. Nat Med 2000; 6: 790-796.
43. Hansson GK. Cell-mediated immunity in atherosclerosis. Curr Opin Lipidol 1997; 8: 301-311.
44. Newby AC, Zaltsman AB. Fibrous cap formation or destruction--the critical importance of vascular smooth muscle cell proliferation, migration and matrix formation. Cardiovasc Res 1999; 41: 345-360.
45. Kockx MM, Herman AG. Apoptosis in atherosclerosis: beneficial or detrimental? Cardiovasc Res 2000; 45: 736-746.

Correspondence:

Dr Barbara Rolfe
Centre for Research in Vascular Biology
School of Biomedical Sciences
University of Queensland
Queensland 4072, Australia

Phone: +61-7-3365-1296
Fax: +61-7-3365-2719
e-mail: b.rolfe@uq.edu.au

Biomedical Research

Volume 11 Number 2 **Special issue on Smooth Muscle*** **May-August 2000**

CONTENT

*Guest Editor: *Professor C.Y. Kwan, Ph.D.* **Price: US$ 50.00**

Order could be placed directly to: Biomedical Research, 6-B Manzar, Sir Syed Nagar, Aligarh 202 002, India

Biomedical Research

Volume 11 Number 2 | Special issue on Smooth Muscle* | May-August 2000

CONTENT

*Guest Editor: *Professor C.Y. Kwan, Ph.D.*

Price: US$ 50.00

Order could be placed directly to: Biomedical Research, 6-B Manzar, Sir Syed Nagar, Aligarh 202 002, India

Biomedical Research

CONTENTS

Volume 15 Number 1

January-April 2004

Cover illustration: Attraction of phagocyte to dying cells in the uterine epithelium (*see Shimizu, Yamada Biomed Res 2003; 14: 121-125)*

GUIDELINES TO THE AUTHORS

Biomedical Research is an International Research Journal for the publication of original research work in all the major disciplines of Pediatrics. Invited and submitted review articles on current topics will also be included. Interesting case reports will be considered for prompt publication.

Manuscripts are received with the understanding that they have not been published or are not under consideration for publication elsewhere. Manuscripts are accepted after the recommendations of the referees. Published papers become the sole property of Biomedical Research and will be copyrighted by the Scientific Publishers of India.

The journal considers for publication manuscripts prepared in accordance with the Guidelines laid down by the *International Committee of Medical Journal Editors (Br Med J 1988; 296: 48-50).*

Preparation of Manuscripts

Manuscripts should consist of the following subdivisions: Title page, Key words, Abstract, Introduction, Material and Metods, Results/ Observations, Discussion, Acknowledgements, References, Tables, Figures and Legends. All manuscripts should be written in English and typed double-spaced throughout on one side of A4 (206x294 mm) with a wide margin. Number all the pages consecutively beginning with the title page.

The original and two copies of the manuscript along with 3 sets of figures should be sent to any one of the Receiving Editors, member of Editorial Advisory Board or directly to: tor:

Editor-in Chief
Biomedical Research
6-B Manzar, Sir Syed Nagar
Aligarh 202 002
India

e-mail: biomedical44@hotmail.com

Moble: 0091-571-3155814

Professor D. Higgins
Deputy Editor-n Chief
Biomedical Research
Dept. of Pharmacology & Toxicology
State Univ. of New York at Buffalo
USA

e-mail: dhiggins@acsu.buffalo.edu

Title Page

The title page should include the complete title of the manuscript, the authors (s) name, address of the institute where the work was conducted, running title and the name and address of the author to whom the correspondence could be sent. 3-8 key words are essential.

Abstract

The abstract should not exceed 250 words. It should be written in complete sentences and should give factual information.

Abbreviations

Abbreviations of units should confirm with those shown below:

Decilitre	dl	Kilgram	kg
Milligram	mg	Hour/s	h
Micrometer	µm	Minute/s	m
Molar	mol/L	Millilitre/s	ml
Percent	%		

Other abbreviations and symbols should follow the recommendations on units, symbols and abbreviations : A guide for Biological and Medical Editors and Authors (The Royal Society of Medicine London 1977).

References

A list of all the references cited in the text should be given at the end of the manuscript. The references should be cited according to the Vancouver agreement. They should be numbered consecutively in the order in which they are first mentioned in the text. Identify references in the text by Arabic numerals [in square brackets]. Authors must check and ensure the accuracy of all references cited. All authors should be cited. Abbreviations of titles of medical periodicals should conform to those used in the latest edition of Index Medicus. The volume of the periodical should be followed by the page number of each reference cited. Some examples are below:

Journal article

Gendron F-P, Newbold NL, Vivas-Mejia PE, Wang M, Neary JT, Sun GY, Gonzalez FA, Weisman GA. Signal transduction pathways for P2Y2 and P2X7 nucleotide receptors that mediate neuroinflammatory responses in astrocytes and microglial cells. Biomed Res 2003; 14: 47-61.

Personal authors' book

Carr KE, Toner PG. Cell structure: An introduction to Electron Microscopy. 3rd Ed Edinburgh Churchill Livingstone 1962.

Edited Book

Dauset J, Columbani J eds. Histocompatability 1972. Copenhagen Muksgaard 1973.